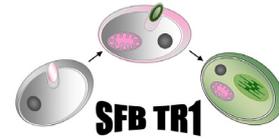# Dissertation

Cytochrome c_{6A} – Functional Evolution of a Plastidial Protein

Michael Scharfenberg

October 2011

Cytochromes c_{6A} – Functional Evolution of a Plastidial Protein

Dissertation

zur Erlangung des Doktorgrades der Fakultät für Biologie

der Ludwig-Maximilians-Universität München

Michael Scharfenberg

October 2011

Erstgutachter: Prof. Dr. Daro Leister

Zweitgutachter: Prof. Dr. Peter Geigenberger

Abgabe der Dissertation: 19/10/2011

Tag der mündlichen Prüfung: 02/12/2011

Cytochromes c_{6A} – Functional Evolution of a Plastidial Protein

Summary

In photosynthetic light reactions of cyanobacteria and green algae, cytochrome c_6 works as a carrier that transfers electrons from the cytochrome b_6f complex to photosystem I. In 2002 a homolog of cytochrome c_6 has been found in higher plants by genomic sequence analyses. Experiments aimed at characterizing the "new" protein, called cytochrome c_{6A}, showed that during evolution its function as electron carrier between the photosynthetic complexes has been lost. Up to now, its function could not be clarified, but hypotheses regarding a putative new function of cytochrome c_{6A} have been developed. The first, known as the hypothesis of Schlarb-Ridley (2006), describes cytochrome c_{6A} as a redox regulating protein in the thylakoid lumen. In this thesis this hypothesis, together with others developed during the study, were adressed by genetic and biochemical approaches.

A detailed characterization of the *Arabidopsis thaliana* T-DNA insertion line *atc6* focusing on the photosynthetic complexes and their performances shows that photosynthesis is unaffected by to the loss of cytochromes c_{6A}. Concerning the *atc6* knock-out line a genome wide expression profile by microarray analyses has been performed. This experiment revealed interdependency between the expression of cytochrome c_{6A} and the two genes *CDC48* and *BAG6*, whose proteins are involved in the programmed cell death process. Furthermore, to identify possible interaction between cytochrome c_{6A} and other proteins, co-immuno precipitation experiments in *Arabidopsis* and protein interaction studies in yeast were applied. The results showed an interaction between cytochrome c_{6A} and stromal components of photosystem I, predominantly with a part of PSI-F, as well as with the RNA-editing-factor OTP86. An interaction with lumenal redox proteins or plastocyanin could not be confirmed. Additionally, localization of cytochrome c_6 in the thylakoid lumen could not be verified.

Considering these results together, previous hypotheses could be at least partially refused. Cytochrome c_{6A} is unlikely to play a role in the linear electron transport of the light reaction and it is not a redox regulator in the lumen. The subplastidial localization of the protein remains obscure. Anyway, as suggested by the interaction studies, a function in the stroma can be assumed, where it interacts with photosystem I and could be involved either in redox regulation or programmed cell death processes.

Cytochromes c_{6A} – Functional Evolution of a Plastidial Protein

Zusammenfassung

Die Funktion von Cytochrom c_6 in der Elektronentransportkette der Lichtreaktion in Cyanobakterien und Grünalgen besteht darin, Elektronen vom Cytochrom b_6f Komplex zum Photosystem I zu transportieren. Im Jahr 2002 konnte ein Cytochrom c_6 Protein in höheren Pflanzen nachgewiesen werden. Experimente mit dem „neuen" Protein, Cytochrom c_{6A} genannt, zeigten, dass im Laufe der Evolution die Funktion des Elektronentransports zwischen den photosynthetischen Komplexen verloren ging. Bis heute konnte die Funktion von Cytochrom c_{6A} nicht geklärt werden, jedoch wurden Hypothesen bezüglich der Funktion von Cytochrom c_{6A} entwickelt. Als erstes ist die Hypothese von Schlarb-Ridley im Jahr 2006 hervorzuheben, die eine Funktion von Cytochrom c_{6A} als redox-regulatorisches Protein im Thylakoidlumen beinhaltet. In dieser Dissertation wurden die Hypothesen unter Verwendung verschiedener genetischer und biochemischer Untersuchungen überprüft.

Eine detaillierte Charakterisierung der *Arabidopsis thaliana* T-DNA-Insertionslinie *atc6* bezüglich ihrer photosynthetischen Komplexe und deren Leistungsfähigkeit zeigte, dass das Fehlen von Cytochrom c_{6A} die Photosynthese nicht beeinflußt. Die *atc6* Mutante betreffend wurde ein genomumfassendes Expressionsprofil mithilfe von Microarray-Analysen erstellt. Hiermit wurde ein Zusammenhang zwischen der Expression von Cytochrom c_{6A} und den beiden Genen CDC48 und BAG6. Des Weiteren wurden zur Überprüfung möglicher Interaktionen von Cytochrom c_{6A} mit anderen Proteinen Co-Immunopräzipitations-Experimente in *Arabidopsis* und Interaktionsstudien in Hefe durchgeführt. Die Ergebnisse bestätigten eine Interaktion von Cytochrom c_{6A} mit stromalen Untereinheiten des Photosystems I, insbesondere mit einem Teil der Untereinheit PSI-F, sowie mit dem RNA Editierungsfaktor OTP86. Eine Interaktion mit lumenalen Redoxproteinen oder Plastocyanin konnte nicht nachgewiesen werden. Außerdem konnten mehrere experimentelle Ansätze die Lokalisierung von Cytochrom c_{6A} im Thylakoidlumen nicht bestätigen.

Anhand dieser Ergebnisse lassen sich die vorherigen Hypothesen zumindest teilweise widerlegen. Cytochrome c_{6A} ist nicht am Elektronentransport der Lichtreaktion beteiligt und es agiert nicht als Redoxregulator im Lumen. Die Lokalisierung des Proteins innerhalb des Chloroplasten bleibt ungeklärt. Durch die Interaktionsstudien kann man von einer Lokalisierung im Stroma ausgehen, wo es an redoxregulatorischen Prozessen oder dem programmierten Zelltod beteiligt sein könnte.

Summary

Zusammenfassung

Index

1. Introduction

1.1. Photosynthesis

Life on Earth is based on solar energy and the process in plants to collect and to process the light energy is photosynthesis of plants. The energy is used to synthesize carbohydrates and to generate oxygen from carbon dioxide and water. The fundamental equation of this process is

$$6 \ CO_2 + 6 \ H_2O + \text{light energy} \rightarrow C_6H_{12}O_6 + 6 \ O_2.$$

Energy stored in carbohydrates drives cellular processes in plants, eventually supplying energy to all forms of life. Around 200 billion tons of CO_2 are converted into biomass each year and around 40% of it by marine phytoplankton (Taiz and Zeiger, 2006).

Photosynthesis can be divided into two functional and regional separated parts, the light reactions (Fig. 1.1) and the carbon reactions (Calvin cycle). The light reactions include the conversion of light energy into chemical energy by the generation of the high-energy compounds adenosine triphosphate (ATP) and reduced pyridine nucleotide (NADPH), which are needed in the carbon fixation. Functional units of the light conversion are two photosystems localized, in higher plants, in the thylakoid membrane of chloroplasts. Energy is used to drive electron transfer through a cascade of electron donors and acceptors from H_2O to the ultimate acceptor $NADP^+$ generating a proton motive force across the thylakoid membrane that propel ATP synthesis (Taiz and Zeiger, 2006).

The initial step of light harvesting is carried out by pigments arranged in antenna complexes that are transferring energy to the reaction center complex. There, energy drives a charge separation of a specialized *chlorophyll a* (P680 in photosystem II (PSII) and P700 in photosystem I (PSI)) by excitation of electrons that are channeled into the electron transport chain. In case of PSII two electrons are transferred to the primary electron acceptor *pheophytin a* and subsequently to two quinones Q_A and Q_B. The oxidized reaction center of the photosystem is re-reduced by electrons obtained via water oxidation by the manganese containing oxygen-evolving complex. The reduced plastoquinone PQ_B takes two protons

from the stromal side becoming a plastohydroquinone PQH_2 that dissociates from the reaction center and diffuses into the membrane layer, where, in turn, it transfers the electrons to the cytochrome b_6f complex. PQH_2 is oxidized close to the lumenal side releasing protons into the lumen. One of the electrons is transferred to a b-type cytochrome of the complex. This electron undergoes a cyclic process via another b-type cytochrome back to a quinone to build a new plastohydroquinone taking protons from the stromal side. The other electron is taken up by the Rieske protein and passed to the cytochrome f that is the lumenal docking side of plastocyanin and cytochrome c_6, the electron carriers to PSI. Both are small, water-soluble proteins in the lumen of thylakoid membranes and accomplish a distant electron transfer between the two photosystems (Taiz and Zeiger, 2006).

Solar energy, which is directed to PSI, leads to a charge separation of the specialized *chlorophyll a*, P700. The electron gap in the reaction center is filled by the electron coming from plastocyanin or cytochrome c_6. The excited electron coming from P700 is accepted by a chlorophyll a (A_0) and a phylloquinone, (A_1) known as vitamin K_1. Passing three membrane-associated iron sulfur proteins, F_X, F_A and F_B, the electron is transported through the protein complex to the stromal docking side of ferredoxin (Fig. 1.2A). After uptake of the electron the negatively charged ferredoxin reduces $NADP^+$ to NADPH catalyzed by the membrane associated flavoprotein ferredoxin-NADP oxidoreductase (FNR) (Taiz and Zeiger, 2006).

Next to the reducing power of NADPH, light reaction produces ATP via photophosphorylation, a chemiosmotic process. The proton gradient generated during the electron transport chain leads to differences in ion concentrations and electric potential across the membrane. This chemiosmotic force can be utilized by the enzyme complex ATP synthase to synthesize ATP starting from ADP and P_i (Taiz and Zeiger, 2006).

Function and structure of the four light reaction complexes were extensively studied and reviewed (Nield *et al.*, 2000; Ben-Shem *et al.*, 2003; Nelson and Yocum, 2006; Baniulis *et al.*, 2008).

Carbon fixation reactions in the stroma require ATP and NADPH in a ratio of 3:2 while according to Arnons view the linear electron transport chain generates a ratio of unity (Arnon et al., 1954; Allen, 2002). To produce more proton motive force, electrons of the acceptor side of PSI can be re-injected into the cytochrome b_6f complex of the electron transport chain. Two possible ways of the cyclic electron flow are discussed, a ferredoxin

dependent way (Munekage *et al.*, 2002; DalCorso *et al.*, 2008) and a NADPH dehydrogenase dependent way (Shikanai, 2007).
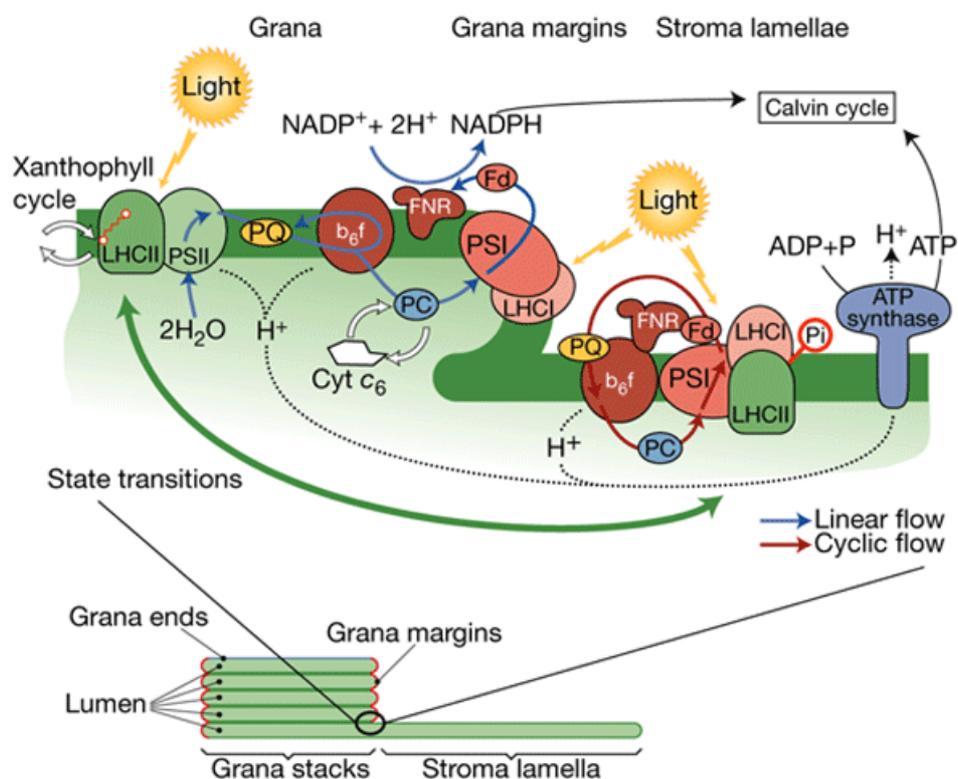
Figure 1.1: Thylakoid Membranes, Their Domains, and the Dynamics of the Photosynthetic Electron-flow Machinery. In the thylakoid membranes (lower panel), photosynthetic activity results from the balance between light absorption and utilization. Several dynamic processes regulate the absorption of light: thermal dissipation in the photosystem II (PSII) outer antenna light-harvesting complex II (LHCII) is modulated by the xanthophyll cycle. Phosphorylation induces the reversible migration of this subcomplex from PSII to PSI (a state transition), which adjusts the relative absorption properties of the two photosystems and allows for the optimization of their relative activities. In addition, supramolecular structures, granal stacks, the uneven distribution of complexes, and protein–protein interactions result in compartmentalization of the photosynthetic complexes and electron carriers. This is likely to modulate the efficiency of linear (blue) and cyclic (red) electron flow, and thus that of ATP synthesis, through the generation of an H^+ gradient. Fd, ferredoxin; FNR, Fd:NADP$^+$ reductase; PQ, plastoquinone (Finazzi *et al.*, 2003).

1.2. Adaption of Photosynthesis to Light Conditions

Due to their sessile life style, land plants are exposed to changes in light quality and quantity without the possibility to escape by moving. Therefore, new mechanisms were evolved to balance the energy distribution between the two photosystems known as long- and short-term acclimation. Redox state of the plastoquinone pool is crucial for the activation of acclimation responses. During long-term acclimation, imbalances in energy distribution are adjusted by changing the stoichiometry of the photosystems within hours and days (Wagner *et al.*, 2008). In short-term conditions, acclimation is accomplished by movements of the light harvesting complex II (LHCII) between the two photosystems within minutes, the state transitions. Under light conditions that favor PSII the kinase STN7/STT7 becomes active and phosphorelates the LHCII that is associated to PSII (State I). This phosphorylation leads to a migration of LHCII to the PSI (State II) to increase the uptake of energy (Bellafiore et al., 2005; Bonardi et al., 2005; Pesaresi et al., 2009b). In PSI favoring light, the LHCII becomes dephosphorylated by the phosphatase TAP38 and migrates back to PSII (Pribil *et al.*, 2010; Pesaresi *et al.*, 2011).

Photosynthetic systems are designed to collect large amount of light energy and to convert it in chemical energy even under low light conditions. In high light the amount of solar energy overcharges the photosynthetic system and excited electrons of reaction center pigments cannot be processed in the same proportion they raise. Electrons react with molecular oxygen that leads to an increased production of toxic species such as superoxide (O_2^-), singlet oxygen ($^1O_2^*$) and peroxide (H_2O_2) (Taiz and Zeiger, 2006).

Plants developed different level of protective and scavenging systems, creating non-photochemical quenching (NPQ), the major process to regulate the delivery of energy to the reaction center. Most of the excess energy is quenched as heat by carotenoids, because their excited state does not provide enough energy to generate toxic oxygen species. Violaxathin (Vx), Antheraxanthin (Ax) and Zeaxanthin (Zx) are precursors of abscisic acid (ABA) and are involved in NPQ. Under high light conditions Vx is converted via Ax to Zx that binds to the light harvesting complexes leading to conformational changes and heat dissipation. The conversion is catalyzed by the enzyme Violaxanthin-de-epoxidase (VDE, NPQ1) and is reverted by the enzyme Zeaxanthin-epoxidase (ZEP, ABA1) (Demmig-Adams

and Adams, 1993). Important factors for this mechanism, also called xanthophyll cycle, are the pH of the thylakoid lumen and the aggregation state of the antenna complexes. Furthermore the heat dissipation is preferentially associated with the peripheral antenna complex protein PsbS protein (Li *et al.*, 2000).

Other components of NPQ are state transitions and photoinhibition that is based on inactivation damage of the PSII. The D1 protein of the reaction center is the main target of the damage by toxic radical oxygen species and has to be replaced with a new synthesized polypeptide by a repair cycle (Baena-González and Aro, 2002).

1.3. Structure of Photosystem I, a Plastocyanin/Ferredoxin-Oxidoreductase

In plants and green algae, PSI is a large monomeric multi-subunit complex with a molecular mass of more than 500 kDa, embedded in the thylakoid membrane. It consists of the peripheral Light Harvesting Complex I (LHCI) and the core complex including the 12-14 subunits PsaA-PsaL, PsaN and PsaO (Fig. 1.2A). The P700 and the primary electron acceptors A_0, A_1 and F_X are bound to the central large subunits PsaA and PsaB. The terminal members of the inner electron transport chain, F_A and F_B are bound by PsaC. The lumenal part is dominated by the subunits PsaN and PsaF. The last-mentioned protein exposes a helix-loop-helix domain stabilizing the interaction between plastocyanin and PSI. PsaC, PsaD and PsaE are forming the stromal side and the binding domain for ferredoxin. The LHCI (Lhca1-4) is associated with the photosystem by the subunits PsaK, PsaG, PsaJ and PsaF and interaction with the LhcII during state transition are realized by the subunits PsaI, PsaH and PsaL (Fig. 1.2B) (Ben-Shem *et al.*, 2004).

In cyanobacteria, the core of the reaction center is very similar to the eukaryotic version, but in prokaryotes the peripheral LHCI is missing. The subunits PsaG, PsaH, PsaN and PsaO are exclusively present in plant photosystems, whereas the subunits PsaM and PsaX are characteristic for cyanobacteria. Furthermore, the PSI in cyanobacteria is organized in a trimeric structure modulated by the subunit PsaL (Ben-Shem *et al.*, 2004).

A   B
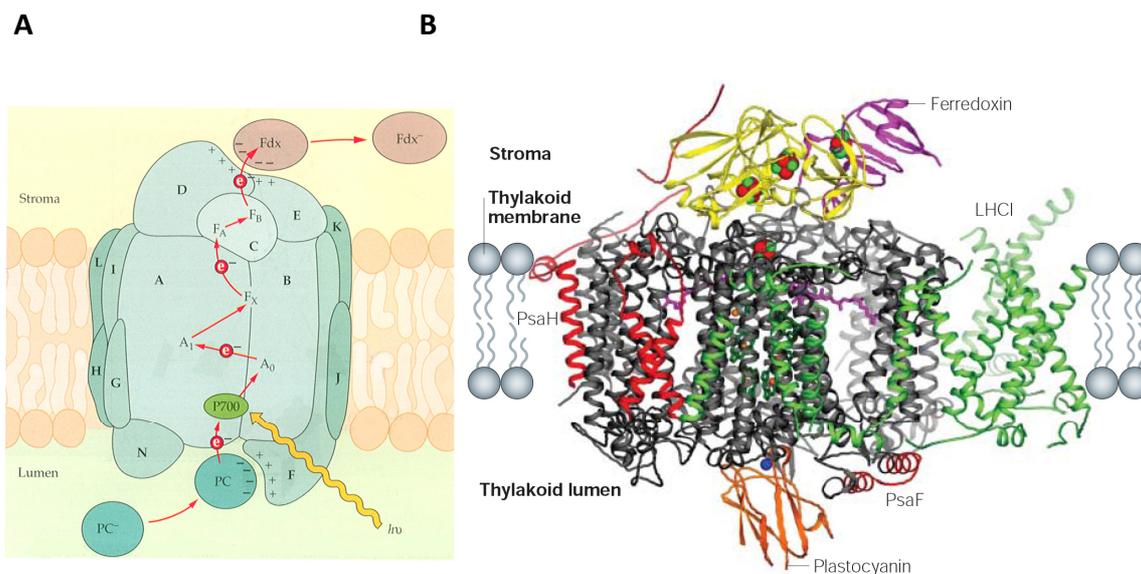
Figure 1.2: Structure of Photosystem I in Higher Plants. Simplified model of the PSI of higher plants is shown (Buchanan *et al.*, 2002). Components of PSI are organized around two major core Proteins, PsaA and PsaB. Minor proteins PsaC to PsaN are labeled C to N. The red arrows indicate the electron transfer through the PSI as described before (chapter 1.1.).

A side view of the putative interactions between plant photosystem I (PSI), plastocyanin and ferredoxin (B). The structural coordinates for PSI were taken from the Protein Data Bank (PDB) file 1QZV. The coordinates for plastocyanin and ferredoxin were taken from PDB files 1AG6 and 1A70, respectively. The reaction centre comprises 12–14 subunits that are denoted PsaA–PsaL, PsaN and PsaO, and two of these subunits are labeled in this figure. The stromal subunits are shown as yellow ribbon structures, and novel structural elements in the reaction centre that are not present in the cyanobacterial counterpart are shown as red ribbon structures. The conserved features of the reaction centre are shown as grey ribbon structures, and the light-harvesting complex I (LHCI) is shown as a green ribbon structure. The electron-transfer components of PSI are: chlorophylls (dark-green stick representations, in which the central orange spheres represent magnesium ions); quinones (dark-pink stick representations); and three Fe_4S_4 clusters that are highlighted by red and green spheres. Plastocyanin is shown as an orange ribbon structure and its copper atom is represented by a blue sphere. Ferredoxin is shown as a dark-pink ribbon structure and its Fe_2S_2 cluster is also represented by red and green spheres (Ben-Shem *et al.*, 2004).

1.4. Interaction between Plastocyanin or Cytochrome c_6 and Photosystem I

In eukaryotic organisms the electron transfer between plastocyanin or cytochrome c_6 and photosystem I can be divided in a multistep model: donor binding, complex formation,

electron transfer and donor release. The binding of plastocyanin or cytochrome c_6 is basically driven by two forces, the electrostatic attraction and the hydrophobic contact.

In *Clamydomonas reinhardtii*, it was shown that a positively charged domain of PsaF is crucial for the binding of both electron donors to PSI (Hippler *et al.*, 1998). Hereby, three lysine residues seem to be the most important for the electrostatic interaction. Two of these residues are located in a helix-loop-helix domain that is conserved in eukaryotic systems (Ben-Shem *et al.*, 2003). In prokaryotes the basic patch of PsaF is missing and the fast electron transfer is independent of PsaF. A chimeric PsaF containing the N-terminal basic patch of *Chlamydomonas* integrated into PsaF of *Synechocystis* was designed and expressed in *Synechocystis*: after PSI isolation the electron transfer rate between *Chlamydomonas* cytochrome c_6 and PSI was determined showing a 30% higher electron transport rate of the chimeric form compared to the wildtype PSI of *Synechocystis* proving the essential role of the N-terminal domain of PsaF for efficient binding and electron transfer from the donor molecule to PSI (Hippler *et al.*, 1999).
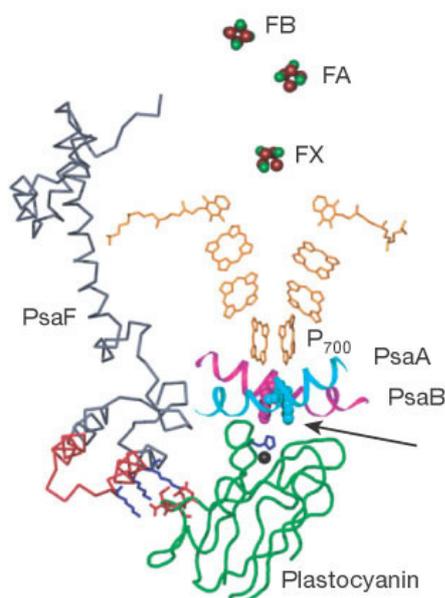
Figure 1.3: Electron Transfer Chain and Plastocyanin Binding. Residues 18–47 of plant PsaF, which include the 18 residues exclusive to eukaryotes and that form a helix–loop–helix domain, showed in red. A cluster of four negatively charged residues (red) on the surface of plastocyanin (green) interacts with three lysines (blue) from the N terminus of PsaF, two of which are from the extra 18 residues. The two tryptophan residues (indicated by the arrow) crucial for the electron transfer from the reduced copper to the oxidized P700, and that contribute

to the hydrophobic interaction with plastocyanin, are shown as spherical atoms (cyan and magenta). The histidine residue that coordinates the copper atom in plastocyanin depicted in blue (Ben-Shem *et al.*, 2003).

In contrast, the hydrophobic interaction site of PSI that is formed by PsaA and PsaB is conserved between prokaryotes and eukaryotes. A tryptophan residue of a luminal helix in loop *i* of PsaA and a tryptophan of a luminal helix in loop *j* of PsaB are adjusted close to the reaction center of PSI. Exchange of either of the tryptophanes prevents the formation of a functional electron transfer complex indicating its requirement for pending of plastocyanin to PSI (Sommer *et al.*, 2004).

According to eukaryotic electron donors, electrostatic and hydrophobic recognition sites of plastocyanin have been dissected by site-directed mutagenesis. A conserved negatively charged patch at the south-end and a hydrophobic patch at the north-end of plastocyanin were identified as the key players in the interaction with photosystem I (Fig. 1.3) (Nordling *et al.*, 1991; Haehnel *et al.*, 1994; Hyun Lee *et al.*, 1995; Hippler *et al.*, 1996).

1.5. Cytochrome c_6 in Cyanobacteria and Algae

The first studies concerning cytochrome c_6 occurred 50 years ago, when Katoh (1960) characterized cytochrome c_6 in the red algae *Porphyra tenera*. Later studies extended to its characteristics and function in cyanobacteria and algae.

Cytochrome c_6 is a low molecular weight (9.3 kDa in *Monoraphidium braunii*), soluble protein with a surface charge distribution and redox potential (358 mV in *Monoraphidium braunii*) similar to plastocyanin (Molina-Heredia *et al.*, 2003). Its 83-90 amino acid sequence contains the c-type cytochrome motif CXXCH (X: any amino acid) which serves as the binding domain for a heme group ensuring the ability to transfer electrons (Fig 1.4). Localized in the thylakoid lumen, cytochrome c_6 oxidizes cytochrome *f* of the cytochrome b_6f complex and reduces PSI to maintain the electron flow of photosynthesis (Merchant and Dreyfuss, 1998). Additionally, in prokaryotic organisms it can provide electrons for the cytochrome oxidase (Nicholls, 1992).

Cytochrome c_6 is widely distributed in lower photosynthetic organisms (e.g. cyanobacteria, brown-, red- and some green-algae). To consider environmental changes in the history of evolution is an attempt to reconstruct its functional evolution (Fig 1.5).

The present opinion describes the c-type cytochromes as the ancient electron donors to both Type I and Type II reaction centers like in *Chlorobium* and *Rhodobacter*, respectively. This supposes that an ancestor of the current cytochrome c_6 was the first electron donor to PSI. Because of the photosynthetic active organisms, the concentration of oxygen in the atmosphere rose and, due to the oxidative environment, free iron was rarely available. Additionally, the access of iron could be influenced by geographic differences causing selective pressure by iron limitation. To apply an electron carrier based on a copper depending polypeptide, instead of an iron depending cytochrome, turned out to be an advantage (Howe et al., 2006). This was the moment, 2.3 billion years ago, when plastocyanin occurred as an alternative to cytochrome c_6 in the photosynthetic electron transport chain (Howe et al., 2006). Cytochrome c_6 was still an important alternative under copper deficient conditions. Both proteins are present in several green algae lineages, providing evidence for their coexistence during the "endosymbiosis event" of plastids 1.5 billion years ago. Through divergence of the green algae lineages, the ancient cytochrome c_6 got lost and plastocyanin took over the function to shuttle electrons from the cytochrome b_6f complex to PSI entirely. This indicates that for many green algae and their evolutionary offspring copper limitation plays only a minor role (Fig. 1.5) (Howe *et al.*, 2006).

1.6. Discovery of Cytochrome c_{6A} in higher plants

In 2002, two groups discovered independently a homolog of cytochrome c_6 in higher plants and green algae by sequence similarity analysis that showed up to 30% identity to other cytochrome c_6 proteins. The peptide sequence of the "new" cytochrome showed two characteristic features conserved in all species, the heme binding domain CXXCH and a twelve amino acid loop (loop insertion peptide or LIP) that is lacking in the original cytochrome c_6 form. This loop carries two invariant cysteine residues that are able to form a disulphide bridge (Fig 1.4) (Gupta *et al.*, 2002; Wastl *et al.*, 2002; Weigel *et al.*, 2003b; Wastl *et al.*, 2004).

```
Anabaena variabilis             1 ..........................................................
Cyanidioschyzon merolae         1 ..........................................................
Synechocystis sp.               1 ..............................................MFKLFNQASR
Chlamydomonas reinhardtii (1)   1 ....................MLQLANRSVRAKAARASQSARSVSCAAAKRGAD
Monoraphidium braunii           1 ..........................................................
Chlorella vulgaris (1)          1 ..........................................................
Aureococcus anophagefferens     1 ..........................................................
Chlamydomonas reinhardtii (2)   1 ........MAKVT......SVQHGPLAAPRVRGVAVRADTPQNL....TPAAPTQPAQRQ
Volvox carteri                  1 .......MASLHPFKFRSATNHTHHRTRAITGVACSK..PR......TSDIATHGPHVH
Chlorella vulgaris (2)          1 ..........................................................
Micromonas sp.                  1 .....MISLAPTTKPTARPGPWRSDRHGPVVAAGRVASEAPRTRRTRGASPVAVQSAARP
Oryza sativa                    1 MHRLPLASRPPGPHRAAAAAHRAPQRTTTACCGRLKQEATPSFASLAVAASAAAERAATP
Arabidopsis thaliana            1 ...........MRLVLSGASSFTSNLFCSSQQVNGRG.KELKNPISLNHNKDLDFLLKK
Carica papaya                   1 ...........MRLLSVAPNAGDQIFALSIKVKGKANEEGQNLVTLKQRHVT..IFKK
Physcomitrella patens           1 ..........................................................


Anabaena variabilis             1 MKKIFSLVLLGIALFTFAFSSPALAADVAN....GAKIFSANCASCHAGGKNLVQAQKTL
Cyanidioschyzon merolae         1 .....MKSLLTFILTTIFCIQQVWAADIAH....GEQIFSANCAACHAGGNNVIMPEKTL
Synechocystis sp.              11 IFFGIALPCLIFLGGIFSLGNTALAADIAH....GKAIFAGNCAACHNGGLNAINPSKTL
Chlamydomonas reinhardtii (1)  34 VAPLTSALAVTASILLTTGAASASAADIAL....GAQVFNGNCAACHMGGRNSVMPEKTL
Monoraphidium braunii           1 ..........................EADIAL....GKAVFDGNCAACHAGGGNNVIPDHTL
Chlorella vulgaris (1)          1 ..................AADISA....GEEVFSNNCAACHTGGANVVQAEKTL
Aureococcus anophagefferens     1 ..............DVES....GATIFAGNCAACHAGGNNVIAAEKTL
Chlamydomonas reinhardtii (2)  43 APAAVAIAAAAAILLGAS..APVLAAEA.......PELFANKCAGCHMGGNILAVGATL
Volvox carteri                 45 ATAAPLILAAISTLLTA...APAFAAGA.......PELFTNKCAGCHMNGANVLAVGATL
Chlorella vulgaris (2)          1 ....................RIAIS..........FLRLSPGCHVGGGNVVQAGATL
Micromonas sp.                 56 LASPSTAAAILAIALNASAVQPSFASSE.......ELFTRTCAGCHAAGGNVVQAGATL
Oryza sativa                   61 LLAAAALLLSAASPGFLASTPSAFAQSE.......GALFRKACIGCHDMGGNILQPGATL
Arabidopsis thaliana           48 LAPPLTAVLLAVSP..ICFPPESLGQTL..DIQRGATLFNRACIGCHDTGGNIIQPGATL
Carica papaya                  46 FAPPLMAAIVALSP..IFNTPVSFGQSI..DIQKGATLFRRACIGCHDAGENVIQPGATL
Physcomitrella patens           1 ..........................................................
                                                                          ^^^^^


Anabaena variabilis            57 KKEDLEKF..GMYSAEAIIAQVTNGKNAMPAFKG...................RLKPDQI
Cyanidioschyzon merolae        52 KLDALFAN..QVNSVEAISTQVRNGKNAMPSFS...................RLTDSDI
Synechocystis sp.              67 KMADLEAN..GKNSVAAIVAQITNCNGAMPGFKG...................RISDSDM
Chlamydomonas reinhardtii (1)  90 DKAALEQYLDGGFKVESIIYQVENGKGAMPAWAD...................RLSEEEI
Monoraphidium braunii          33 QKAAIEQFLDGGFNIEAIVYQIENGKGAMPAWDG...................RLDEDEI
Chlorella vulgaris (1)         33 QKDALVSYLDGGFSVDSIVTNGKN...AMPAWAG...................RLSEDEI
Aureococcus anophagefferens    31 RKEALDSYLAGGRKESSVVTQVTNGKNAMPAFGG...................RLSDEEI
Chlamydomonas reinhardtii (2)  94 FSEDLRKN..GVDSPEALYKIIYSGKGKMPGFGKECAPK.......GACTFGARLSDEEV
Volvox carteri                 95 FPDDLRRN..GVDSSEALYKIIYSGKGKMPGFGKECAPK.......GACTFGPRLSDEEV
Chlorella vulgaris (2)         28 REGDLKRN..SVATVESIYDLVYSGKGKMPGYGTGCTPKASSPALQGKCTFGPRLSDEEI
Micromonas sp.                108 FPADLTRN..GVNDADAVYDIIYGGKGKMPGYGEGCAPK.......GQCTFGARLSDEDV
Oryza sativa                  115 YMKDLERN..GVATEDELYNITYYGKGRMPGFGEKCTPR.......GQCTFGPRLVEDDI
Arabidopsis thaliana         104 FTKDLERN..GVDTEEEIYRVTYFGKGRMPGFGEKCTPR.......GQCTFGPRLQDEEI
Carica papaya                102 FTNDLQRN..GVDTEDKLFRITYYGKGRMPGFGENCTPR.......GQCTFGPRLQDEEI
Physcomitrella patens          1 ......RN..GMANVENIFQITYSGKGRMPGYGEKCAPR.......GQCTFGPRLSDSDI
                                                                        ******************
                                                                        *

Anabaena variabilis            96 EDVAAYVLGQA.DKSWK.......
Cyanidioschyzon merolae        90 EDVANYVLAQA.KKGW........
Synechocystis sp.             106 EDVAAYVLDQA.EKGW........
Chlamydomonas reinhardtii (1) 131 QAVAEYVFKQATDAAWKY......
Monoraphidium braunii          74 AGVAAYVYDQAAGNKW........
Chlorella vulgaris (1)         71 QDVAAYVYDQASNDKW........
Aureococcus anophagefferens    72 GDVAAYVIDQANGDKWDE......
Chlamydomonas reinhardtii (2) 145 TSLASYVAERA.AACWKS......
Volvox carteri                146 AALATYVQERA.AEGWKS......
Chlorella vulgaris (2)         86 QRLSQYVVDQA.AADWK.......
Micromonas sp.                159 RGLAGYVLERS.AAEWK.......
Oryza sativa                  166 KLLAAFVKSQA.ENGWPKIDGDGD
Arabidopsis thaliana          155 KILAEFVKFQA.DQGWPTV.STD.
Carica papaya                 153 KLLAQLVKFQA.DQGWPDLPSTDD
Physcomitrella patens          46 RALAEFVRLQA.DQGWTK......
```

Figure 1.4: Sequence Alignment of *Arabidopsis* Cytochrome *c*_{6A} and Its Homologues from Other Species. The protein sequence of *Arabidopsis thaliana* cytochrome *c*_{6A} was aligned to its homologues from *Anabaena variabilis, Cyanidioschyzom merolae, Synechocystis sp., Chlamydomonas reinhardtii, Monoraphidium braunii, Chlorella vulgaris, Aureococcus anophagefferens, Volvox carteri, Micromonas sp., Oryza sativa, Carica papaya*

and *Physcomitrella patens* using AlignX. The heme binding motif and the cytochrome c_{6A} specific loop are indicated with small arrows and asterisks, respectively. The transit peptide of the *Arabidopsis* sequence predicted by ChloroP is underlined. In presence of both cytochrome forms, cytochrome c_6 is labeled with (1) and cytochrome c_{6A} with (2).

The detection of cytochrome c_{6A} mRNA by Northern blot analysis and protein by Western blot analysis in leaves, but not in roots, of *Arabidopsis thaliana* suggests a limitation of cytochrome c_{6A} to photosynthetic active tissue. Furthermore the protein was detected in the lumenal fraction of isolated protoplast indicating localization in the thylakoid lumen (Gupta *et al.*, 2002). Proteomic approaches have failed to detect cytochrome c_{6A} (Peltier *et al.*, 2002; Schubert *et al.*, 2002; Baginsky *et al.*, 2004; Friso *et al.*, 2004; Kleffmann *et al.*, 2004).
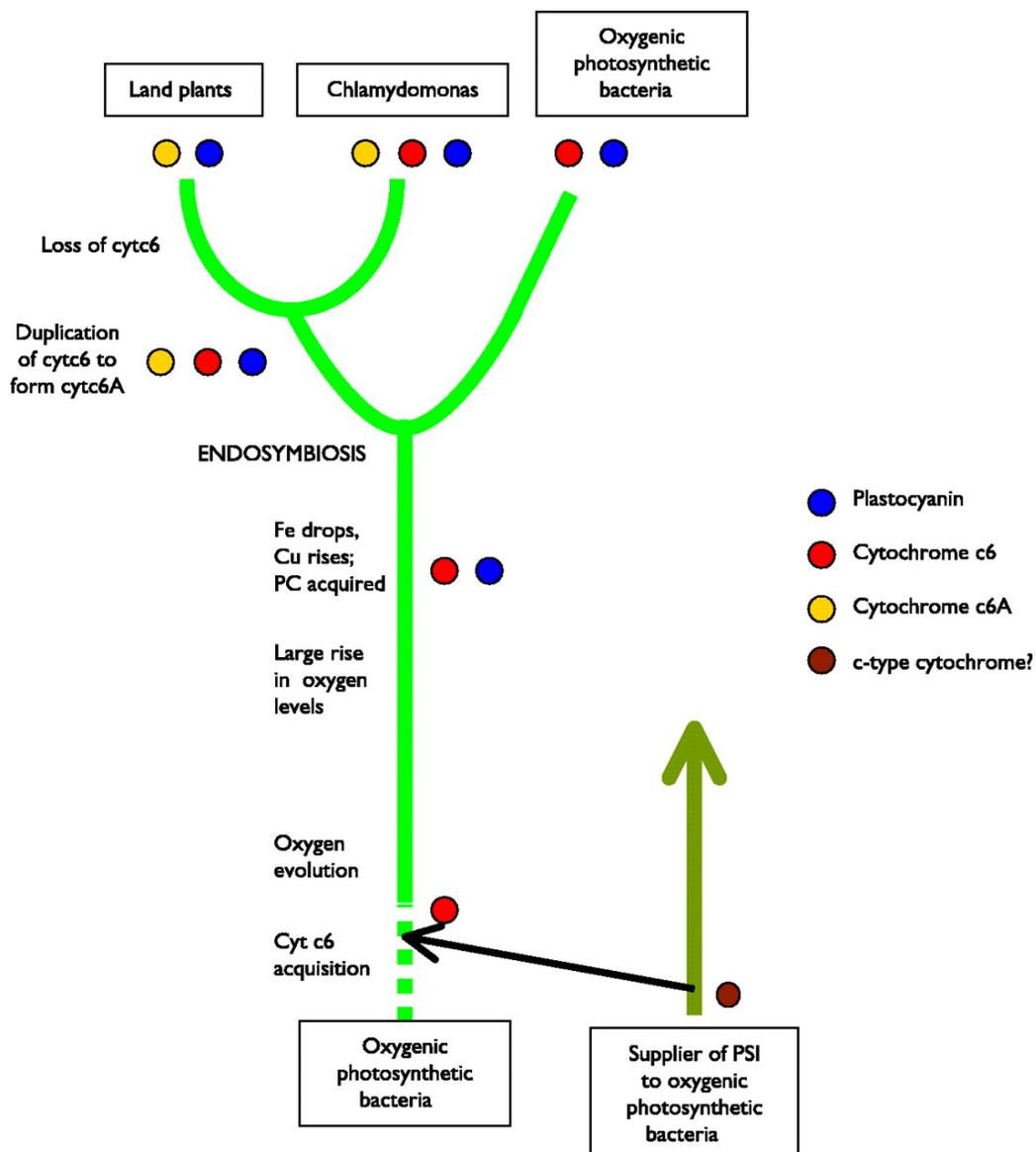
Figure 1.5: Proposed Evolutionary Pathway for Cytochrome c_{6A}. A simplified evolutionary overview of cytochrome c_6, cytochrome c_{6A} and plastocyanin related to environmental changes is shown (Howe *et al.*, 2006). The diagram supposes that the ancestor to Photosystem I was transferred laterally into the oxygenic photosynthetic bacterial lineage, although other origins for two photosystems in these organisms have been proposed (Allen, 2005).

1.7. Three Dimensional Structure of Cytochrome c_{6A}

The structure of cytochrome c_{6A} from *Arabidopsis* was analyzed by X-ray crystallography (Fig. 1.6A). It belongs to a typical class I c-type cytochromes with four α-helices and a heme group. The heme is covalently bound to two cysteines (Cys16 and Cys19) of the heme binding motif and the heme iron is coordinated by histidine (His20) and methionine (Met60). The backbone of the protein is very similar to the structure of cytochrome c_6 of *Monoraphidium braunii* (Fig. 1.6B). The LIP is well defined lying on the external surface of the protein (Marcaida *et al.*, 2006; Worrall *et al.*, 2008).

Comparison of the protein structure of a protein carrying oxidized or reduced heme, showed no significant differences between these two forms. In contrast, the change of the heme redox state of the ancient cytochrome c_6 leads to both a rearrangement of the heme coordination and of neighboring side-chains. Neither changes of the LIP conformation in cytochrome c_{6A} could be observed contradicting a function as a redox state indicator to other proteins (Marcaida *et al.*, 2006).

A

B

Figure 1.6: X-Ray Crystal Structure of Cytochrome c_{6A} and Cytochrome c_6. X-ray crystal structure of *Arabidopsis* ferri-cytochrome c_{6A} with its fou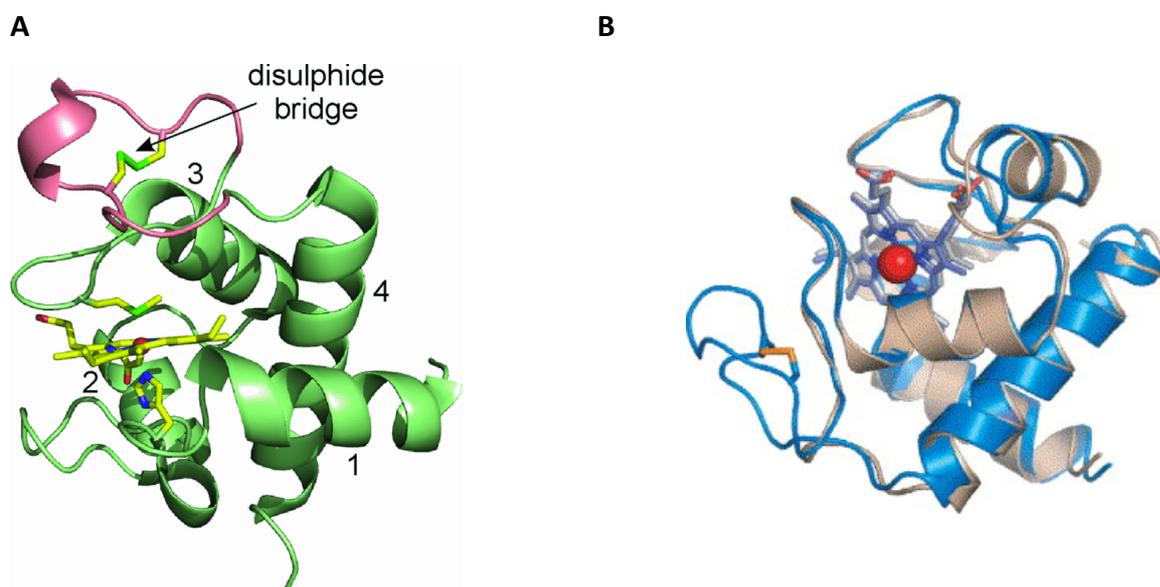r alpha helices (1-4) and the LIP (pink). The disulphide bridge, the heme and the axial methionine and histidine ligands to the iron (red sphere) are shown in sticks (A) (Worrall *et al.*, 2008). The superposition of the *Arabidopsis* ferri-cytochrome c_{6A} (blue) and the *Monoraphidium* ferro-cytochrome c_6 (brown) show a very similar architecture (B) (Marcaida *et al.*, 2006).

1.8. Cytochrome c_{6A}: Incapable to Transport Electrons to Photosystem I

In cyanobacteria and some algae cytochrome c_6 transports electrons from the cytochrome b_6f complex to PSI (chapter 1.5.). Therefore first investigations regarding the function of cytochrome c_{6A} focused on a possible function in the electron flow of photosynthesis similar to the function of the original cytochrome. In 2002, studies with transgenic *Arabidopsis* plastocyanin RNAi lines were performed: plants carrying a T-DNA insertion to knock-out cytochrome c_{6A} expression were not able to survive, when also plastocyanin levels were reduced. Furthermore, evolution of oxygen in inside-out thylakoids were measured in the presence of heterologously expressed cytochrome c_{6A}. It was claimed, that cytochrome c_{6A} was able to replace plastocyanin, providing electrons to the PSI, when plastocyanin was absent (Gupta *et al.*, 2002).

In the following years this hypothesis was contradicted by genetical *in vivo* and biochemical *in vitro* approaches and a loss of the original function of cytochrome c_{6A} was suggested.

Arabidopsis plants lacking plastocyanin by mutation in both plastocyanin-encoding genes, *PETE1* and *PETE2*, were generated: these plants could not grow autophototrophically and showed a high chlorophyll fluorescence phenotype indicating a blocked photosynthetic electron flow (Weigel et al., 2003a). Cytochrome c_{6A}, even overexpressed under the control of the 35S CaMV promoter, was incapable to rescue the defect. Survival of the above mentioned plastocyanin RNAi silencing lines could be explained by leakage of the silencing and a residual expression of plastocyanin (Weigel *et al.*, 2003a).

The midpoint redox potential of *Arabidopsis* cytochrome c_{6A} was determined at +140 mV (Molina-Heredia *et al.*, 2003) and in a later approach even lower than +100 mV (Worrall *et al.*, 2008*)*. In contrast to the midpoint redox potential of *Monoraphidium* cytochrome c_6 at +358 mV and *Arabidopsis* plastocyanin at +365 mV, the potential of cytochrome c_{6A} is not

positive enough, and therefore thermodynamically unsuitable, to oxidize cytochrome f, which has a potential of +320 mV (Fig. 1.7).
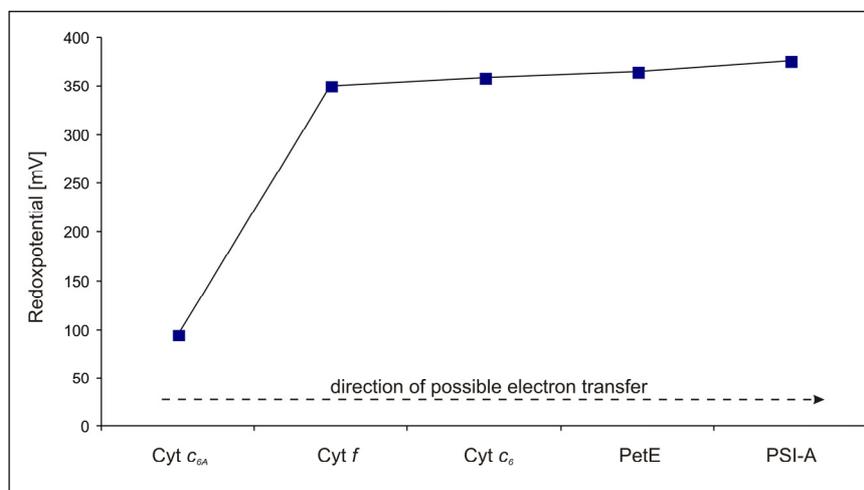
Figure 1.7: Redoxpotential of cytochrome c_{6A} and Components of the Photosynthetic Electron Transport Chain. Redoxpotential of the cytochrome c_{6A} (Cyt c_{6A}) heme is compared to components of the photosynthetic electron transport chain (*Arabidopsis* cytochrome f, Cyt f; *Monoraphidium* cytochrome c_6, Cyt c6; *Arabidopsis* plastocyanin, PetE; *Arabidopsis* photosystem I subunit A, PSI-A). The direction of a possible electron transfer is indicated by a black arrow.

Nevertheless, the midpoint redox potential allows electron donation to PSI. Kinetic analysis of laser-flash induced reduction of *Arabidopsis* photosystem I in the presence of heterologous electron donors was performed. *Arabidopsis* cytochrome c_{6A} was 100 times less effective than plastocyanin, whereas *Monoraphidium* cytochrome c_6 and *Arabidopsis* plastocyanin showed a similar rate of PSI reduction. These results indicate that an electron transfer from cytochrome c_{6A} to PSI *in vivo* is unlikely (Fig. 1.8A) (Molina-Heredia *et al.*, 2003).

As described (chapter 1.4.) in eukaryotes, electrostatic interactions between the electron donor and PSI are indispensable for the formation of a functional electron transfer complex. *Arabidopsis* plastocyanin and *Monoraphidium* cytochrome c_6 have a negative surface electrostatic potential that supports interaction with positively charged domains of PsaF. *Arabidopsis* cytochrome c_{6A} has a positively charged domain close to the solvent heme,

confirming the observation of the laser-induced kinetic analysis (Fig. 1.8B) (Molina-Heredia *et al.*, 2003).

Taking together both genetic and biochemistry data, a role of cytochrome c_{6A} as an electron carrier between the cytochrome b_6f complex and PSI can be excluded.

A   **B**
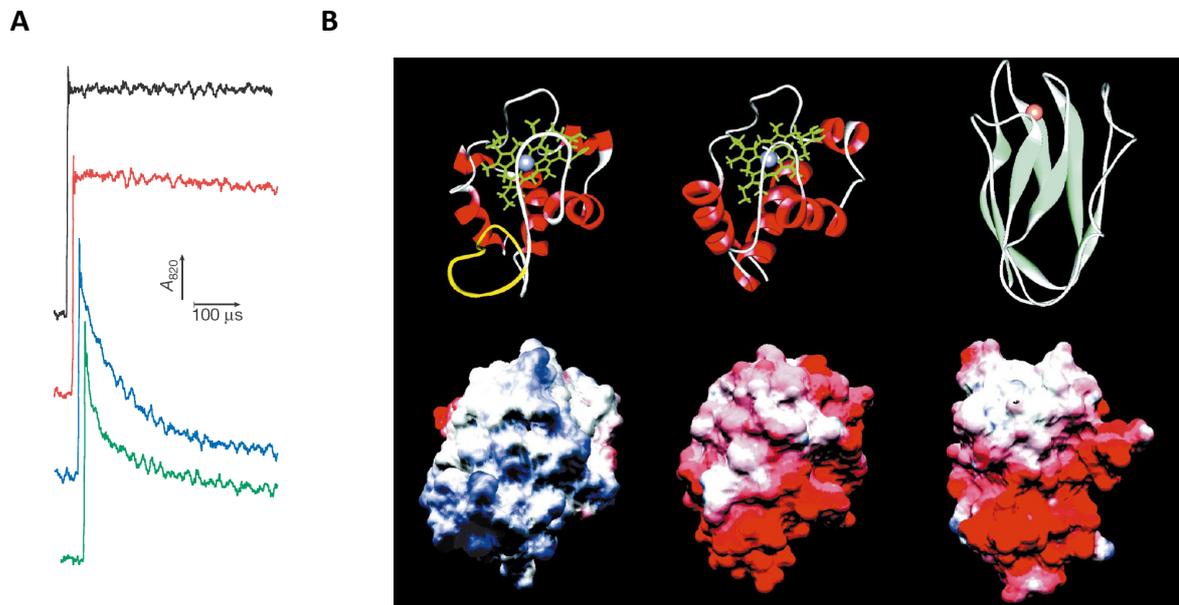
Figure 1.8: Functional Comparison of *Arabidopsis* Cytochrome c_{6A}, Plastocyanin and *Monoraphidium* Cytochrome c_6. Reduction of Arabidopsis photosystem I by cytochrome c_6 of *Arabidopsis* (red) or *Monoraphidium* (blue) and by plastocyanin of *Arabidopsis* (green) was measured by Laserflash-induced kinetic traces at 820 nm with 150 mM protein as electron donor, and a control without added protein (black, A). Structural models (top) and surface electrostatic-potential distribution (bottom) of, from left to right, *Arabidopsis* cytochrome c_{6A}, *Monoraphidium* cytochrome c_6 and *Arabidopsis* plastocyanin. The molecules are similarly orientated: *Monoraphidium* cytochrome c_6 and *Arabidopsis* plastocyanin are placed with their respective negatively charged areas towards the front; *Arabidopsis* cytochrome c_{6A} is placed with its haem group in the same orientation as that of *Monoraphidium* cytochrome c_6. Heme groups are shown in green; the extra loop of *Arabidopsis* cytochrome c_{6A} is shown in yellow; negatively and positively charged regions are shown in red and blue, respectively. Surface electrostatic-potential distributions were calculated at an ionic strength of 40 mM and pH 7.0 (B) (Molina-Heredia *et al.*, 2003).

1.9. Searching the Function of Cytochrome c_{6A}

After rejection of the original hypothesis that cytochrome c_{6A} could replace plastocyanin in the photosynthesis electron transport chain the real function of the protein remained obscure. Due to its conservation in all higher plants, it seems likely that the LIP and its cysteine bridge are related to a possible new function.
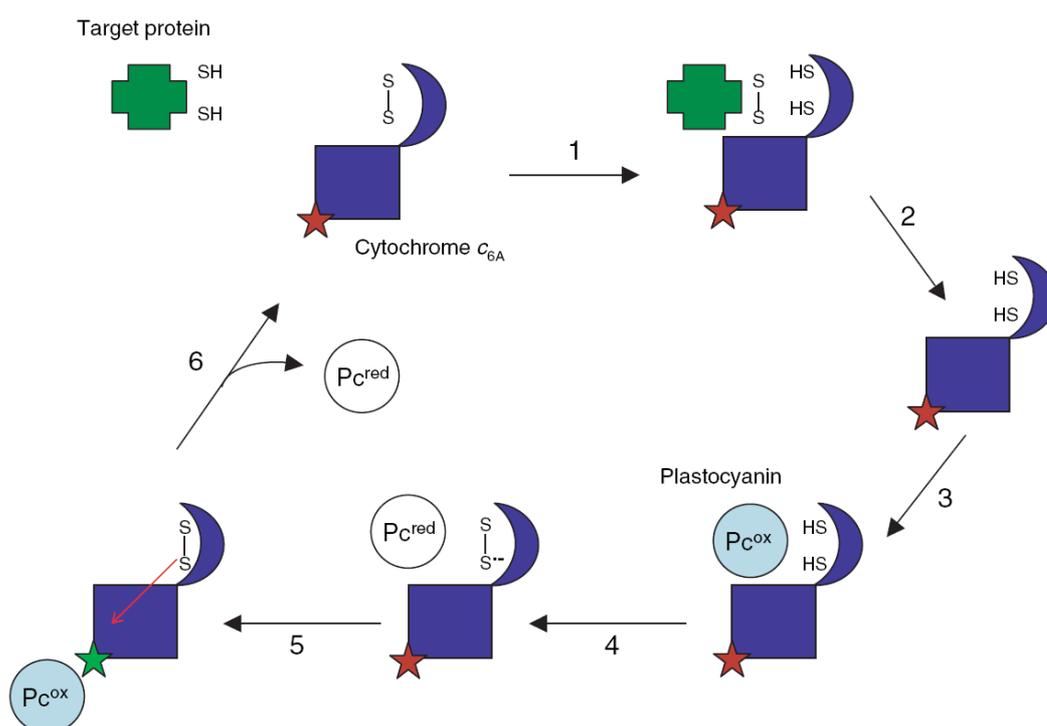
Figure 1.9: Scheme for the Hypothesis Concerning the Function of Cytochrome c_{6A}. In stage (1) a disulphide is formed in the target protein by exchange with cytochrome c_{6A}, leaving (2) cytochrome c_{6A} in the dithiol form. In stage (3) oxidized plastocyanin binds and removes a single electron in a slow reaction (4) generating a disulphide anion radical. This is followed by rapid electron transfer to the heme (5), which helps pull reaction (4) over and leads to resolution of the radical and reduction of the heme (green star). In stage 6, the reduced heme is reoxidized by plastocyanin (Schlarb-Ridley *et al.*, 2006).

Schlarb-Ridley *et al.* (2006) designed a model in which the function of cytochrome c_{6A} is to catalyze the formation of disulphide bridges in the thylakoid lumen. An oxidized Cytochrome c_{6A} could interact with lumenal target proteins that contain reduced disulphides. By a disulphide exchange reaction, the electrons are transferred to cytochrome c_{6A} reducing its

disulphide bridge and oxidizing cysteine residues of the target protein. From the reduced cysteine residues of cytochrome c_{6A} the electrons are transferred to plastocyanin by a two step reaction involving the heme to facilitate the reaction thermodynamically. Thereby target proteins in the lumen were oxidized by channeling the electrons into the photosynthesis electron transport chain and cytochrome c_{6A} acts as a coupler between the two-electron reaction of disulphide bridges and the single-electron turnover of plastocyanin (Fig 1.9) (Schlarb-Ridley *et al.*, 2006). This hypothesis was supported by many evidences coming from different studies: the lack of cytochrome c_{6A} has no phenotype in wild type, but seems to be lethal when plastocyanin is reduced (Gupta *et al.*, 2002); cytochrome c_{6A} interacts with the disulphide containing luminal protein FKBP13 in a yeast two-hybrid assay (Gupta *et al.*, 2002); it is present in low amounts (Howe *et al.*, 2006); cytochrome c_{6A} has an insertion containing conserved cysteine residues (Gupta *et al.*, 2002; Wastl *et al.*, 2002); it can reduce plastocyanin *in vitro* (Marcaida *et al.*, 2006); structural analysis suggests that intramolecular electron transfer between the heme and the LIP is possible (Worrall *et al.*, 2008). Nonetheless, in spite of many achieved hints and sophisticated assumptions, a direct evidence for the function of cytochrome c_{6A} is still missing.

1.10. Aim of the thesis

The project's goal is to reveal the function of cytochrome c_{6A} in higher plants. To achieve this aim, established hypotheses were tested and new ideas regarding the role for cytochrome c_{6A} developed.

To find a *loss-of-function* phenotype that indicates the role of the protein, an *Arabidopsis* mutant lacking cytochrome c_{6A} was investigated in a reverse genetic approach. The characterization was focused on development and growth performance, photosynthesis, in particular the photosystem I, and overall mRNA expression analysis via microarrays.

Proteins interacting with cytochrome c_{6A} were searched with yeast interaction studies and screens against an *Arabidopsis* cDNA-library. Co-immunoprecipitation of a GFP-labeled cytochrome c_{6A} in chloroplasts was applied to identify possible interactors *in vivo*.

Data available in literature about the protein localization are controversial. To verify the subcellular localization, *in silico* prediction, chloroplast *in vitro* import assay and *in vivo* fluorescence and immuno detection were performed.

To investigate new scenarios in which cytochrome c_{6A} could play a putative role, environmental stress conditions, which only land plants have to endure, were applied and the expression profile of *ATC6* monitored.

2. Materials and Methods

2.1. Plant Material and Screening for T-DNA Insertion Lines

T-DNA insertion lines of the SALK (Alonso *et al.*, 2003) or the SAIL (Sessions *et al.*, 2002) collection were identified by screening the SIGNAL database (http://signal.salk.edu/cgi-bin/tdna express) and obtained from the NASC stock centre (http://arabidopsis.info/).

Genomic DNA of *Arabidopsis* leaf tissue was extracted as described (Liu *et al.*, 1995). Mutant alleles were screened by PCR using a combination of primers designed for the left border of the T-DNA insertion and primers specific for the target gene. PCRs (1x Quiagen PCR buffer, 1mM dNTPs, 1mM forward primer, 1mM reverse primer, Qiagen Taq polymerase) were performed according to the following protocol: 3 min 94°C; [30 sec 94°C d, 30 sec 55-60°C and 30 sec -1 min 72°C]$_{x35}$; 5 min 72°C. PCR products were visualized on 1% agarose gel stained with ethidium bromide.

pete1-1.1 (*pete1*) and *pete2-1.3* (*pete2*) mutant lines derived from an *En*1-transposon mutagenesis and showed a frame shift in the coding region. The excision of the transposon in the *pete1* mutant, led to a 52 bp deletion that can be verified by the size of the PCR amplicon. In the *pete2* mutant, the transposon excision led to the creation of a recognition site for the digestion enzyme *AlwI*. Mutant alleles were therefore proven by digestion of the PCR amplicons.

The *psad1-1* (*psad*) mutant was identified by a dSpm-mutagenized *Arabidopsis* population(Tissier *et al.*, 1999). The *psae1-3* (*psae*) mutant was identified by a mutagenized *Arabidopsis* collection at INRA-Versailles (Lines are listed in Table 2.1).

Name	AGI Code	Insertion/NASC ID	Background	Forward Primer	Reverse Primer	Left Border Primer
atc6	AT5G45040	N511266	Col-0	C6seq1s	2Cyt6as	LBb1
pete1	AT1G76100	*En*1-transposon	Col-0	dMWs	dR4as	/
pete2	AT1G20340	*En*1-transposon	Col-0	139sl	75as	/
psad	AT4G02770	dSpm1	Col-0	psaD1-1s	psaD1-999as	dSpm-1-3´7
psae	AT4G28750	INRA	Ler	At4g28750-F	At4g28750-R	Taq3 (right border)
psaf	AT1G31330	N871197	Col-0	psaf-100s	psaf732as	LB3
aba1	AT5G67030	N559469	Col-0	aba1.2s	aba1.2as	LBb1
aba3	AT1G16540	N554454	Col-0	aba3.2s	aba3.2as	LBb1
abi1	AT4G26080	N576309	Col-0	abi1.2s	abi1.2as	LBb1
abi2	AT5G57050	N515166	Col-0	abi2.1s	abi2.1as	LBb1

Table 2.1: Summary of Mutant Lines Used in this Work. Mutant lines are listed together with the AGI code of the affected gene, the type of insertion or the NASC identity code, the corresponding background and the primer combination used for screening. Col-0, ecotype *Columbia 0*; Ler, ecotype *Landsberg erecta*.

2.2. Growth Conditions, Growth Measurements and Germination Assay

A. thaliana seeds were sterilized by washing with 70% Ethanol (v/v) and 5% NaOCl (v/v) and kept for 2 days at 4°C in order to break dormancy and synchronize germination. Afterwards, plants were grown on Petri dishes containing 1 x Murashige & Skoog medium (MS) including vitamins (Duchefa®) under 90 µE/(m²sec) illumination with a 16h /8h day/night cycle.

Alternatively, seeds were stratified on water soaked Whatman® paper at 4°C for 2 days and sown on soil for germination. Plants were grown under greenhouse controlled conditions (70-90 µE/(m²sec)) with a 16h/8h day-night cycle). Fertilization with "Osmocote Plus" (Scotts Deutschland GmbH, Nordon Germany) was performed according to manufacturer's instructions.

For each genotype the leaf area of at least 15 plants grown on soil each genotype was measured every week for a total of 5 weeks using ImageJ (image processing and analysis software; http://rsbweb.nih.gov/ij/).

Hypocotyl length measurements were performed placing the culture Petri-dishes vertically, as described (Bolle, 2009).

Germination was determined by sowing more than 100 seeds each genotype on MS media containing 0 µM, 0.5 µM or 1 µM abscisic acid (ABA). After 2 days of vernalization at 4°C plants were shifted for 6 h to the growth chamber light conditions and afterwards placed in the dark for 36 h: seeds that showed broken peel or visible cotyledons were considered germinated.

2.3. Computational Analyses of Protein Sequences

Amino acid sequences were obtained browsing publicly available databases (SUPERFAMILY 1.75 database; http://supfam.cs.bris.ac.uk/SUPERFAMILY/index.html, and the National Center for Biotechnology Information, NCBI; http://www.ncbi.nlm.nih.gov/). Sequences were aligned and phylogeny trees were calculated by mean of the Vector NTI software by

Invitrogen®. Alignments were shaded according to sequence similarity using the Boxshade server 3.21 (www.ch.embnet.org/software/BOX_form.html).

2.4. Cyt c_{6A} Overexpressing and Tagged Lines

To obtain Cyt c_{6A} overexpressing lines, the coding sequence of *ATC6* was cloned under the control of the Cauliflower Mosaic Virus 35S promoter into the plant expression vector pH2GW7 (Invitrogen®) by a Gateway Cloning strategy using the GWc6as/GWc6ps primer combination. After PCR, following manual descriptions of a proofreading polymerase (Phusion polymerase, NEB®) the fragment was subcloned into the pDonor207 vector (Invitrogen®) by BP reaction and transferred by LR reaction into pH2GW7 vector. *atc6* mutant plants were transformed by floral dipping (Clough and Bent, 1998). Plants were transferred to the greenhouse and seeds were collected after approximately 3 weeks. Overexpressing plants were identified after *in vitro* selection on hygromycin (15µM) -containing MS medium, and the expression level of *ATC6* was detected by Real-Time PCR, using C6seq1s and 2Cyt6as as primers (chapter 2.5.).

To fuse Cyt c_{6A} to the HA-tag (derived from Influenza hemagglutinin) or the green fluorescent protein GFP the stop codon was removed by using the GWc6s and GWc6tagas primers. After subcloning into the pDonor207, the fragment was transferred into the destination vectors pGWB14 (carrying the sequence for the HA fusion) and pB7FWG2 (harboring the GFP-coding sequence). After transformation by floral dipping of *A. thaliana* Col-0 wild type plants, transformants were selected on hygromycin (15 µM) -containing plates (pGWB14 transformation) or after BASTA treatment on plantlets (pB7FWG2 transformation). The expression level of *Cyt c_{6A}::HA* and *Cyt c_{6A}::GFP* was detected by Real-Time PCR using C6seq1s and 2Cyt6as as primers (chapter 2.5.).

As positive control for luminal localization, the coding sequence of plastocyanin was fused to the HA and GFP polypeptides using the described strategy and the PETE2GWs/PETE2GWframeas primer combination. As a stromal control the coding sequence of Cyt $c_{6A,}$ without the predicted transit peptide, was fused to the plastidial signal peptide of the Rubisco small subunit and cloned into the pB7fWG2 vector as described above (primer combinations: cTPGWs/cTPas and C6cTPs/GWc6tagas).

2.5. Real-Time PCR

Total leaf RNA was extracted from frozen tissue by TRIzol (Invitrogen®) reagent following manual instructions or by RNA isolation protocols according to Oñate-Sánchez and Vicente-Carbajosa (2008). RNA quality was checked using 2% (w/v) agarose gel containing ethidium bromide and RNA specific pattern was visualized under UV light. The quantity and purity were determined spectrophotometrically (A_{260}/A_{280} ratio). First-strand cDNA synthesis from 1 μg of total RNA was performed either using the iScript cDNA Synthesis Kit (Bio-Rad®) or using the SuperScript™ III Reverse Transcriptase (Invitrogen®). Both preparations were performed according to manufacturer's instructions. cDNA quality was checked by standard PCR program (chapter 2.1.) performed with the ubis/ubias primer combination for the housekeeping gene *Ubiquitin* (*UBI*).

For Real-Time PCR analysis, the cDNA (1:10 dilution) and specific primers were added to a iQ™ SYBR® Green containing Supermix (Bio-Rad®), and the thermal cycling consisted of an initial step at 95°C for 3 min, followed by 40 cycles of 10 s at 95°C, 30 s at 55°C and 10 s at 72°C, after which a melting curve was performed. The housekeeping *UBI* gene was considered as reference-gene. Real-Time primers are listened in (Appendix 1). Gene expression and standard deviation were calculated by the iQ5™ Optical System Software (Bio-Rad), using the following formula (Pfaffl, 2001):

$$\text{Ratio} = \frac{(E_{target})^{\Delta Ct,\ target\ (calibrator-\ test)}}{(E_{ref})^{\Delta Ct,\ ref\ (calibrator-\ test)}}$$

E_{target} and E_{ref} are the amplification efficiencies of the target gene and *UBI*, respectively. All experiments were performed with an iQ5™ Multi Colour Real-Time PCR Detection System (Bio-Rad®), using reactions in triplicate with at least two biological replicates.

2.6. Affymetrix ATH1 Array Hybridization and Quantification

10 micrograms of total RNA from leaves of four-week-old plants were extracted as described (chapter 2.5.).Each sample represents rosette-leaves of at least five plants and two to three biological replicates were performed. RNA was hybridized to a GeneChip Arabidopsis ATH1 Genome Array using the One-Cycle Target Labelling and control reagents according to the manufacturer's instructions (Affymetrix®). Reverse transcription was employed to generate first-strand cDNA. After second-strand synthesis, double-stranded cDNA was used in an *in vitro* transcription reaction to generate biotinylated cRNA. The fragmented, biotinylated cRNA was used for hybridization. Hybridization, washing, staining, and scanning procedures were performed as described in the Affymetrix technical manual. A Hybridization Oven 640, a Fluidics Station, and a GeneChip Scanner 3000 were used. Transcriptome Data Analysis CEL files were imported into FlexArray 1.6 (http://www.gqinnovationcenter.com/services/) for further analysis. Intensity raw data were normalized using the *robust multiarray average algorithm* (Irizarry *et al.*, 2003). The Local-pooled-error test (Jain *et al.*, 2003) was applied to identify differentially expressed genes. Differential gene expression was defined by thresholds of fold change expression higher than 2 or lower than 0.5. False discovery rate was calculated for p-value correction (Benjamini and Hochberg, 1995). A significance p-value threshold of 0.05 was defined for differentially regulated genes.

2.7. Leaf Pigment Analysis

For pigment extraction, leaves were frozen in liquid nitrogen and disrupted with beads in microcentrifuge tubes in the presence of acetone. After centrifugation at 10.000 g for 10 min, pigment extracts were filtered through a membrane filter (pore size 0.2 µm) and either used directly for HPLC analysis or stored for up to 2 d at −20°C. Pigments were analyzed by reverse-phase HPLC as described (Farber et al., 1997).

2.8. 77K Measurements

Fluorescence spectra of thylakoids were recorded after light adaption as described (Tikkanen *et al.*, 2006). Thylakoids were isolated by grinding leaves in presence of the *77K-buffer* (50 mM Hepes/KOH pH 7.5, 100 mM Sorbitol, 10 mM $MgCl_2$, 10 mM NaF) followed by filtration through a nylon mesh. After filtration, samples were diluted to a chlorophyll concentration of 10μg/ml, filled in a small glass tube and frozen in liquid nitrogen. 77 K fluorescence spectra were obtained by excitation at 475 nm using a Spex Fluorolog mod.1 fluorometer (Spex Industries). Emission between 600 and 800 nm was recorded, and spectra were normalized to the peak height at 685 nm. Data frequency was of 0.5 nm with an integration time of 0.1 s. More than 10 independent measurements were made from each genotype.

2.9. Blue Native PAGE and 2D SDS PAGE

Rosette-leaves of four-week-old plants were homogenized in ice cold *buffer 1* (0.4 M Sorbitol and 0.1 M Tricine-KOH pH 7.8) and filtered through four layers of Miracloth (Calbiochem). Intact chloroplasts were collected by centrifugation at 2,000 g for 10 min at 4 °C (JA 25.5 rotor, Beckmann®), resuspended and lysed in ice cold *buffer 2* (20 mM HEPES/KOH pH 7.5, 10 mM EDTA) for 20 min. Thylakoids were collected by centrifugation at 12,000 g for 10 min at 4°C and resuspended in *TMK buffer* (10 mM Tris/HCl pH 6.8, 10 mM $MgCl_2$ and 20 mM KCl). The chlorophyll concentration was measured after acetone precipitation (Porra, 2002). For the first dimension of Blue Native PAGE analysis, proteins corresponding to 30 μg of chlorophyll were washed with *TMK buffer* and incubated in *solubilization buffer* (750 mM ε-aminocaproic acid, 50 mM Bis-Tris pH 7.0, 5 mM EDTA pH 7.0, 50 mM NaCl, 1.5% β-dodecyl maltoside (β-DM) or 1.5% digitonin) for 20 min in case of β-DM or 1 hour in case of digitonin on ice. After precipitation of non soluble material at 19,000 g for 15 min or 1 hour at 4 °C the supernatant was supplemented with 5 % Coomassie-blue in 750 mM ε-aminocaproic acid and loaded onto BN gel (4-12% acrylamide (37.5:1), 0.5 M ε-aminocaproic acid, 50 mM Bis-Tris pH 7.0, 10% glycerol). The first half of the run was carried out over night at 4 °C at 20 V in cathode buffer (50 mM Tricine, 15 mM Bis-Tris pH7.0, 0.02% Coomassie G250) and anode buffer (50 mM Bis-Tris pH 7.0). After the front reached half of the gel length, the cathode

buffer was exchanged by cathode buffer without Coomassie and the voltage was raised to 300 V. First dimension gel slices were solubilized in denaturing buffer (0.125 M Tris-HCl pH 6.8, 4% SDS and 1 mM DTT) and separated by 12% acrylamide Tris-Tricine SDS-PAGE gels (Schägger and von Jagow, 1987). Proteins were visualized by Coomassie blue (G250) staining.

2.10. Isolation of Chloroplasts, Stroma and Thylakoid Fraction

About 20 g of four-week-old dark adapted (16h) leaf material were ground in *homogenizing buffer* (0.45 M Sorbitol, 20 mM Tricine/KOH pH 8.4, 10 mM EDTA, 10 mM NaHCO$_3$, 0.1% BSA). The suspension was filtered through two layers of Miracloth (Calbiochem®) and chloroplasts were sedimented at 500 g for 1 min (JA 25.5 rotor, Beckman). The pellet was resuspended in 0.8 ml *resuspension buffer* (0.3 M Sorbitol, 20 mM Tricine/KOH pH 8.4, 2.5 mM EDTA, 5 mM MgCl$_2$) and loaded on a 40/80 Percoll (GE Healthcare®) gradient. Gradients were centrifuged in a swing rotor (JS 13.1 rotor, Beckman) at 6500 g for 20 minutes without break. After centrifugation the lower green band, which contains the intact chloroplasts, was collected by pipetting using a cut-off tip and diluted with *resuspension buffer.* Chloroplasts were collected by centrifuging at 1500 g for 4 min (JA 25.5 rotor, Beckman) and incubated for 30 min on ice in *lysis buffer* (20 mM HEPES/KOH pH 7.5, 10 mM EDTA) for further separation. To separate thylakoids from the stroma, ruptured chloroplasts were centrifuged at 42,000 g for 30 min at 4°C. Stromal proteins were recovered from the supernatant, whereas thylakoids were collected as pellet.

2.11. PSI Isolation

Thylakoids were isolated from four-week-old plants as previously described in chapter 2.10.. For the isolation of PSI complexes, membranes were washed twice with 5 mM EDTA pH 7.8, centrifuged (5 min, 10,000 g) and resuspended in ddH2O to a final concentration of 2 mg/ml of total chlorophyll. After solubilization with 2% (w/v) β-dodecyl maltoside (10 min, 4°C), not soluble material was removed by centrifugation (5 min, 16,000 g). Supernatant was loaded on a 0.4 M sucrose gradient and centrifuged at 39,000 rpm (SW40Ti, Beckmann®) for at least 21 hours. After centrifugation the lower band was collected and proteins were separated by

16–23% gradient SDS PAGE as described (Jensen et al. 2000). Proteins were stained with Coomassie Blue (G250).

2.12. Immunoblot Analysis

Protein fraction was isolated as described (chapter 2.10.) and standardized to 5 µg chlorophyll content. Separation on SDS-PAGE (12% acrylamide) was performed after resuspension in *loading buffer* (6 M Urea, 50 mM Tris-HCl pH 6.8, 100 mM DTT, 2% SDS, 10% glycerol, 0.1% bromophenol blue). Protein transfer from gel to PVDF membrane was performed by means of a semi-dry blotting apparatus (Bio-Rad®) with constant current corresponding to 1mA cm^{-2} (cathode buffer: 25 mM Tris, 10% Methanol and 40 mM glycine pH 9.4; anode buffer 1: 0.3 M Tris pH 10.4 and 10% methanol; anode buffer 2: 25 mM Tris pH 10.4 and 10% methanol).

Membranes were probed with antibodies against several subunits of PSI, PSII, Cyt b_6/f and other plastid proteins according to standard protocols (Sambrook et al., 1989). Signals were detected by enhanced chemo-luminescence (ECL kit, Amersham Bioscience®) in an ECL reader (Peqlab®).

2.13. Chlorophyll Fluorescence Measurements

Chl-a fluorescence in leaves was measured by using the Dual-PAM 100 system (Walz GmbH, Effeltrich, Germany) system according to Pesaresi *et al.* 2009. For standard PSII measurements dark adapted leaves were exposed to a single far red pulse (5,000 mmol m^{-2} s^{-1}, 800 ms) and maximum fluorescence (F_M) was determined as well as fluorescence with measuring light illumination (F_0). The functionality of PSII (F_V/F_M) was calculated by the formula $F_V/F_M = (F_M - F_0)/F_M$. After a 10 min exposure to actinic red light (22, 72, 95 or 1,095 µmol m^{-2} s^{-1}) a second pulse was applied to measure the maximum fluorescence under illumination ($F_M´$) and the steady state fluorescence (F_S). Values for the effective PSII quantum yield (Φ_{II}), photochemical quenching (qP) and non-photochemical quenching were calculated (Maxwell and Johnson, 2000). The contribution of each NPQ component was analyzed by performing an induction curve as described (Eberhard *et al.,* 2008). For

detection of the PSI activity P_m', the maximum P700$^+$ absorption under illumination, and the photochemical quantum yield Φ_I were calculated. Φ_I is defined as the fraction of total P700 that is reduced in a given state and is not limited by the acceptor side. For donor side and acceptor side limitations the values Y(ND) and Y(NA) were measured, respectively, according to the manual instruction of the Dual PAM 100.

2.14. Prediction of Sub-Cellular Location

Amino-acid sequences of proteins were obtained from the TAIR database (www.arabidopsis.org/index.jsp) and analyzed with the following prediction programs (all available online): TargetP (Emanuelsson *et al.*, 2007); ChloroP (Emanuelsson *et al.*, 2000); Predotar (Small *et al.*, 2004); iPSORT (Bannai *et al.*, 2002); WoLF PSORT (Horton *et al.*, 2007); PSORT (Nakai and Horton, 2007); BaCelLo (Pierleoni *et al.*, 2006); PCLR *(Schein et al.*, 2001); ProteinProwler (Hawkins and Bodén, 2006).

2.15. *In Vitro* Import

The coding sequences of *AT5G45040* and *AT1G20340* were cloned into the pF3A (Promega®) vector and the coding region of *AT1G67090* was cloned into the pGEM-Teasy vector (Promega®) downstream the SP6 promoter region. mRNA was transcribed *in vitro* using the SP6 RNA polymerase (MBI Fermentas®). Precursor proteins were synthesized in a Reticulocyte Extract System (Flexi; Promega®) in the presence of a [^{35}S]methionine-[^{35}S]cysteine mix. Aliquots of the translation reaction were incubated with intact chloroplasts corresponding to 45 µg chlorophyll, and protein uptake was analyzed after treatment of isolated chloroplasts with thermolysin (Calbiochem®) as described (Bölter and Soll, 2007). Chloroplasts were ruptured by adding *lysis buffer* (chapter 2.10.) followed by centrifugation at 14,000 g for 10 min. Stromal proteins were recovered from the supernatant, whereas thylakoids were represented by the pellet. Labeled proteins were subjected to SDS-PAGE and detected by phosphorimaging (Typhoon; Amersham Biosciences®)

2.16. Subcellular Localization with GFP

The green fluorescent protein (GFP) from the hydrozoan jellyfish *Aequorea victoria* (Tsien, 1998) was used as reporter to determine the intracellular localization of the protein of interest. The coding sequence of the gene was cloned in frame upstream the sequence coding for GFP as described before (chapter 2.4.). Leaves of four-week-old transgenic *Arabidopsis* plants expressing a GFP fusion protein were cut and incubated for several hours at room temperature in the dark in an appropriate *cell wall lysis buffer* [20 mM KCl, 10 mM MES pH 5.7, 10 mM CaCl$_2$, 0.5 M Mannitol, 0.1% BSA, 0.1 g/ml macerozyme (Duchefa®), 0.1 g/ml cellulase (Duchefa®)]. Protoplasts were collected by centrifugation at 50 g for 5 min and washed with *washing buffer* (20 mM KCl, 10 mM MES pH 5.7, 10 mM CaCl$_2$, 0.5 M Mannitol). Microscopic analyses were carried out using Axio Imager fluorescence microscope with integrated ApoTome (Zeiss). Fluorescence was excited via an X-Cite Series 120 fluorescence lamp (EXFO) and detected at wavelength ranges of 505 - 530 nm (GFP fluorescence) and 670 - 750 nm (chlorophyll autofluorescence).

2.17. Yeast Two-Hybrid and Ternary-Trap Assays

YPAD, SD, and appropriate drop-out media have been previously described (Sherman *et al.*, 2002). The yeast two-hybrid and the ternary-trap assays were performed using the yeast strain AH109 supplied by Clontech® (Palo Alto, CA) (James *et al.*, 1996). The pGBTKT7 vector (Clontech®), carrying the GAL4 DNA-binding domain, was used to express the bait proteins, whereas the pGADT7 vector (Clontech®), carrying the GAL4 activation domain, was used to express Cyt c_{6A}. For the ternary-trap test, the vector pTFT1 (Egea-Cortines *et al.*, 1999) was employed to express Cyt c_{6A} additionally. Two-hybrid protein interactions were evaluated by growing the yeast colonies at 28°C on media lacking either histidine or adenine and supplemented with different amounts of 3-amino-1,2,4-triazole (3-AT). Ternary-trap assays were evaluated on media containing 3-AT but lacking histidine. For the ternary-trap screen the pGADT7 vector containing the mature Cyt c_{6A} was combined with an expression cDNA library of *Arabidopsis thaliana* in pGBTKT7. The vector sequences of positive clones were blasted against the genome of *Arabidopsis thaliana* (NCBI BLASTN) and interaction has been

confirmed by performing a ternary-trap assay with either the coding sequence of the mature form either a distinct domain of the proteins in pGBTKT7.

Mutagenesis of Cyt c_{6A} and PsaF were performed via PCR site-directed mutagenesis using C6wtps, C6SERas, C6SERs, c6TAGas and PSAFADBDmut1bs, PSAFmut2bas, PSAFmut2bs, PSAFADBDas primer combinations, respectively. Primers for cloning are listed in appendix 1.

2.18. Split-Ubiquitin Assay

In the split-ubiquitin assay, NubG (N-terminal domain of ubiquitin with a mutation leading to an exchange of isoleucine at position 13 to glycine, preventing auto-reconstitution of the protein) and Cub (C-terminal domain of ubiquitin) are able to reconstitute ubiquitin only when brought into close proximity by two interacting test proteins that are expressed as fusion proteins with NubG and Cub. To test for interactions, Cyt c_{6A} was fused to the NubG by cloning the sequence of its mature form into the multiple cloning site of pADSL-Nx (Dualsystems Biotech) and putative interacting proteins were fused to the N terminus of Cub by cloning into pAMBV4 (Dualsystems Biotech). As negative control, the plasmid pAlg5-NubG, which encodes the endoplasmic reticulum membrane protein Alg5 fused to NubG (Alg5^{NubG}), was used for co-transformations. Because NubI (the wild-type Nub) and Cub spontaneously reassemble to reconstitute ubiquitin, Alg5 fused to NubI (Alg5^{NubI}) was used as positive control. The specificity of the pADSL-Nx constructs was confirmed by co-transformation with a control vector encoding Alg5 fused to Cub (Alg5^{Cub}). Yeast transformation was performed as described (Gietz and Woods, 2006). Yeast colonies were plated on *permissive medium* (synthetic medium lacking Leu and Trp; -LT; Clontech) and *selective medium* (synthetic medium lacking Leu,Trp and His; -LTH; Clontech). Primers for cloning are listed in table appendix 1.

2.19. Environmental Stress Induction

Four-week-old plants grown in the greenhouse were exposed to environmental stress conditions, like high light, dark, heat, drought and wounding, to check the *ATC6* expression. To induce light-depending-stress plants were shifted either to 2,500 mmol m^{-2} s^{-1}, for high

light conditions either into the dark for 3 hours. Heat stress was applied by exposing the plants to 45°C for 3 hours, while wounding-induced-stress was applied by cutting pieces of the rosette-leaves. Drought stress was induced by placing the plants into the air flow of a fan over night. After the different stress treatment, rosette-leaves were collected and immediately frozen in liquid nitrogen for RNA isolation (chapter 2.5.).

2.20. Antibody Production

The coding sequence of Cyt c_{6A} without its predicted cTP was cloned into the pET151-Topo vector (Invitrogen®) using MC6TOPOs and C6TAGas primers providing Cyt c_{6A} with an N-terminal His-Tag. This construct was used to transform the BL21 *E. coli* strain which is suitable for the overexpression of recombinant proteins. Overexpression of Cyt c_{6A} was induced adding 1 mM IPTG to the bacterial media and *E. coli* cells were harvested after 6 hours at 37°C. His-tagged Cyt c_{6A} protein was purified according to a Ni-NTA batch purification protocol under denaturing conditions (Qiagen®). The purified Cyt c_{6A} protein was injected into rabbits to generate polyclonal antibodies. To produce an antibody with higher specificity, in particular against the Cyt c_{6A} dimer, the protein sequence of the mature Cyt c_{6A} was cloned in a tandem repeat version using MC6TOPOs, Doubleas, Doubles and C6TAGas primer combinations. Expression, purification and injection of the protein were performed as described before.

2.21. Lumen Preparation

Thylakoids were isolated from 100 g leaf tissue as described before (chapter 2.10.) and chlorophyll concentration was determined. Membranes were diluted with *PPlysis buffer* (10 mM Na-Pyrophosphate pH 7.8) to a chlorophyll concentration of 0.2 mg/ml and centrifuged (5 min, 10,000 g, 4°C, JA 25.5 rotor, Beckmann®). Two washing steps with *PPlysis buffer* followed by other two with *fragmentation buffer* (30 mM Na-Phosphate pH 7.8, 100 mM sucrose, 50 mM NaCl, 5mM $MgCl_2$) were performed and the pellet was resuspended in fragmentation buffer to the final concentration of 3.5-4.5 mg/ml chlorophyll, with a total yield of 25-30 mg chlorophyll. Suspension was applied to a YEDA press and exposed twice to

an atmospheric pressure of 10 MPa. After centrifugation (200,000 g for 1 hour at 2°C SW40Ti, Beckmann®) the supernatant was recovered and centrifuged (200,000 g for 1 hour at 2°C SW40Ti, Beckmann®). The soluble fraction was concentrated using Centricons (Milipore®) and quantification was carried out according to Bradford (1976) using bovine serum albumin as standard.

2.22. Co-Immunoprecipitation

Isolated chloroplasts corresponding to 100 µg chlorophyll (chapter 2.10.) isolated from N-term RbcS-Cyt c_{6A}-GFP and wild type plants were resuspended in 120 µl *CoIP buffer* (50 mM Hepes pH 8, 330 mM Sorbitol, 150 mM NaCl, 1 mM PMSF), 30 µl 5% (w/v) digitonin were added and solubilization was carried out by rotating samples on a rotary shaker at 4°C for 1 hour. After centrifugation (10,000 g for 1 hour at 4°C) supernatant was recovered and diluted to 600 µl with *CoIP buffer*. Adding 20 µl of GFP specific antibody (Invitrogen®) samples were incubated 2 hours at 4°C by a rotary shaker. Afterwards the incubation step was repeated in presence of 100 µl Agarose-Protein A (Thermo Scientific®). Samples were washed 5 times with *CoIP buffer* containing digitonin as in the binding procedure. Proteins were recovered adding 100 µl SDS-loading dye and incubating for 10 min at 65°C. Agarose beads were spun down by centrifugation (10.000 g for 2 min at RT) and supernatant was loaded on a SDS-PAGE. Total gel lane containing the proteins was cut from the gel and sent to mass spectrometry analysis.

3. Results

3.1. Changed Cytochrome c_{6A} Expression in Transgenic Lines

To reveal the function of a protein, reverse genetic approaches are often successfully applied. The phenotype of plants lacking the protein of interest often can help to understand its function or gives an indication in which cellular processes the protein is involved. A knock-out mutant line of cytochrome c_{6A} was already mentioned in literature (Gupta 2002, Weigel 2003b), but its phenotype has never been described in detail.

In *Arabidopsis thaliana*, cytochrome c_{6A} is encoded by a single gene: At5g45040. From the start to the stop codon the sequence on the genomic DNA strand scales 1286 base pairs (bp) and six exons build the coding sequence (528 bp). The transgenic mutant line SALK_011266 in the Columbia-0 (Col-0) background was obtained from the SALK collection and will be referred as *atc6*. In this mutant, the gene sequence is interrupted in the first intron, 126 bp downstream of the start codon, by a T-DNA insertion of the vector pROK2 (Fig 3.1).
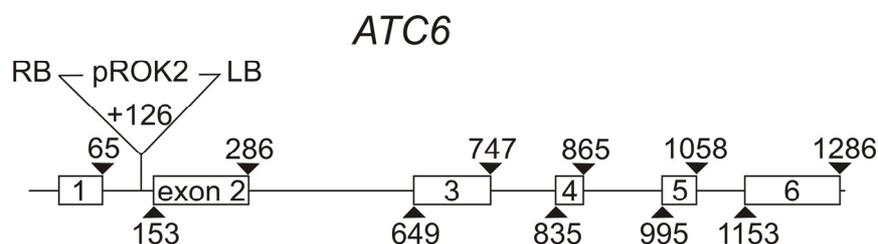
Figure 3.1: Tagging of the *ATC6* Gene Coding for Cytochrome c$_{6A}$. In *atc6* (SALK_011266), the *ATC6* gene is disrupted by an insertion of the pROK2 T-DNA in the first intron, 126 bp downstream the start codon (Pesaresi et al., 2009a).

The interruption of the gene prevents the accumulation of mRNA, thus resulting in a full knockout *Arabidopsis* line. The transcript level of *ATC6* was not detectable in atc6 by Real-Time PCR, confirming the complete suppression of the gene expression (Fig. 3.2).

To generate plants containing a higher amount of the desired protein, the complete coding sequence of cytochrome c_{6A} was cloned under the control of the constitutive 35S promoter of the Cauliflower Mosaic Virus and transferred, by *Agrobacterium* transformation, into the *atc6* line. The transcript level of *ATC6* in the lines Cyt c_{6A} OE#1 (in further experiments

designated as Cyt c_{6A} OE) and Cyt c_{6A} OE#2 showed an increased expression of *ATC6* of 64 and 23 times, respectively, compared to the wild type level (Fig. 3.2).

For a more sensitive detection of the protein, lines expressing cytochrome c_{6A} fused to tag-peptides were designed and their transcript level was determined. A fusion with the HA polypeptide should facilitate the detection of the desired protein with a commercially available HA-specific antibody via immunoblot analysis. The expression in the generated lines Cyt c_{6A} HA#1 and Cyt c_{6A} HA#2 was increased up to 20 and 30 times compared to wild type level. Furthermore, plants were transformed with a construct that fuses cytochrome c_{6A} to the green fluorescent protein (GFP) to enable detection via immunoblot analysis and fluorescence microscopy. Cyt c_{6A} GFP#1 and Cyt c_{6A} GFP#2 overexpressing lines accumulated Cyt c_{6A} mRNA around seven folds more than the wild type (Fig. 3.2).
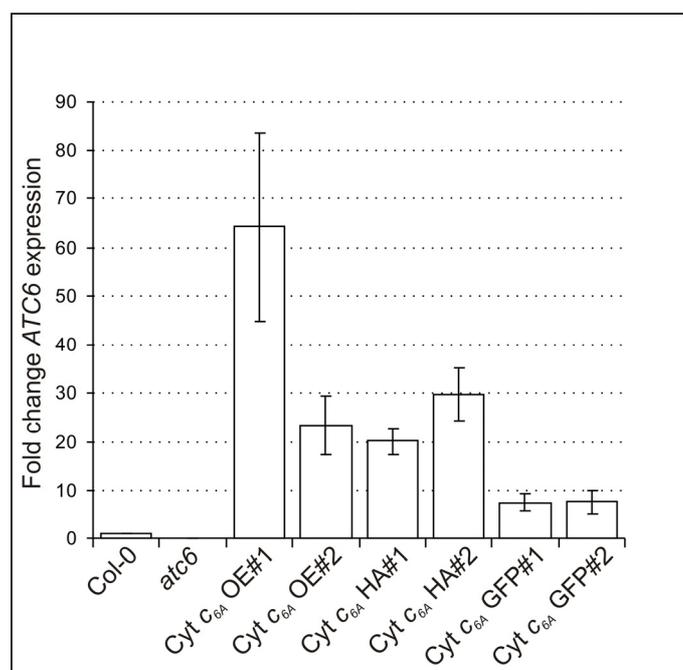
Figure 3.2: *ATC6* Expression Level in Transgenic Lines. Real-time PCR based analyses of *ATC6* transcript accumulation in transgenic lines carrying the following constructs: 35S CAMV::cds-*ATC6* (Cyt c_{6A} OE#1 and Cyt c_{6A} OE#2), 35SCAMV::cds-*ATC6*-HA (Cyt c_{6A} HA#1 and Cyt c_{6A} HA#2) and 35S CAMV::cds-*ATC6*-GFP (Cyt c_{6A} GFP#1 and Cyt c_{6A} GFP#2). Results were normalized using ubiquitin as internal standard.

Although the abundance of the cytochrome c_{6A} mRNA was strongly increased in all overexpressor lines, the cytochrome c_{6A} protein could never be reliably detected by

immunoblot analysis. A collection of antibodies raised against an epitope, the mature form and a double repeat version of cytochrome c_{6A} were tested on total leaf protein extract, chloroplast fraction (data not shown), thylakoid fraction and isolated lumen fraction. Fractions were checked with specific compartment-marker proteins, the LHCII subunit 2 (LhcB2) for thylakoid membranes and plastocyanin (PetE) for the thylakoid lumen (Fig. 3.3A,B).
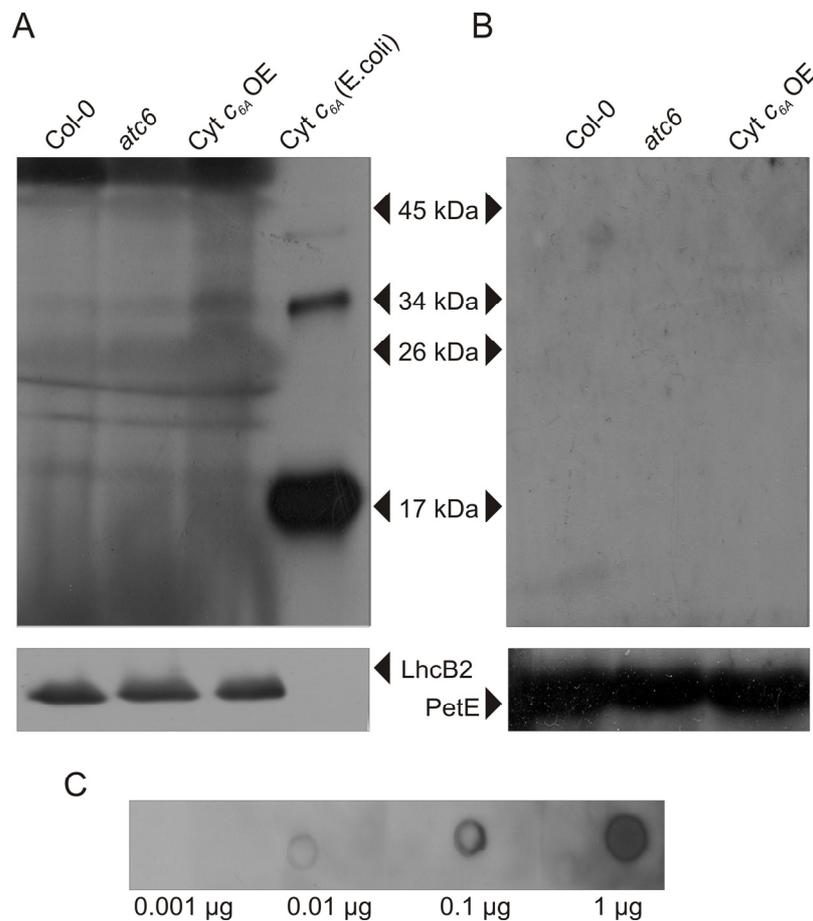
Figure 3.3: Cyt c_{6A} Protein Detection by Immunoblot. Tylakoids (A; 10 µg chlorophyll) and thylakoid lumen (B; 36 µg proteins) were extracted and loaded on SDS-PAGE for immuno blot analyses. LhcB2 and PetE detection was used as control. The specificity and sensitivity of the Cyt c6A antibody was analyzed by loading the recombinant protein expressed in *E. coli* (A) on a SDS-PAGE and by a dot blot analysis, respectively (C).

The cytochrome c_{6A}-antibody recognized the recombinant cytochrome c_{6A} expressed in *E. coli*, when the protein amount loaded on the gel was less than 0.01 µg (Fig. 3.3C) indicating that neither the immune-blot procedure nor the quality of the antibody prevents the detection of the polypeptide. Gupta et al. 2002 described changed electrophoretic mobility

of the protein in leaf extract and suggested a post-translational processed form of cytochrome c_{6A}. In case of the *ATC6* processed form, it is possible, that the antibody is not capable to recognize the changed protein version and the detection fails. Nevertheless, this would not explain the absence of a signal in the overexpressor lines, where the protein is fused to an HA or GFP polypeptide. Although the fused protein should not be influenced by post-translational modification, it could not been detected, neither via immuno blot with antibodies against GFP and HA nor via fluorescence microscopy of the GFP lines (data not shown).

It is more likely that the protein is present in a very low, not detectable concentration in the cell and post-transcriptional mechanisms prevent its over-accumulation independently of the transcript level. This might also explain why all published proteomics approaches fail to detect cytochrome c_{6A} (chapter 1.6.), so far.

In summary, a line without the capability to express cytochrome c_{6A} could be confirmed, whereas any trial to obtain a line overexpressing the protein failed.

Due to the fact that the accumulation of cytochrome c_{6A} in overexpressor lines could not been obtained, the transgenic lines were not considered for the most of the experiments.

3.2. Phenotypic Characterization of *atc6* Mutant Line

The modification of the expression level of genes involved in photosynthesis often determines a visible change of the plant phenotype, such as reduced growth or altered leaf pigment composition. A complete knock-out of key-players in photosynthesis usually leads to a loss of autotrophic growth, whereas a down regulation of these genes or the knocking-out of non-essential proteins normally results in a milder phenotype. Due to their impaired photosynthetic performance, mutant plants affected in the concentration of plastocyanin (*pete2*) or the PSI subunits D (*psad*) and E (*psae*), are smaller and pale green compared to wild type plants (Ihnatowicz *et al.*, 2004; Ihnatowicz *et al.*, 2007; Pesaresi *et al.*, 2009a).

After four weeks, plants of the lines *atc6* and Cyt c_{6A} OE were compared to wild type (Col-0 ecotype). No significant difference between transgenic plants lacking or overexpressing cytochrome c_{6A} and the wild type could be observed (Fig. 3.4). The only phenotypical

changes related to cytochrome c_{6A} were shown by the transgenic line N-term RbcS-Cyt c_{6A}-GFP that is presented and discussed in chapter 3.6.2.
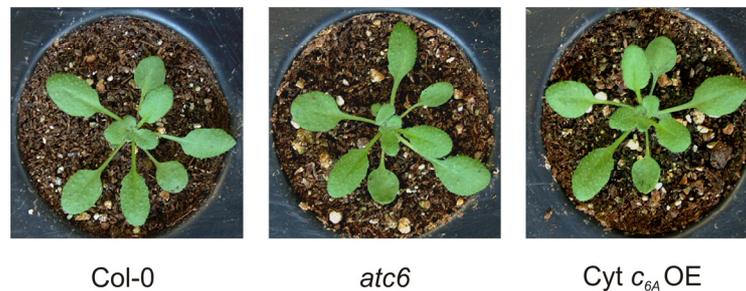
Col-0   *atc6*   Cyt c_{6A} OE

Figure 3.4: Phenotype of Col-0, Mutant *atc6* and Overexpressor Plants at 8 leaf rosette stage. Four-week-old plants of Col-0, *atc6* and Overexpressor Cyt c_{6A} OE propagated in greenhouse are shown.

To survey growth performances, a growth curve of five-week old *atc6* plants was generated by measuring the leaf area every seven days (Fig. 3.5). Similar leaf size of wild type and mutant plants indicates that the growth is neither inhibited nor promoted by cytochrome c_{6A}.
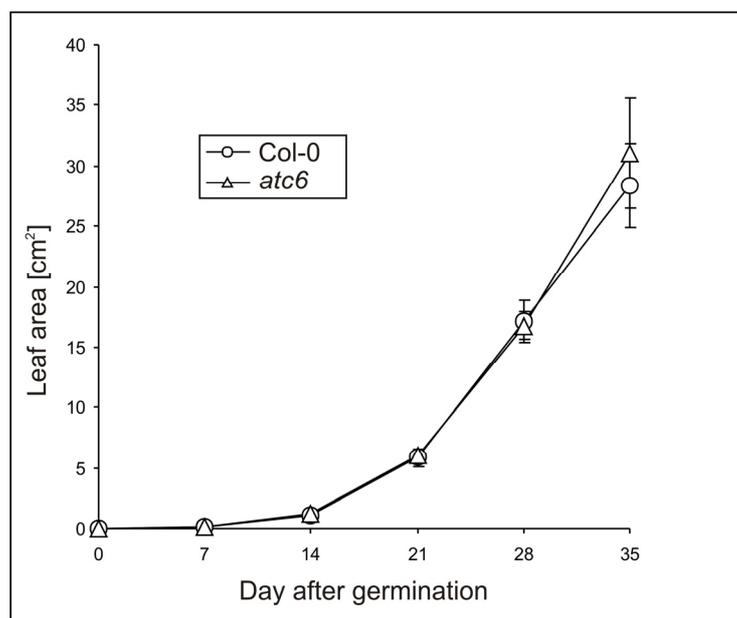
Figure 3.5: Growth Kinetics of Wild Type (Col-0) and Mutant (*atc6*) plants. Leaf area of Col-0 and *atc6* was measured during a period of 35 days growth under greenhouse conditions. At least 10 plants per genotype were analyzed.

Elongation of the hypocotyl at the early stage of plant development is mainly a process of cell expansion, which is regulated by photoreceptors (mainly phytochromes and cryptochromes) and hormones such as gibberellins, brassinosteroids and auxins (Bolle, 2009). Hypocotyl length of wild type and *atc6* plants grown in dark and light conditions was measured. Both genotypes showed the same hypocotyl growth performance disclaiming impact on the process of cell elongation (Fig. 3.6).
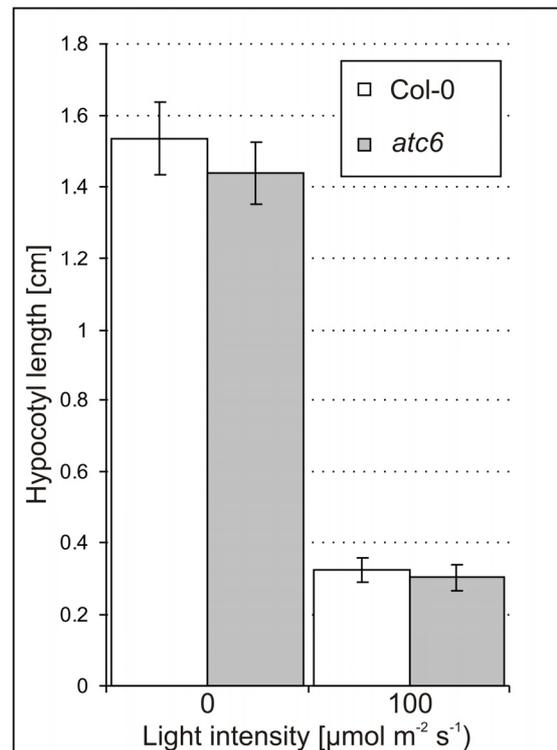
Figure 3.6: Hypocotyl Length of Wild Type (Col-0) and Mutant (*atc6*) Plants. The hypocotyl length of Col-0 and *atc6* plants grown on MS media in the dark and at a light intensity of 100 µmol photons m^{-2} s^{-1} was analyzed. At least 30 plants per genotype and condition were measured.

Testing the germination efficiency of *atc6*, seeds were sown out on MS plates containing different concentrations of ABA to apply hormonal pressure on the germination processes. Without ABA application the cotyledons of all wild type, *atc6* and *abi1* (ABA insensitive 1, affected in ABA perception) plants were visible after 36 hours, but only one third of the *aba1* mutant (that is affected in ABA synthesis). During germination on 0.5 µM ABA, around 90% of wildtype and *atc6* seeds broke dormancy, but the cotyledons were still inside the teguments after 36 hours, indicating a delay of development. Dormancy in *abi1* and *atc6*

was broken in similar level to the wild type, but cotyledons were not exposed. The impact of ABA was even more evident in the *aba1*mutant, where more than 50% of the seeds did not germinate. Application of 1 µM ABA increased the observed effect of germination delay (Fig. 3.7). These data show that *atc6* seeds germinated slightly better than wild type seeds, in the presence of 1 µM ABA. The mutant *abi1* showed only minor changes in comparison to the wild type, possibly due to functional redundancy of the ABI1 and ABI2 proteins. Germination of *aba1* was totally impaired by the lack of an important enzyme in the ABA synthesis pathway.
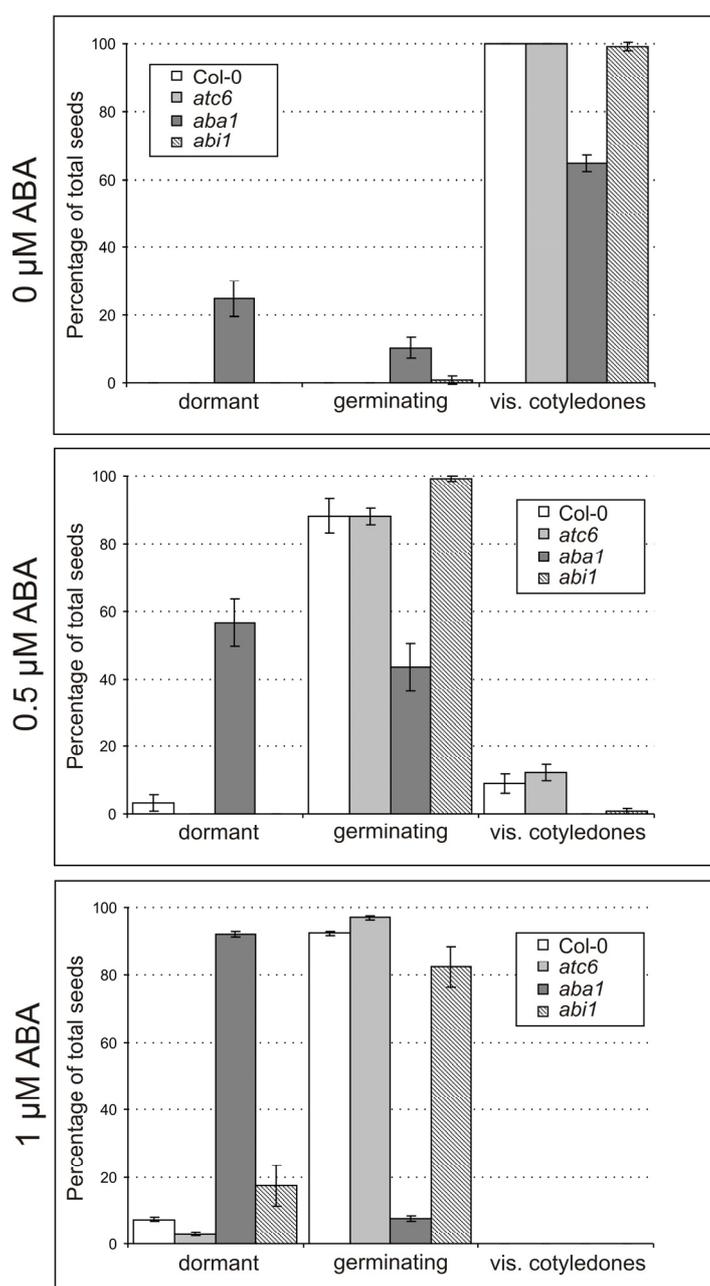
Figure 3.7: Abscisic Acid Dependent Seed Germination of *atc6*. More than 200 seeds per genotype were sown out on plates containing different concentration of abscisic acid (ABA). After 36 hours seeds were classified in three groups: dormant seeds, germinating seeds with broken peel and germinated with visible cotyledones.

Considering 4-week old plants (Fig. 3.4), there seems to be no major change in pigment composition between the genotypes. Pigments were extracted from *atc6* and wild type plants and analyzed by high-performance liquid chromatography (HPLC). Carotenoids are important protective components during excessive light and for the formation of NPQ. The overall concentration of carotenoids and of single pigments like neoxanthin (a precursor of abscisic acid), lutein and the VAZ pool are indicators of insufficient energy processing by the photosystems. More, an increased conversion of violaxanthin to zeaxanthin is required for an effective NPQ formation (chapter 1.2.). The concentration of chlorophylls and the ratio between chlorophyll a and chlorophyll b, give indications about the stoichiometry between photosystems and light harvesting complexes. In the *atc6* mutant, neither carotenoid nor chlorophyll concentrations differ from the wild type level suggesting a similar energy processing and NPQ formation in both genotypes (Fig. 3.8).
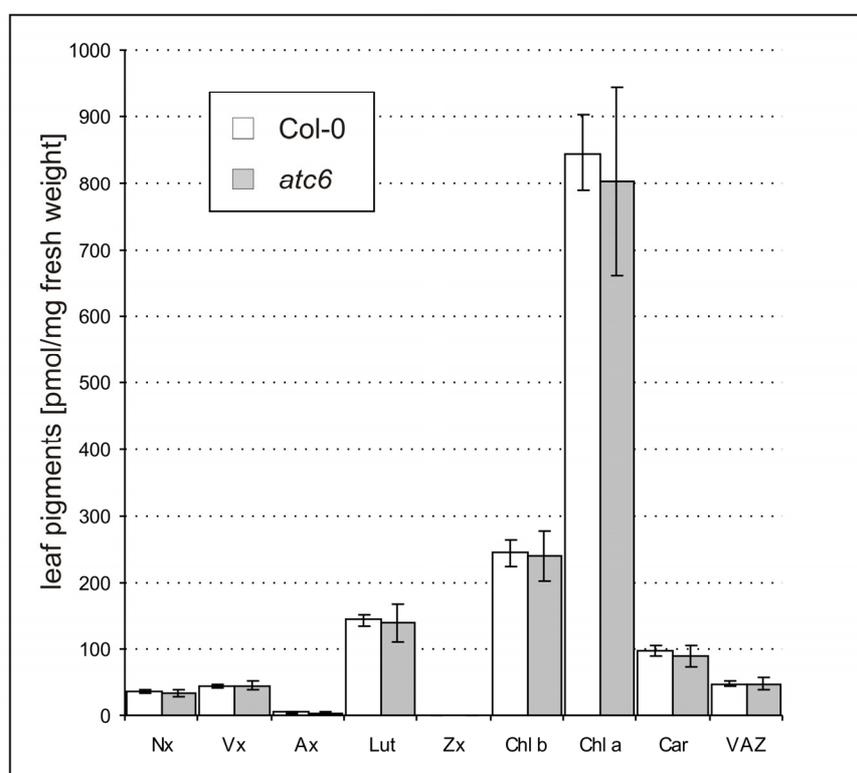
Figure 3.8: Leaf Pigment Composition in *atc6* Compared to Col-0. Pigment composition of four-week old mutant, *atc6*, and wild type, Col-0, plants was investigated by HPLC analysis. Pigment amount was normalized on leaf weight. Nx, neoxanthin; Vx, violaxanthin; Ax, antheraxanthin; Lut, lutein; Zx, zeaxanthin; Chl b, chlorophyll b; Chl a, chlorophyll a; Car, carotenoide; VAZ, Vx+Ax+Zx).

Plants lacking cytochrome c_{6A} do not show any major difference to the wild type according to the visible phenotype, growth, pigmentation and germination.

3.3 Photosynthesis without Cytochrome c_{6A}

3.3.1. Dissection of Photosynthetic Complexes in *atc6*

Energy processing of photosynthesis requires a functional electron transport chain through thylakoid membrane complexes (chapter 1.1.). Major changes in the mutant *atc6* in photosynthetic performances can be excluded by the former previously described observations regarding the phenotype. To reveal minor changes in photosynthetic performances, a more detailed analysis was carried out.

With a value of 3.33 ± 0.09 in *atc6* the chlorophyll a to chlorophyll b ratio is not significantly different from the wild type (3.47 ± 0.08) indicating a similar stoichiometry between PSI and PSII (Fig. 3.8).
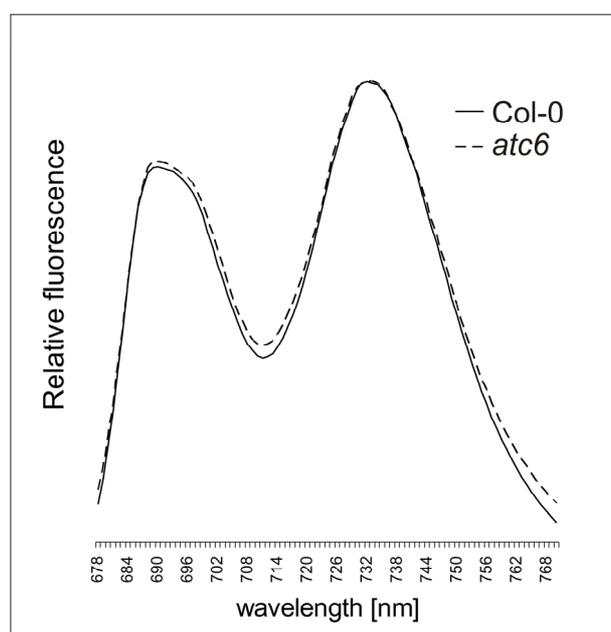
Figure 3.9: 77 K Fluorescence Emission Spectra of Col-0 and *atc6*. The 77 K fluorescence emission spectra of light adapted Col-0 and *atc6* plants were recorded. The spectra were normalized at 685 nm.

To analyze the surface of the light harvesting antenna of the photosystems, fluorescence spectra of thylakoids at 77 K were applied. The first peak around 690 nm represented the antenna complexes of PSII, whereas the second peak around 735 nm represented the PSI antenna complexes. The ratio of light harvesting between the two photosystems in *atc6* compared to the wild type is not imbalanced (Fig. 3.9). Considering the results of the pigment composition (Fig. 3.8) and the 77 K fluorescence, a different composition of the light harvesting apparatus in the mutant *atc6* can be excluded.

Photosynthetic machinery of higher plants contains four major complexes, PSII, Cyt b_6/f, PSI and ATPase, that build even larger super complexes *in vivo*. Blue Native PAGE (BN-PAGE) analysis of thylakoid membranes allows a fine separation of protein complexes, maintaining their structure. To solubilize the membranes, β-DM or digitonin are commonly used for nice separation of PSII or PSI complexes, respectively. No difference between *atc6* and the wild type complex or super complex formation could be observed in the first dimension BN-PAGE (Fig. 3.10).
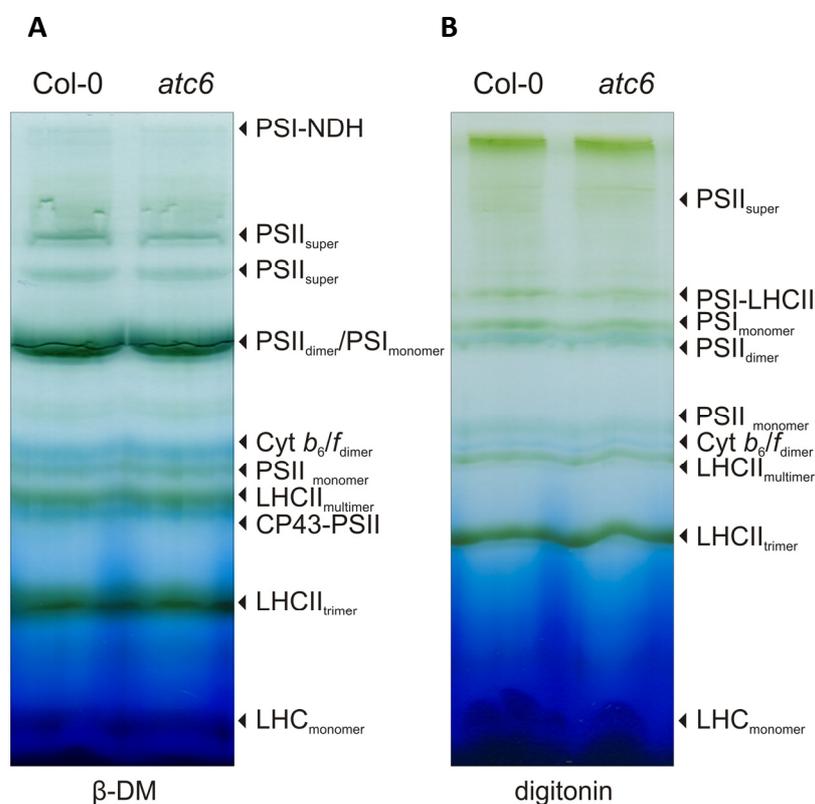
Figure 3.10: BN-PAGE Analysis of Thylakoid Multiprotein Complexes. Thylakoids were isolated from equal amounts of fresh leaf material (~100 mg), normalized on chlorophyll amounts (30 µg) and solubilized with 1.5% (w/v) β-DM (A) or 1.5% (w/v) digitonin (B). Extracts were fractionated by BN-PAGE. Bands identify specific protein complexes in accordance with previously published profiles (Granvogl *et al.*, 2006; Peng *et al.*, 2006; Schwenkert *et al.*, 2006).

To analyze the complex composition, the subunits were fractionated by denaturing second dimension conditions (2D SDS-PAGE). However, both genotypes showed the same pattern of protein composition (Fig. 3.11). Considering these results, presence or absence of cytochrome c_{6A} does not affect the assembly, amount and composition of photosynthetic complexes and super complexes.
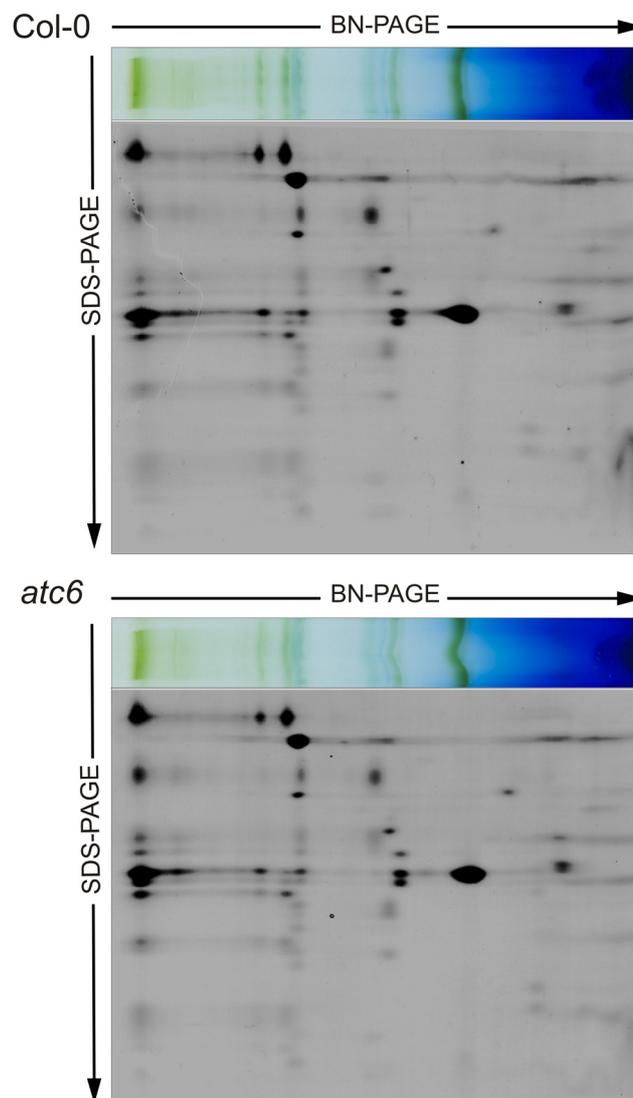
Figure 3.11: 2D BN/SDS-PAGE Separation of Thylakoid Protein Complexes. Individual lanes from BN-PAGE gels as in figure 3.10 were analyzed in presence of SDS by electrophoresis on 10 to 16% PA gradient gels, stained with colloidal Coomassie blue (G 250). Arrows indicate the PAGE migration.

The original cytochrome c_{6A}, which is present in cyanobacteria and green algae, transfers electrons from the cytochrome b_6f complex to PSI. The redox potential of cytochrome c_{6A} is anyway too low to permit the uptake of electrons from the cytochrome b_6f complex, but electron transfer to PSI could still be possible (chapter 1.8.).

Gene expression data were obtained from microarray studies (chapter 2.6.) to determine the mRNA accumulation of PSI subunits (Fig. 3.12A). The difference of expression levels of most of the PSI subunits is less than 0.2 fold and appeared to be very similar between *atc6* and wild type plants. psaA and psaB are slightly down-regulated and psaC looks slightly upregulated though this increment is not significant ($0.5 \geq FC \geq 2$).

PSI was isolated from leaf tissue and separated by SDS-PAGE analysis. Neither the pattern nor the concentration of the PSI subunits was changed between the genotypes (Fig. 3.12B).
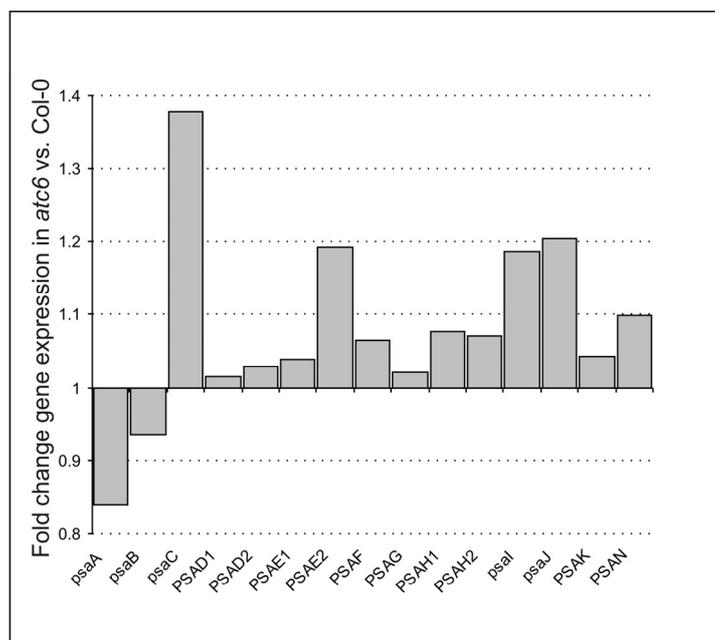
A   **B**
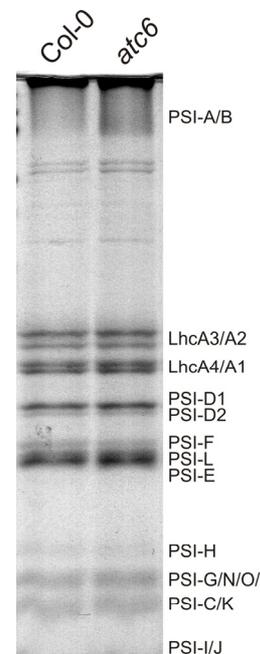
Figure 3.12: Composition of Photosystem I in *atc6*. The fold change expression levels of genes encoding for PSI subunits in the mutant *atc6* were normalized on the wild type (set as 1). (A) Data derived from microarray

studies. (B) Polypeptide Composition of PSI complexes isolated from 4-week-old Col-0 and *atc6* leaves were analyzed by 16-25% SDS-PAGE.

A more detailed view was obtained by performing immuno blot analysis with specific antibodies against different subunits of PSI and representative members of the photosynthetic machinery, such as plastocyanin and subunits of Cyt b_6/f, PSII, ATPase, LHCII and Rubisco (Fig. 3.13). Modification of the protein concentration in *atc6* samples did not occur, confirming the results of PSI isolation and BN-PAGE analysis.
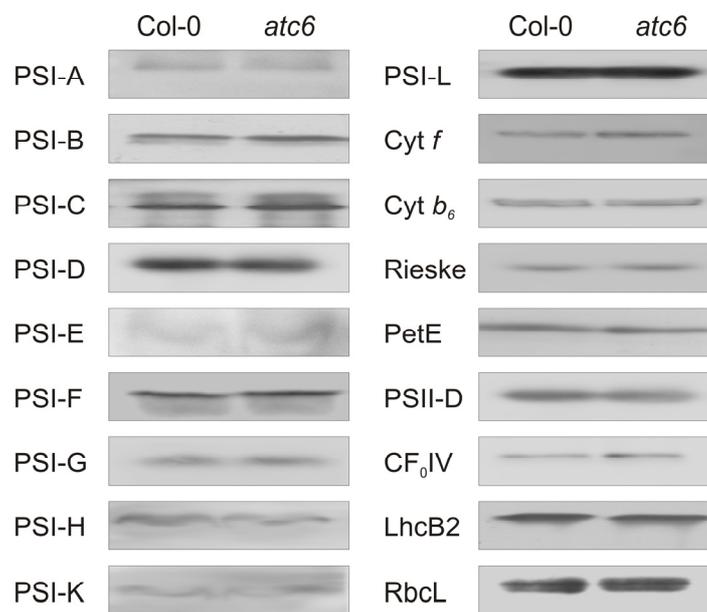
Figure 3.13: Protein Composition of Chloroplast Proteins in Col-0 and *atc6*. Chloroplast proteins normalized by chlorophyll content (10 µg) of 4 week old Col-0 and *atc6* plants, were fractionated by SDS-PAGE, blotted on nylon filters and probed with specific the antibodies indicated on the left.

Summarizing, the absence of cytochrome c_{6A} does not affect concentration, composition, arrangement and stoichiometry of subunits of LHC and photosystems. Therefore, a major role of cytochrome c_{6A} in photosynthetic processes can be excluded.

3.3.2. Photosynthetic Electron Flow in *atc6*

Beside analysis of the electron transport chain components, the performance of the light reaction can be visualized by fluorescence and absorption measurements using the so-called

pulse amplitude modulation (PAM) technique. The fluorescence of open PSII reaction centers detected by the PAM fluorometer provides information regarding the distribution of photosynthetic energy between photochemical and non-photochemical quenching. Light energy, collected by the antenna of both photosystems, is utilized by processes of photochemical quenching that drive the photosynthetic electron transport chain. In excess light conditions, the capacity of the electron transport chain is not sufficient to quench the high amount of incoming energy and processes of non-photochemical quenching are therefore activated. (Eberhard *et al.*, 2008).

The energy processing ability of *atc6* mutant was analyzed and compared to the wild type performance. F_V/F_M describes the PSII maximum efficiency, Φ_{II} specifies the effective yield of PSII and (1-qP) is related to the photochemical quenching. The non-photochemical quenching, NPQ, is divided into heat dissipation (qE), state stransitions (qT) and photoinhibition (qI).

The values of F_V/F_M and Φ_{II} in *atc6* was comparable to wild type plants indicating a similar fraction of open PSII reaction centers after dark and light adaption. Photochemical (1-qP) and non-photochemical energy distributions were not changed, as well as heat dissipation and photoinhibition (Tab. 3.1).

Absorption measurements were applied to visualize the reactivity of PSI. The activity, P_m,P_m', the yield, Φ_I, and the limitation of the acceptor, Y(NA), and donor, Y(ND), sides were determined, revealing no anomalies in the mutant (Tab3.1).

Parameter	Fv/Fm	Φ_{II}	1-qP	NPQ	qE	qI
Col-0	0.835 ± 0.001	0.773 ± 0.003	0.045 ± 0.002	0.19 ± 0.02	0.07 ± 0.01	0.12 ± 0.02
atc6	0.837 ± 0.002	0.774 ± 0.002	0.047 ± 0.006	0.19 ± 0.02	0.08 ± 0.01	0.11 ± 0.02

Parameter	Pm, Pm'	Φ_I	Y(ND)	Y(NA)
Col-0	0.085 ± 0.004	0.81 ± 0.02	0.049 ± 0.007	0.14 ± 0.02
atc6	0.091 ± 0.003	0.84 ± 0.03	0.049 ± 0.020	0.11 ± 0.01

Table 3.1: Photosynthetic Performance of Photosystem II and Photosystem I. Parameters of the chlorophyll a fluorescence (F_V/F_M, maximum quantum yield of PSII; Φ_{II}, effective quantum yield of PSII; 1-qP, excitation pressure; NPQ, non-photochemical quenching; qE, heat dissipation; qI, photoinhibition) and parameters of the P700 absorption (P_m,P_m', maximum PSI reduction; Φ_I, effective quantum yield; Y(ND), donor side limitation;

Y(NA) acceptor side limitation) were measured by pulse amplitude modulation (PAM) at 72 μmol photons m^{-2} s^{-1} actinic light. At least five leaves of five independent four-week-old plants each genotype were measured.

Due to balancing and rescue mechanisms the photosynthetic machinery is a flexible system, by which changes of components often remain hidden and do not lead to visible effects. A form of photosynthetic stress was applied to the system to remove a part of the flexibility and to elicit a phenotype in the mutant's performance. Therefore, *atc6* was crossed with *pete1*, *pete2*, *psad*, *psae* and *psaf* mutants that are known to have a reduced expression of crucial photosynthetic genes. *pete1*, *pete2*, *psad* and *psae* are well described (Ihnatowicz *et al.*, 2004; Ihnatowicz *et al.*, 2007; Pesaresi *et al.*, 2009a), whereas the mutant *psaf*, which carries a stable T-DNA insertion in the promoter region of PSI-F (Fig. 3.14), has not been described yet.

Figure 3.14: Tagging of the *PSAF* Gene Coding for PSI-F. In *psaf* (SAIL_351_H11), the *PSAF* gene is disrupted by an insertion of the pCSA110 T-DNA in the 5'UTR region, at 77 bp upstream the start codon.

Plants of this line remain small and pale green, but viable on soil (Fig. 3.16). The insertion leads to a decrease of the *PSAF* transcript level in the single mutant *psaf* down to 10% compared to wild type level that is not influenced by the presence of cytochrome c_{6A} (Fig. 3.15A). Plants without PSI-F are not viable (Haldrup *et al.*, 2000) proving the presence of the protein in the mutant. Nevertheless, the protein concentration is strongly reduced and remained not-detectable by immuno blot analysis (Fig. 3.15B).

Comparison of the created double mutants with the corresponding single mutants showed that the lack of both proteins do not give additional phenotypes (Fig. 3.16).

A   **B**
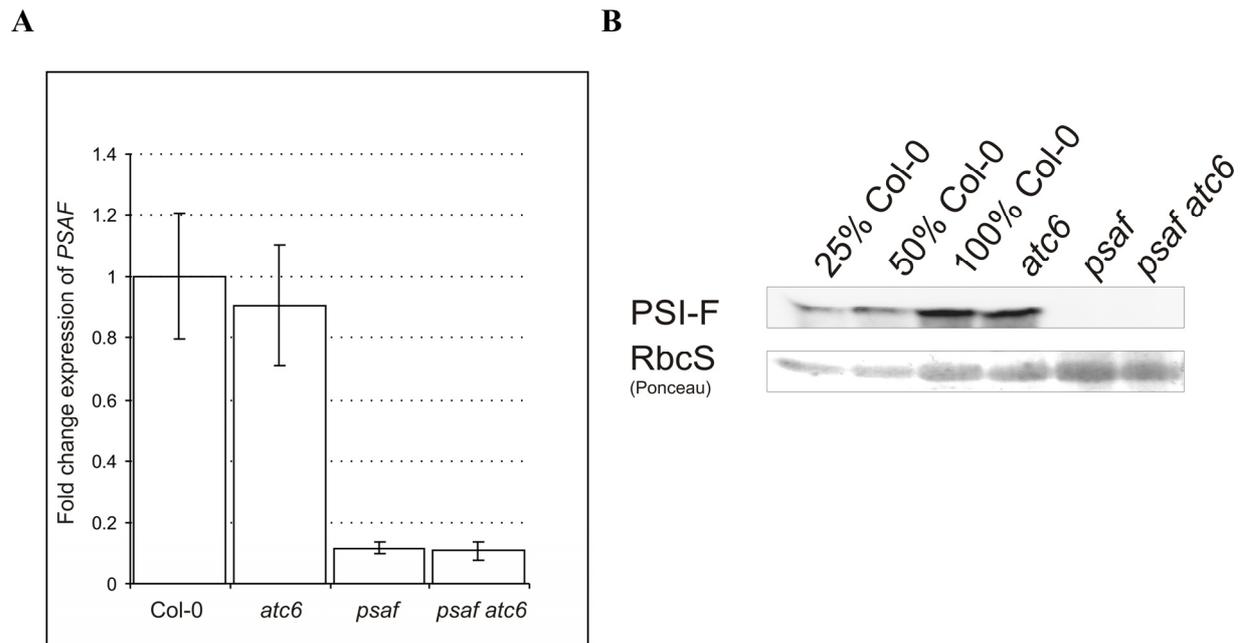
Figure 3.15: PSI-F Expression in Wild Type (Col-0) and Mutant (*atc6*, *psaf*, *psaf atc6*) Plants. (A) The mRNA expression level of the gene *PSAF* in wild type (Col-0) and mutant (*atc6, psaf, psaf atc6*) plants was measured by real time PCR. Results were normalized by the expression of ubiquitin. (B) Chloroplast fractions of 6 week old wild type and mutant plants were normalized by the amount of chlorophyll (5 µg) and separated by SDS-PAGE. Filters were probed with a PSI-F specific antibody. For loading control the Ponceau staining of the small subunit of Rubisco is shown.

Changes of photosynthetic electron flow in the mutants were analyzed by PAM measurements as described before, but under different light condition. Low (22 µmol m^{-2} s^{-1}), growth (95 µmol m^{-2} s^{-1}) and high (1028 µmol m^{-2} s^{-1}) light conditions were applied and photosynthetic parameters determined. Defects in electron flow of mutants with reduced plastocyanin levels, *pete1* and *pete2*, were not enhanced by the absence of cytochrome c_{6A}, supporting the loss of the function typical of the ancient cytochrome c_6 (Tab. 3.2).
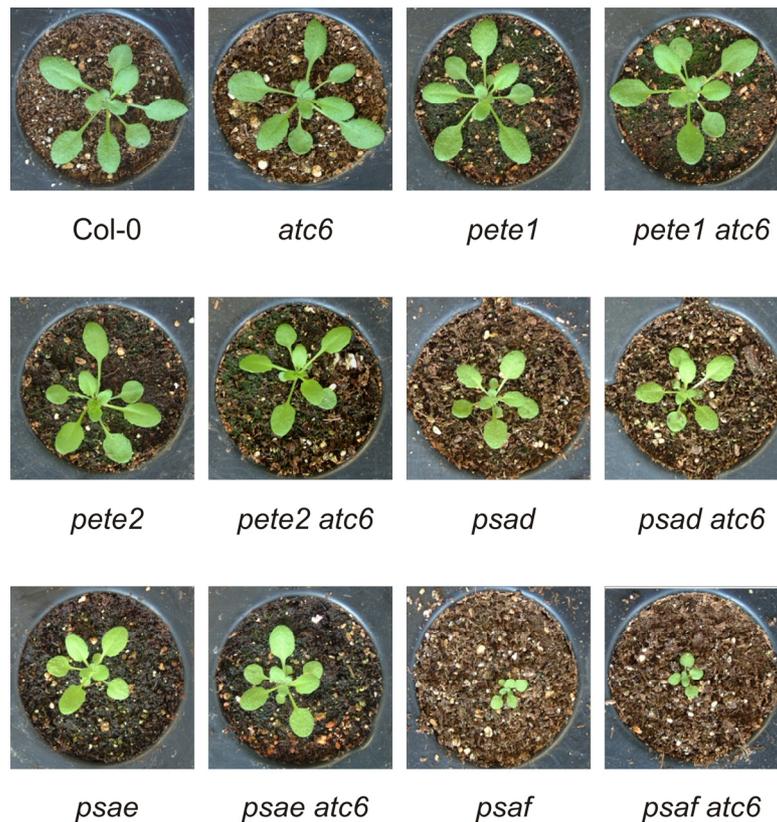
Figure 3.16: Phenotypes of Double Mutants with Defects in Linear Electron Flow. Double mutants between *atc6* and established mutants with defects in the linear electron flow (*pete1*, *pete2*, *psad*, *psae* and *psaf*) are compared to their corresponding single mutants. Four-week-old plants grown in greenhouse are shown.

Additionally, this observation contradicts the functional redundancy of plastocyanin and cytochrome c_{6A} as a lumen redox regulator, suggested by the Schlarb-Ridley hypothesis. Performance of *psad1-1* and *psae1-3*, which are affected in PSI, were also not changed by cytochrome c_{6A}. A significant difference could be observed in the NPQ value of the *psaf atc6* double mutant under low and growth light conditions. In several independent experiments NPQ formation was decreased to 30% of the *psaf* level, but in some cases it appeared without changes to the single mutant. It is possible that an environmental factor, which could not be isolated, supports the different NPQ formation in the plants. However, it is more likely that the difference is due to the individual fitness of the small, fragile plants during the experimental procedure (Tab. 3.2).

Actinic light	0 µE	22 µE			95 µE			1028 µE		
Parameter	Fv/Fm	ΦII	1-qP	NPQ	ΦII	1-qP	NPQ	ΦII	1-qP	NPQ
Col-0	0.818 ± 0.003	0.806 ± 0.001	0.030 ± 0.008	0.15 ± 0.01	0.753 ± 0.005	0.089 ± 0.012	0.18 ± 0.01	0.148 ± 0.031	0.762 ± 0.049	2.44 ± 0.14
atc6	0.818 ± 0.001	0.807 ± 0.004	0.036 ± 0.006	0.14 ± 0.06	0.755 ± 0.007	0.093 ± 0.008	0.18 ± 0.06	0.161 ± 0.021	0.745 ± 0.029	2.43 ± 0.11
pete2	0.825 ± 0.003	0.814 ± 0.008	0.036 ± 0.005	0.13 ± 0.04	0.726 ± 0.016	0.127 ± 0.019	0.22 ± 0.03	0.119 ± 0.032	0.826 ± 0.039	1.85 ± 0.37
pete2 atc6	0.822 ± 0.008	0.811 ± 0.003	0.032 ± 0.008	0.09 ± 0.04	0.742 ± 0.020	0.112 ± 0.020	0.19 ± 0.02	0.137 ± 0.018	0.800 ± 0.020	1.81 ± 0.08
psad	0.782 ± 0.017	0.469 ± 0.014	0.431 ± 0.009	0.12 ± 0.02	0.394 ± 0.016	0.502 ± 0.014	0.38 ± 0.06	0.095 ± 0.031	0.833 ± 0.053	3.10 ± 0.60
psad atc6	0.800 ± 0.010	0.491 ± 0.009	0.411 ± 0.010	0.12 ± 0.01	0.400 ± 0.011	0.494 ± 0.014	0.47 ± 0.05	0.106 ± 0.008	0.816 ± 0.015	3.07 ± 0.05
psae	0.802 ± 0.008	0.471 ± 0.048	0.436 ± 0.059	0.09 ± 0.02	0.386 ± 0.043	0.533 ± 0.052	0.17 ± 0.02	0.113 ± 0.021	0.807 ± 0.037	2.98 ± 0.34
psae atc6	0.824 ± 0.007	0.537 ± 0.038	0.372 ± 0.047	0.08 ± 0.03	0.437 ± 0.029	0.484 ± 0.035	0.14 ± 0.02	0.146 ± 0.009	0.758 ± 0.015	3.18 ± 0.05
psaf	0.728 ± 0.009	0.391 ± 0.025	0.459 ± 0.043	0.46 ± 0.05	0.287 ± 0.024	0.572 ± 0.045	0.87 ± 0.17	0.081 ± 0.014	0.843 ± 0.031	2.56 ± 0.09
psaf atc6	0.733 ± 0.010	0.399 ± 0.052	0.490 ± 0.060	0.15 ± 0.05	0.335 ± 0.039	0.561 ± 0.051	0.28 ± 0.04	0.094 ± 0.038	0.822 ± 0.065	2.73 ± 0.19

Table 3.2: Performance of Photosynthesis Affected Mutants Lacking Cytochrome *c₆ₐ*. Parameters of the chlorophyll a fluorescence (F_v/F_m, maximum quantum yield of PSII; Φ_{II}, effective quantum yield of PSII; 1-qP, excitation pressure; NPQ, non-photochemical quenching) are measured by pulse amplitude modulation (PAM) at the indicated actinic light. At least five leaves of five independent four-week-old plants each genotype were measured.

3.4. Dissecting Putative Cytochrome *c₆ₐ* Functions

3.4.1. Transcriptomic Analysis of *atc6*

Transcriptomic dissection by microarrays is a powerful tool providing an overview of processes that are changed in certain conditions. Using Affymetrix chip analysis, the transcription level of more than 22,000 genes was compared among wild type, *atc6* and Cyt *c₆ₐ* OE plants. It has to be taken into account that Cyt *c₆ₐ* OE were created in *atc6* background and that the accumulation of cytochrome *c₆ₐ* protein could not be verified (chapter 3.1.).

Changes in transcript expression level between the genotypes were visualized in scatter blots (Fig. 3.17). The yellow line is consistent with identity between mRNA levels in two conditions and the blue lines describe the fold change threshold for significant changes. The pattern displayed in the scatter blots is very similar between the genotypes and remained mainly between the fold change thresholds. This implies no major changes in the transcription profile between Col-0 and *atc6*, between Col-0 and Cyt *c₆ₐ* OE and between *atc6* and Cyt *c₆ₐ* OE (Fig. 3.17A,B,C). Nevertheless, the transcriptomic analysis was

summarized in a Venn diagram to display the number of single genes with significant different expression (Fig. 3.17D).

A

B

C

D
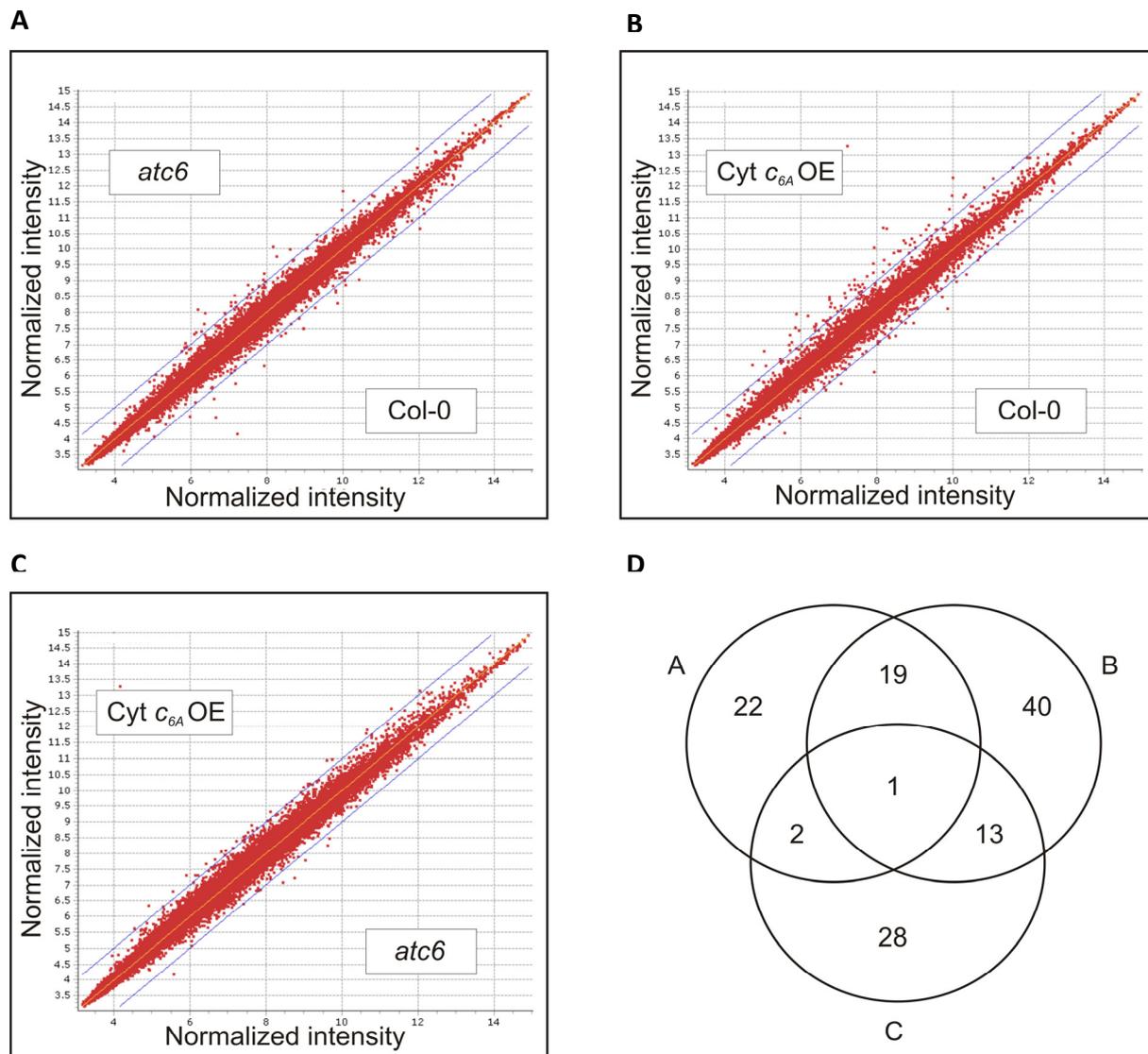
Figure 3.17: Detection of Changes in Transcript Level by Using Affymetrix Chip Analysis. RNA of four-week-old plants grown in greenhouse has been hybridized to Affymetrix chips including probes for more than 22,000 genes of the Arabidopsis genome. The expression data of the three genotypes were compared to each other in the scatter plots A (Col-0 vs. *atc6*), B (Col-0 vs. Cyt c_{6A} OE) and C (*atc6* vs. Cyt c_{6A} OE).The thresholds of significance (a fold change of more than 2 and less then 0.5) are indicated by the blue lines. Among the 22,000 genes the different regulated genes are summarized in a Venn diagram (D). The data in the scatter plots were derived as average expression values from at least two independent replicates.

ATC6 was the only gene showing different expression in all genotypes: in *atc6* it was not detectable, whereas in Cyt *c6A* OE it was expressed more than 65 times higher than the wild type level. Two genes showed a different expression between mutant and wild type and between mutant and overexpressing plants: the cell division cycle protein CDC48 and the BCL-2-associated athanogene BAG6, the best candidates as significantly changed in absence of cytochrome *c6A*.

AGI Code	Description	FC	P-value
AT5G61590	ERF/AP2 transcription factor family protein	3.75	0.0000000
AT1G65390	Disease resistance protein (ATPP2)	3.71	0.0000001
AT4G21870	26.5 kDa class P-related heat shock protein (HSP26)	3.55	0.0000363
AT3G45970	Expansin family protein (EXPL1)	3.00	0.0000000
AT2G41990	Unknown protein	2.59	0.0000173
AT4G34950	Nodulin-like protein (#2)	2.57	0.0000014
AT3G23550	MATE efflux family protein	2.53	0.0001542
AT5G20250	Raffinose synthase family protein (DIN10)	2.47	0.0002683
AT3G59350	Serine/threonine protein kinase	2.42	0.0002984
AT3G01290	Band 7 family protein	2.38	0.0185126
AT5G05440	Unknown protein	2.36	0.0000094
AT1G08930	Sugar transporter (ERD6)	2.35	0.0004089
AT1G74890	Two-component responsive regulator (ARR15)	2.35	0.0004568
AT3G06070	Unknown protein	2.34	0.0042888
AT2G06850	Xyloglucosyl transferase (EXGTA1)	2.33	0.0009508
AT2G25735	Unknown protein	2.28	0.0001774
AT5G51550	Phosphate-responsive 1 family protein (EXL3)	2.21	0.0003968
AT3G30775	Proline oxidase (ERD5)	2.21	0.0042888
AT1G57980	Purine permease-related protein	2.21	0.0016606
AT4G37540	LOB domain protein 39 (LBD39)	2.18	0.0001330
AT5G62920	Two-component responsive regulator (ARR6)	2.13	0.0003322
AT5G12050	Unknown protein	2.13	0.0001437
AT5G28630	Glycine-rich protein	2.13	0.0018271
AT1G06360	Fatty acid desaturase family protein	2.09	0.0036315
AT1G74670	Gibberellin-responsive protein	2.08	0.0063099
AT2G16660	Nodulin family protein (#1)	2.07	0.0495121
AT1G52200	Unknown protein	2.05	0.0031401
AT1G69760	Unknown protein	2.02	0.0008638
AT3G30720	Unknown protein	0.49	0.0191591
AT1G36280	Adenylosuccinate lyase	0.48	0.0001437
AT1G14230	Nucleoside phosphatase family protein	0.47	0.0018271
AT1G56600	Galactinol synthase	0.46	0.0004324
AT3G53230	Cell division cycle protein 48 (CDC48)	0.45	0.0042888
AT4G17470	Palmitoyl protein thioesterase family protein	0.45	0.0007172
AT5G24780	Vegetative storage protein 1 (VSP1)	0.44	0.0112310
AT3G51910	Heat shock transcription factor family protein (HSFA7A)	0.43	0.0001437
AT2G46240	IQ domain-containing protein (BAG6)	0.39	0.0003968
AT4G15210	Beta-amylase (BMY1)	0.38	0.0000186
AT2G24850	Aminotransferase (TAT3)	0.37	0.0265084
AT1G60190	Armadillo/beta-catenin repeat family protein	0.36	0.0000016
AT4G16590	Glucosyltransferase-related (CSLA01)	0.34	0.0000001
AT4G39950	Cytochrome P450 79B2 (CYP79B2)	0.33	0.0000003
AT1G56650	Myb family transcription factor (MYB75)	0.26	0.0000000
AT5G45040	CYTC6A	0.12	0.0000000

Table 3.3: Significant Differently Regulated Genes in the Mutant *atc6*. Affymetrix microarray analysis between the mutant *atc6* and the wild type (Col-0) resulted in 44 significant differently regulated genes. The gene description derives from the Arabidopsis Genome Initiative. The fold change expression (FC) refers to the wild type level.

Focusing on the comparison between *atc6* and wild type arrays, 44 significant differently regulated genes were detected (Tab. 3.3). Interestingly, among them were several genes involved in hormone signaling such as cytokinin (*ARR6*, *ARR15*, *AT2G16660*, *and AT3G06070*), gibberelin (*AT1G74670*), auxin (*CYP79B2*) and brassinosteroide (*AT5G51550*) pathways as well as genes involved in cell development processes such as cell division (*CDC48*), cell elongation (*EXPL1*) and apoptosis (*BAG6*). The second noticeable group includes proteins related to carbohydrate pathways (*DIN10*, *ERD6*, *EXGTA1*, *DESAT.*, *AT1G36280*, *AT1G56600*, VSP1, BMY1).

A subset of nuclear and plastid encoded genes was chosen to be rechecked by real-time PCR to prove the reliability of the microarray results (Fig.3.18A). In most cases the tendency of the microarray analysis could be confirmed, but changes in expression were much lower and did not even exceed the significant fold change threshold (*Desat.*, *ATPP2*, *ARR15*, *NOD-LIKE#1*, *MATE*, *QQS*, *EXPL1*, *HSP26*, *NOD-LIKE#2*, *RCAR8*, *EXL3* and *ARR6*). Genes, which where not significantly changed in microarray analysis, showed similar expression levels when analyzed by real-time PCR (*psbA*, *rps12A*, *psaB*, *psbA*, *rbcL*, *petG*, *psbB* and *rps12C*). Both observations confirm the reliability of the microarrays, even though the level of expression differences is questionable.

MYB75, *CYP79B2* and *BMY1* were regulated in an opposite manner between the two analysis techniques, and therefore the results cannot be considered reliable for these three genes. The most promising candidates derived from the microarray analysis, *CDC48* and *BAG6*, were the only genes, whose down-regulation in *atc6* could be confirmed in tendency and magnitude by real-time PCR (Fig. 3.18B).

A

Name	AGI Code	Name	AGI Code
DESAT.	AT1G06360	CYP79B	AT4G39950
MYB75	AT1G56650	RCAR8	AT5G05440
ATPP2	AT1G65390	EXL3	AT5G51550
ARR15	AT1G74890	ARR6	AT5G62920
NOD.LIKE#1	AT2G16660	psbA	ATCG00020
BAG6	AT2G46240	rps12A	ATCG00065
MATE	AT3G23550	psaB	ATCG00340
QQS	AT3G30720	psaA	ATCG00350
EXPL1	AT3G45970	rbcL	ATCG00490
CDC48	AT3G53230	petG	ATCG00600
BMY1	AT4G15210	psbB	ATCG00680
HSP26	AT4G21870	rps12C	ATCG00905
NOD.LIKE#2	AT4G34950		

B
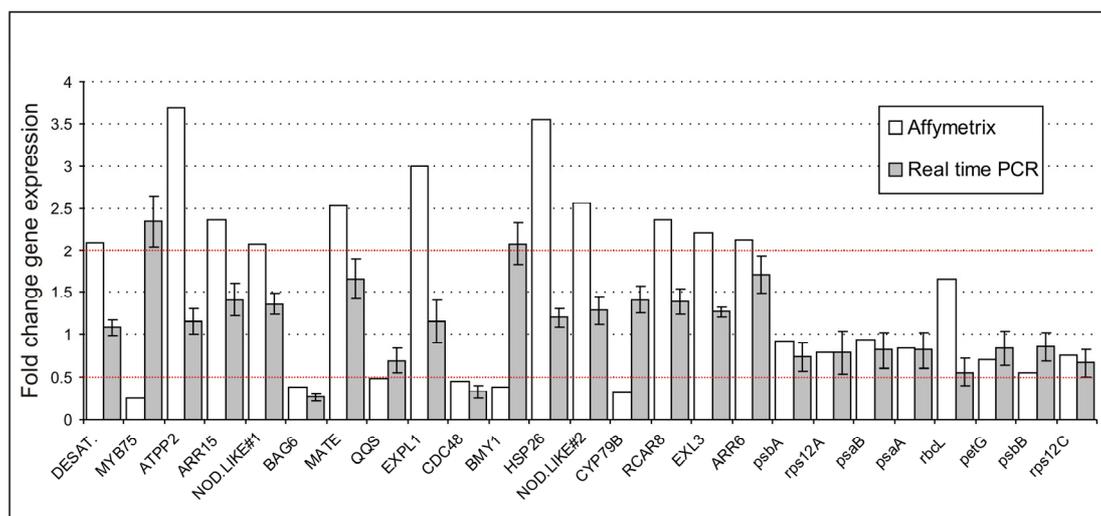
Figure 3.18: Analysis of the Affymetrix Chip Expression Data by Real Time PCR. A subset of differently regulated nuclear and plastid genes, based on Affymetrix microarray data (A), were chosen to be subjected to real-time PCR analyses (B). Thresholds of significance, a fold change expression more than 2 or less than 0.5, are indicated by red lines. Results were normalized using ubiquitin as internal standard.

3.4.2. Stress Treatments

In standard conditions, plants lacking cytochrome c_{6A} do not show any different phenotype compared to the wild type (chapter 3.2.). To analyze a role of cytochrome c_{6A} under stress conditions *atc6* and Cyt c_{6A} OE plants were exposed to high light and dark conditions and to heat and drought stress, but no phenotype could be observed in transgenic plants (data not shown).

By real-time PCR *ATC6* transcript level was determined in wild type plants, which were exposed to high light, dark, heat, drought and wounding, in order to test for differences in gene expression. Even if the detected levels were highly fluctuating, they were not significantly different from the wild type in standard conditions, with the exception of plants under drought treatment. In this case the cytochrome c_{6A} transcript level was reduced to about 35 % from standard conditions (Fig. 3.19).

Figure 3.19: *ATC6* Expression Level in Wild Type (Col-0) under Stress Conditions. Wild type (Col-0) plants were grown four weeks under greenhouse conditions and then shifted to stress inducing environment (chapter 2.19.). *ATC6* expression levels were determined by real time PCR. Results are normalized with ubiquitin expression level and displayed as fold change expression related to the expression level in untreated plants.

The most important hormone involved in drought stress response is ABA (Raghavendra *et al.*, 2010) leading to the idea that the expression of *ATC6* is influenced by its abundance. The ABA level in conditions of changed *ATC6* expression was detected analyzing two ABA reporter genes, *COR15* and *KIN2* (Hoth *et al.*, 2002). Two weeks after germination the transcription level of *ATC6* was increased, in comparison to transcript of the genes in four week old plants kept under growth condition (taken as reference). At the same time, *COR15* and *KIN2* were down-regulated indicating a lower level of ABA. In plants under drought stress, the situation is reversed. *ATC6* was down- and the reporter genes highly up-regulated

confirming high levels of ABA. The *atc6* mutant, without any *ATC6* expression, showed wild type levels of the ABA reporter genes (Fig. 3.20).
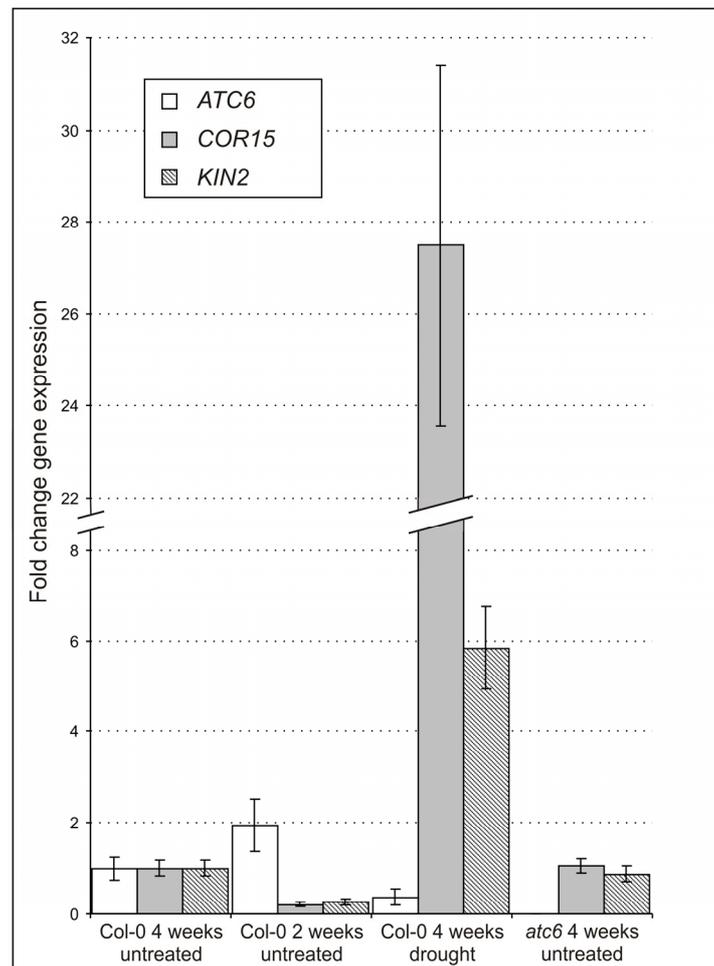
Figure 3.20: Abscisic Acid (ABA) Dependent Expression of *ATC6*. The expression level of ABA induced genes (*COR15* and *KIN2*) in the untreated wild type (Col-0) after four and after two weeks, under drought stress and in the *atc6* mutant was determined by real-time PCR. Fold change expression levels related to untreated four week old wild type plants are displayed in the diagram as standard. Results were normalized on the ubiquitin expression level.

These results indicate that *ATC6* expression does not change ABA concentrations, but its expression is down-regulated in the presence of high ABA levels.

3.4.3. Cytochrome c_{6A} Expression is Increased in the First Days of Plant Development

In the mutant *atc6*, changes in the expression of genes involved in cell development were detected by microarray analysis (chapter 3.4.1.). Real-time PCR was used to monitor *ATC6* expression during the first four weeks of plant development. One day after germination the amount of transcript was about five times higher than in the adult plant (after four weeks). The level of cytochrome c_{6A} mRNA decreased continuously after three days to three times, after 6 days to two times and finally after 28 days to the adult level. Photosynthetic genes showed an opposite behavior. The plastidial encoded *PsbA* and the nuclear encoded *PsaF* were hardly expressed after one day. Expression of *PsbA* increased continuously to the adult level after 28 days, whereas *PsaF* reached the four-weeks expression level already after three days. (Fig. 3.21).
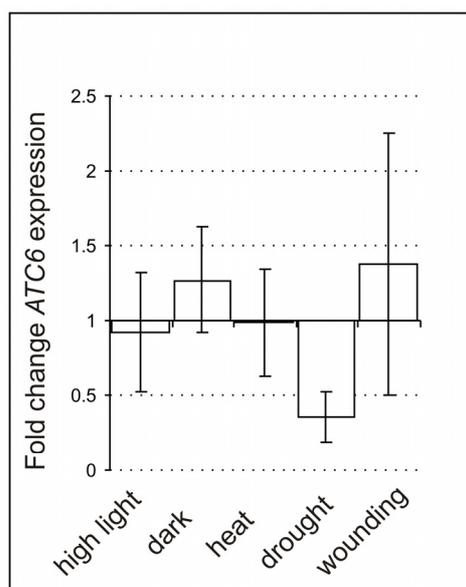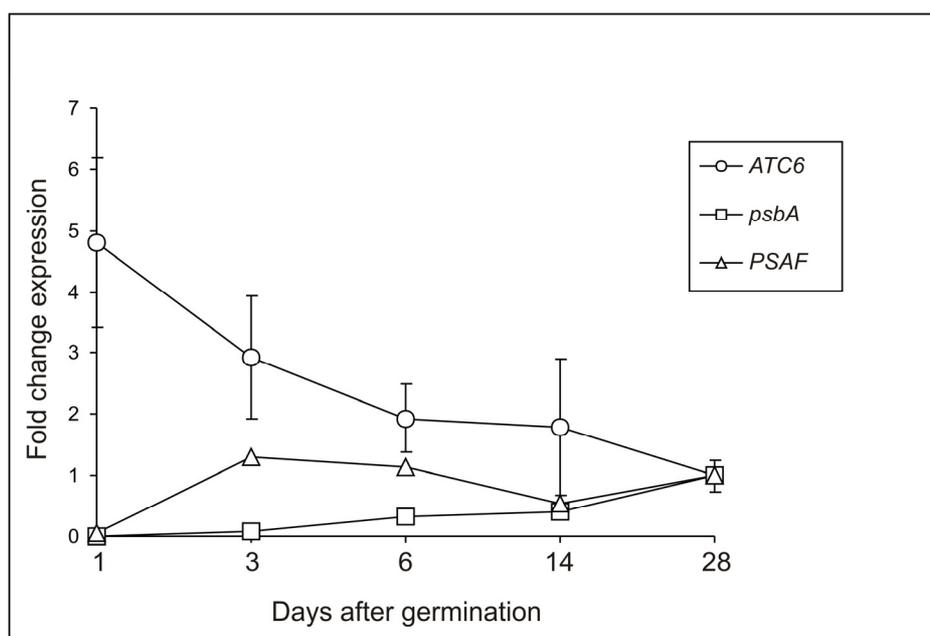

Figure 3.21: *ATC6* Expression Level in Wild Type (Col-0) during Growth. Wild type (Col-0) plants were grown for four weeks under greenhouse conditions. *ATC6*, *PsbA* and *PsaF* expression levels were determined by real time PCR. Results are normalized with ubiquitin expression level and displayed as a fold change expression taking the level at 28 days after germination as standard.

3.4.4. Genetic Dissection of a Relation between Cytochrome c_{6A} and ABA

To reveal a crosslink between ABA pathways and cytochrome c_{6A} a genetic approach, by creating double mutants, was applied. *atc6* was crossed with mutants of the ABA synthesis pathway, *aba1* and *aba3.* ABA1 catalyzes the conversion of zeaxanthin to violaxanthin in the chloroplast and ABA3 the conversion of abscisic aldehyde to abscisic acid in the cytoplasm. Furthermore, ABA insensitive mutants, *abi1* and *abi2*, were crossed with *atc6* and a triple mutant was created to overcome the problem of functional redundancy of ABI1 and ABI2. Between the single and the double mutants no phenotypical difference could be observed in four week old plants and a direct link between ABA and cytochrome c_{6A} could not be proven (Fig. 3.22).

| Col-0 | *atc6* | *aba1* | *aba1 atc6* |

| *aba3* | *aba3 atc6* | *abi1* | *abi1 atc6* |

| *abi2* | *abi2 atc6* | *abi1 abi2* | *abi1 abi2 atc6* |

Figure 3.22: Phenotypes of Double Mutants with Defects in ABA Synthesis and Perception. Double mutants between *atc6* and established mutants with defects in ABA synthesis (*aba1* and *aba3*) and perception (*abi1* and *abi2*) are compared to their corresponding single mutants. Four-week-old plants grown in the greenhouse are shown.

3.5. Subcellular Localization of Cytochrome c_{6A}

3.5.1. *In Silico* Analysis of Cytochrome c_{6A} Localization

Simultaneously to its discovery in 2002, cytochrome c_{6A} was also proposed to be localized in the thylakoid lumen (Gupta *et al.*, 2002). However, the presented immuno blot analysis of subcellular fractions turned out to be doubtful, due to loading peculiarity of the stromal fraction and variant size of the obtained signal for cytochrome c_{6A} (11 kDa).
In silico localization, achieved applying online available prediction programs, showed in most cases a plastidial or mitochondrial localization without a clear tendency (Tab. 3.4).

Prediction Program	Predicted Localization
PSORT	mitochondria
iPSORT	mitochondria
TargetP	chloroplast
BaCelLo	nucleus/cytoplasma
Protein prowler	mitochondria
Predotar	chloroplast
ChloroP	no cTP
WolfPSORT	chloroplast
PLCR	chloroplast

Table 3.4: Prediction of Subcellular Localization of Cytochrome c_{6A}. Amino-acid sequence of cytochrome c_{6A} was obtained from the TAIR database and analyzed with online available localization prediction programs (see material & methods).

3.5.2. *In Vivo* Analysis of Cytochrome c_{6A} Localization

Transient transformation of *tobacco* protoplasts confirmed the localization of cytochrome c_{6A} in plastids (Weigel, 2006), but repetition of the experiment in Arabidopsis protoplast with both the truncated transit peptide and the complete protein, fused to dsRED fluorescent protein failed.

An *in vivo* approach was carried out, in which wild type plants were transformed with a construct expressing the full length protein sequence of the cytochrome c_{6A}, fused to GFP and HA polypeptides. The transcript level was determined (chapter 3.1.), but neither immuno blot analysis nor fluorescence microscopy allowed detecting the protein. In parallel, plants were transformed with localization controls: the full length sequence of plastocyanin was fused to GFP and HA and served as a lumenal marker. A weak GFP signal in chloroplasts could be detected by microscopy (Fig 3.23A) and the HA polypeptide was recognized by immuno blot analysis (Fig. 3.23B).

A **B**
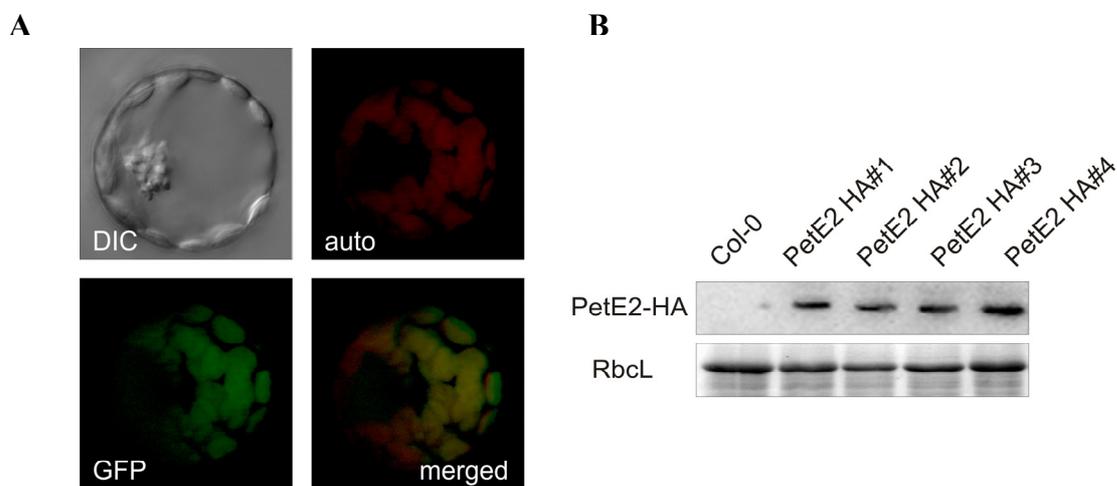
Figure 3.23: Expression of Plastocyanin Fused to a GFP or HA Polypeptide. *Arabidopsis thaliana* plants were transformed by floral dipping with constructs carrying the plasocyanin fused to the GFP polypeptide and protoplasts were isolated. (A) The fluorescence signals were detected and displayed in false colour, chlorophyll autofluorescence (auto) in red, green fluorescent protein (GFP) in green and the overlay (merged) in yellow. (B) Plastocyanin was fused to a HA polypeptide and immunoblot detection was performed with HA antibodies. Ponceau staining confirmed the equal loading of the lanes.

Additionally, the mature protein sequence of cytochrome c_{6A} was cloned fusing at its N-terminal the transit peptide of the small subunit of Rubisco and at its C-terminal the GFP polypeptide to obtain a stromal localized version of the protein. The constructed protein N-term RbcS-Cyt c_{6A}-GFP could be detected in chloroplast via microscopy (Fig. 3.24A) and specifically in the stroma, via immuno blot analysis using GFP specific antibodies (Fig.3.24B).

A   **B**
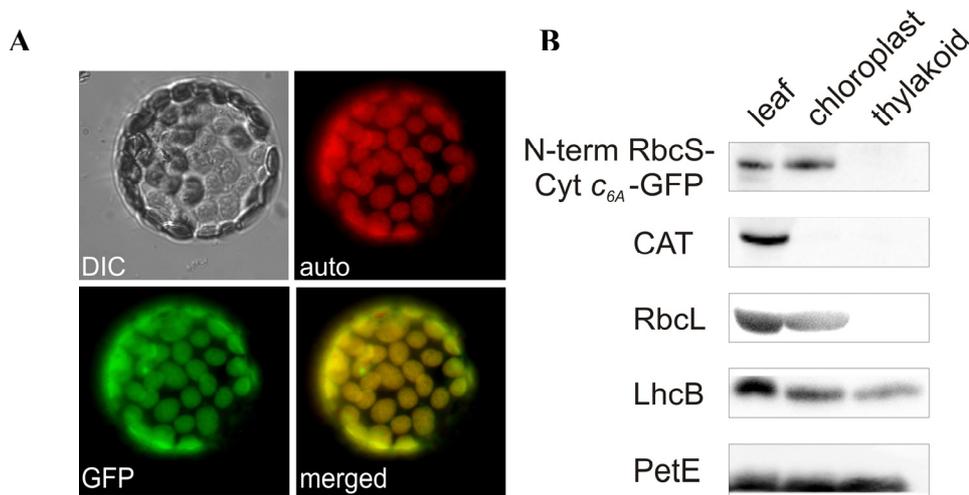
Figure 3.24: Subcellular Localization of Cytochrome c_{6A} Fused to the Transit Peptide of the Rubisco Small Subunit. (A) Protoplasts have been isolated and fluorescence signals were detected (A). The images are presented in false color, chlorophyll autofluorescence (auto) in red, green fluorescent protein (GFP) in green and the overlay (merged) in yellow. (B) Fractionation of leaf total protein (leaf), chloroplasts and thylakoids were tested by specific marker proteins (CAT, catalase; RbcL; LhcB;PetE). Clearly the chimeric protein N-term Rbcs-Cyt c_{6A}-GFP was located in the chloroplast stroma as detected by immune blot with a GFP specific antibody.

3.5.3. *In Vitro* Analysis of Cytochrome c_{6A} Localization

The third approach trying to detect the subcellular localization was based on the *in-vitro* import. Cytochrome c_{6A} was transcript and translated *in vitro* with radioactive labeled amino acids. The radioactive-labelled protein was incubated with wild type chloroplasts and the effective import was proven by its protection to protease degradation. The small subunit of Rubisco and the plastocyanin served as localization controls for stroma and thylakoids, respectively. The premature form (black arrow in Fig. 3.25) of RbcS is imported and processed in the chloroplast (white arrow in Fig. 3.25), where it is protected from thermolysin digestion (Fig. 3.25B). Further separation of the chloroplasts in thylakoid and stroma fractions proves its presence in the stroma and absence in thylakoids. In contrast, due to its lumenal localization, the processed form of the plastocyanin is present in the thylakoid, but missing in the stromal fraction (Fig. 3.25C). For cytochrome c_{6A} the localization is less obvious. Only a small amount of the translation product is imported and processed in

the chloroplast. The weak signal is hardly detectable after thermolysin treatment and it is not present in further sub-fractions of the chloroplasts (Fig. 3.25A).
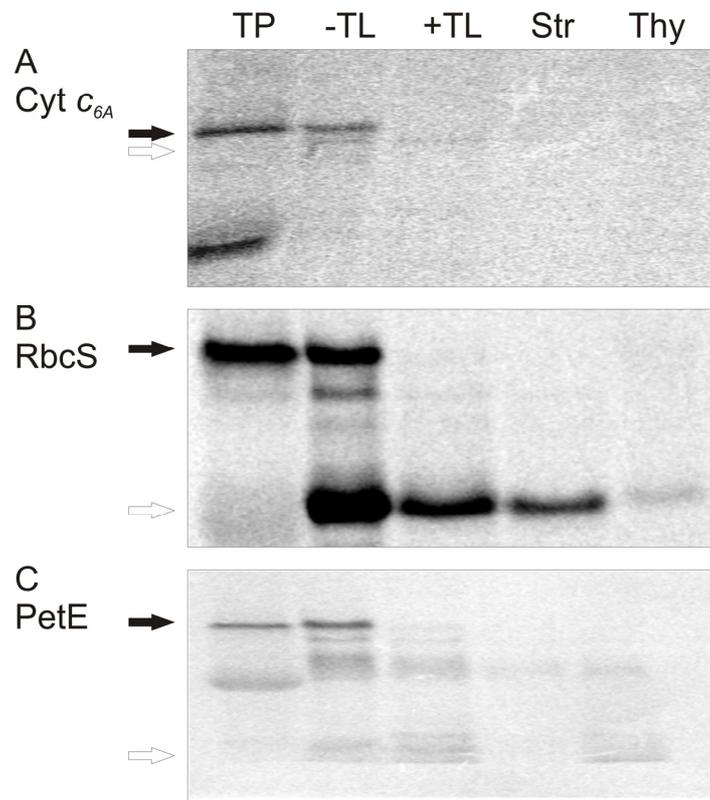
Figure 3.25: Plastidial Localization of Cytochrome *c*$_{6A}$ by *In-Vitro* Import Assays. The plastidial localization of cytochrome *c*$_{6A}$ (A) was analyzed by *In-Vitro* Import Assay using the small subunit (SSU) of Rubisco (B) and the plastocyanin (C) as import controls. Gels were loaded with 1/10 of the radio-labeled translation product added to the import reaction mixture (TP), and the radio-labeled protein recovered from chloroplasts that had (+TL) or had not (-TL) been treated with thermolysin after termination of the import reaction. Chloroplasts treated with thermolysin were further fractionated in stroma (Str) and thylakoids (Thy). The translation product is indicated by black arrows, the mature protein by white arrows.

Localization inside the chloroplast could be confirmed by the in vitro assay, the small amount of processed protein impeded a further discrimination between stromal or thylakoid localization of the protein.

3.6. Dimeric Cytochrome c_{6A} Interacts with the Stromal Region of Photosystem I

3.6.1. Interaction Studies in Yeast

Although hypothesis about the function of cytochrome c_{6A} were suggested, direct evidences have never been delivered. Interaction studies between proteins in yeast and in plants were applied to prove existing hypotheses and to gain new information about cytochrome c_{6A} function.

The yeast two-hybrid system (Y2H) is an established strategy to detect protein-protein interactions. Testing the self-interaction cytochrome c_{6A} with a second cytochrome c_{6A} showed that the protein is capable to build homodimers in yeast, suggesting the same behavior in plants. By changing the cys(67) and cys(73) of the LIP by serine, it could be shown that the dimer formation is independent of the disulphide bridge (Tab. 3.6(Pesaresi et al., 2009a).

Based on the knowledge of its dimerization a yeast ternary-trap screening (Y3H) with cytochrome c_{6A} against a cDNA expression library of *Arabidopsis thaliana* was performed. The method requires an additional cytochrome c_{6A} fused to a nuclear signal peptide allowing the formation of cytochrome c_{6A} dimers within the nucleus. 31 clones containing the sequence of 26 putatively interacting proteins were obtained and information according their function and localization were identified using the TAIR database and prediction programs (Tab. 3.5). Plastidial proteins and peroxin 11C were analyzed further in yeast assays with full length proteins.

Collecting all candidates, interaction studies were performed using yeast two hybrid (Y2H and Y3H) and split-ubiquitin (SU) systems. Candidates derive from the hypothesis of Schlarb-Ridley *et al.* 2006, the ternary yeast screen, the ABA pathway and the photosystem subunits PsaE and PsaF (Tab. 3.6).

Clone	AGI-Code	Description	Localization
1	AT4G02510	TOC132	chloroplast outer envelope
2	AT5G12110	eEF1B	(cytoplasm)
3	AT4G02060	PROLIFERA	(nucleus)
4	AT5G12110	eEF1B	(cytoplasm)
5	AT4G02060	PROLIFERA	(nucleus)
6	AT5G12110	eEF1B	(cytoplasm)
7	AT1G01820	Peroxin 11C	peroxisome
8	AT1G73590	ATPIN1	plasma membrane/cytoplasm
9	AT5G59690	Histone H4	nucleus
10	AT5G38470	RAD23	nucleus
11	AT2G35240	DAG	mitochondrion/(chloroplast)
12	AT5G59690	Histone H4	nucleus
13	AT3G61470	LhcA2	chloroplast thylakoid membrane
14	no match		
15	AT3G25520	ATL5	nucleus/cytoplasm
21	no match		
22	AT3G63370	OTP86	chloroplast stroma
23	AT3G15240	unknown protein	?
24	AT5G45280	pectinacetylesterase	cell wall
25	AT4G19490	ATVPS54	chloroplast stroma
26	AT2G37520	PHD finger family protein	(nucleus)
27	AT1G72370	AP40	nucleus/cytoplasm
28	AT5G45280	pectinacetylesterase	cell wall
29	AT1G22920	AJH1	cytoplasm
30	AT2G46980	unknown protein	nucleus/cytoplasm
31	AT1G28520	unknown protein	?

Table 3.5: Putative Interactors of Cytochrome c_{6A} Derived from Ternary Yeast Screening. Cytochrome c_{6A} fused either to the GAL4 activation domain or together with a nuclear localization signal were incubated in yeast in the presence of an *Arabidopsis* cDNA expression library fused to the GAL4 binding domain. Plasmids of yeast, which is able to grow on selective media, were sequenced and blasted against the genome of *Arabidopsis thaliana* using NCBI nBlast. The localization of the identified putative interactors refers to TAIR database and was rechecked with prediction programs (chapter 2.14).

The hypothesis of Schlarb-Ridley *et al.* 2006 suggests that cytochrome c_{6A} interacts in the lumen with proteins by a disulphide exchange reaction and transfers electrons to plastocyanin(Schlarb-Ridley *et al.*, 2006). Therefore, the interaction of cytochrome c_{6A} with plastocyanin (PetE1 and PetE2) and with lumenal proteins containing a disulphide bridge (FKBP13, PsbO1, PsbO2, HCF164, 17.4kDA protein, PrxQ, STN7 and Rieske protein) was tested. Due to a self-activation of the split-ubiquitin system, the approach testing the Rieske protein was invalid. For the other proteins no interaction could be confirmed, not even for FKBP13 that was described to interact with cytochrome c_{6A} in a yeast screening by Gupta et al. 2002. Considering these studies and the genetic approach analyzing cytochrome c_{6A}

plastocyanin double mutants (chapter 3.3.2.) the proposed function of cytochrome c_{6A} in the thylakoid lumen seems to be unlikely (Pesaresi *et al.*, 2009a). However, it is possible that electron transfer and disulphide bridge exchange reactions might be based on a very transient interaction between proteins that could not be detected by yeast assays.

Some experiments suggested a correlation between abscisic acid levels (chapter 3.4.2.), NPQ formation and cytochrome c_{6A}, as observed in *psaf atc6* (chapter 3.3.2.). ABA1 and NPQ1 are enzymes involved in both pathways, ABA synthesis and NPQ formation, and are localized in the chloroplast. For that reasons they were chosen for interaction studies in yeast assays. Combined with cytochrome c_{6A}, yeast was not able to grow on selective media indicating no direct interaction between the proteins.

To validate their interaction with cytochrome c_{6A}, candidate proteins derived from the Y3H screening were tested by expressing the full length protein in yeast assays. Lhca2 that is a component of PSI was analyzed in several approaches. The polypeptide, which was found in the Y3H screening, consists of the first 136 amino acids of its full protein sequence and contains the transit peptide, the first stromal domain, the first transmembrane domain and the first lumenal domain. The full length protein containing transmembrane regions was tested in a SU approach, whereas the stromal and lumenal domains were checked separately in Y3H assays. LhcA2, both unknown proteins, VPS54 and DAG did not show any detectable interaction and the result of the screening remains the only prove for the interaction between cytochrome c_{6A} and the candidates.

PEX11 is a characteristic domain for peroxisomal division membrane proteins of the peroxin 11 family. Since the PEX11 domain was found in two independent clones, OTP86 and PEX11C were tested, though the latter one is localized in the peroxysome. Due to PEX11C hydrophobicity, both SU and Y3H were applied but without success in confirming the screening result.

OTP86 was the only protein of the Y3H screening, whose interaction with cytochrome c_{6A} could be verified. Its PEX11 domain and the peptide found in the screening were strongly interacting with cytochrome c_{6A}. The reason for the weaker interaction observed with the full length protein could be a result of its size (99 kDa) or its different folding and processing in yeast. OTP86 is a stromal pentatricopeptide repeat (PPR) protein involved in mRNA editing of the ribosomal protein RPS14 (Hammani *et al.*, 2009). *rps14* is a plastidial gene translated

polycistronic with *psaA* and *psaB*. Nevertheless, a crucial role of cytochrome c_{6A} in this mRNA editing process performed by OTP86 can be excluded by sequencing of *rps14* transcripts in *atc6* plants (at least four independent sequencing experiments for *atc6* and wild type plants):

unedited   5'...tgattcgtcgatcctT...3'

Col-0   5'...tgattcgtcgatcctC...3'

atc6   5'...tgattcgtcgatcctC...3'

otp86   5'...tgattcgtcgatcctT...3' (Hammani *et al.* 2009)

Interaction between cytochrome c_{6A} and PSI-F, the interactor of the ancient cytochrome c_6 in cyanobacteria, was investigated extensively. Stromal and several versions of the lumenal regions were tested by Y3H assays and the full length protein by SU approaches due to its transmembrane domain. The lumenal domain of PSI-F did not show any interaction with cytochrome c_{6A}. Surprisingly, the stromal domain showed a weak positive signal in the Y3H assay that could be confirmed by the SU approach.

Y3H assays with the stromal subunit E of PSI suggested no interaction with cytochrome c_{6A}, whereas a hypothetical protein, which shows the highest expression correlation to cytochrome c_{6A} (ATTED-II database), seems to interact very weakly (Tab. 3.6).

Taken together, cytochrome c_{6A} is capable to build homodimers, which are able to interact with the stromal mRNA editing protein OTP86 and the stromal domain of PSI-F, indicating a stromal localization of the protein. No interaction with lumenal proteins could be detected contradicting the present hypotheses about its function.

Put. Interactor	AGI code	Sequence	Yeast Assay	Interaction?
Cyt c_{6A}	AT5G45040	CDS without cTP	Y2H	interaction
Cyt c_{6A}	AT5G45040	CDS without cTP; cys67ser cys73ser	Y2H	interaction
PetE1	AT1G76100	CDS without cTP	Y2H/Y3H	no interaction
PetE2	AT1G20340	CDS without cTP	Y2H/Y3H	no interaction
FKBP13	AT5G45680	CDS without cTP	Y2H/Y3H	no interaction
PsbO1	AT5G66570	CDS without cTP	Y2H/Y3H	no interaction
PsbO2	AT3G50820	CDS without cTP	Y2H/Y3H	no interaction
HCF164	AT4G37200	CDS without cTP	SU	no interaction
17.4kDa protein	AT5G53490	CDS without cTP	Y2H/Y3H	no interaction
PrxQ	AT3G26060	CDS without cTP	Y2H/Y3H	no interaction
STN7	AT1G68830	CDS without cTP	SU	no interaction
Rieske protein	AT4G03280	CDS without cTP	SU	self-activation
ABA1	AT5G67030	CDS without cTP	Y2H/Y3H	no interaction
NPQ1	AT1G08550	CDS without cTP	Y2H/Y3H	no interaction
unknown protein	AT3G15240	full CDS	Y3H	no interaction
unknown protein	AT1G28520	full CDS	Y3H	no interaction
VPS54	AT4G19490	CDS without cTP	Y3H	no interaction
DAG	AT2G35240	CDS without cTP	Y3H	no interaction
LhcA2	AT3G61470	CDS without cTP	SU	no interaction
LhcA2	AT3G61470	lumenal loop	Y3H	no interaction
LhcA2	AT3G61470	stromal loop	Y3H	no interaction
PEX11C	AT1G01820	full CDS	Y3H	no interaction
PEX11C	AT1G01820	full CDS	SU	no interaction
OTP86	AT3G63370	Pex11 domain of AT3G63370	Y3H	interaction
OTP86	AT3G63370	sequence found in Y3H screen	Y3H	interaction
OTP86	AT3G63370	full CDS	Y3H	weak interaction
PsaF	AT1G31330	CDS without cTP	SU	weak interaction
PsaF	AT1G31330	lumenal loop	Y3H	no interaction
PsaF	AT1G31330	lumenal loop; cys75ser cys130ser	Y3H	no interaction
PsaF	AT1G31330	lumenal loop cys75ser	Y3H	no interaction
PsaF	AT1G31330	lumenal loop cys130ser	Y3H	no interaction
PsaF	AT1G31330	stromal loop	Y3H	weak interaction
PsaE1	AT4G28750	CDS without cTP	Y3H	no interaction
hypothetical protein	AT1G73090	CDS without cTP	Y3H	weak interaction

Table 3.6: Overview of Yeast Interaction Studies between Cytochrome *c₆A* and Putative Interactors. Putative interactors of cytochrome *c₆A* derived from Schlarb-Ridley's hypothesis (PetE1, PetE2, FKBP13, PsbO1, PsbO2, HCF164, 17.4kDa protein, PrxQ, STN7 and the Rieske protein), the ternary yeast screening (unknown proteins, LhcA2, VPS54, DAG, PEX11C and OTP86), photosynthesis (PsaF and PsaE) and some other candidates (NPQ1, ABA1, hypothetical protein) were checked by yeast-two-hybrid assays (Y2H: yeast-two-hybrid; Y3H: ternary yeast assay; SU: split-ubiquitin assay). The full length coding sequence (CDS) full length, without the transit peptide, with mutated or single domains, were cloned into the bait and prey vector and interaction studies were performed with the mature cytochrome *c₆A*.

3.6.2. Interaction Studies in Plants

Immunoprecipitation of protein complexes (co-immunoprecipitation) is an established method to prove interactions *in vivo*. By targeting the protein of interest with a specific

antibody, it may become possible to pull it out of a solution, together with attached proteins, which can be identified by mass spectrometry.

Since plants expressing N-term RbcS-Cyt c_{6A}-GFP was the only case, in which a cytochrome c_{6A} fusion protein could be detected via microscopy and immuno-blot, they were used to perform co-immunoprecipitation experiments. The localization of the wild type cytochrome c_{6A} inside the chloroplast could not be clarified in this work (chapter 3.5.) and the stromal localization of N-term RbcS-Cyt c_{6A}-GFP might prevent the protein to find its interactors in case of a lumenal localization of the wild type form. Therefore, for co-immunoprecipitation entire chloroplast were solubilized with digitonin and incubated for a longer period in order to allow interaction between N-term RbcS-Cyt c_{6A}-GFP and lumenal proteins.

Using this strategy it was possible to identify two complexes, which could be precipitated and identified via mass spectrometry. These proteins are putatively interacting with N-term RbcS-Cyt c_{6A}-GFP. The first one includes the small (RbcS1) and the large (RbcL) subunits of Rubisco and the Rubisco activase (RCA). Precipitation of these proteins could be mediated by the transit peptide of RbcS that is fused in front of cytochrome c_{6A}. The second identified complex contains many subunits of the stromal region of PSI (PsaA, PsaD1, PsaE1, and PsaE2) and its light harvesting complex (LhcA2 and LhcA4). PsaB and PsaF were detected in both the N-term RbcS-Cyt c_{6A}-GFP and the control experiment and for that reason their interaction is not reliable. Other identified peptides (AT1G67700, AtpB, LhcB1, ANTR1 and AT1G72300) are most probably unspecific interaction, but should be rechecked by other interaction experiments like yeast assays (Tab. 3.7).

Yeast assays showed association of cytochrome c_{6A} with LhcA2 (Tab. 3.5) and with PsaF (Tab. 3.6) and suggested an interaction with the stromal region of PSI. The co-immunoprecipitation approach confirmed these interactions *in planta*.

Name	AGI-Code	Co-IP	Control
eGFP		2	0
PsaA	ATCG00350	2	0
PsaB	ATCG00340	3	2
PsaD1	AT4G02770	1	0
PsaE1	AT4G28750	2	0
PsaE2	AT2G20260	2	0
PsaF	AT1G31330	1	1
PsaL	AT4G12800	2	0
LhcA2	AT3G61470	1	0
LhcA4	AT3G47470	5	0
RbcL	ATCG00490	3	0
RbcS1	AT1G67090	1	0
RCA	AT2G39730	1	0
unknown protein	AT1G67700	0	1
cleavage stimulation factor	AT1G71800	1	0
AtpB	ATCG00480	2	1
LhcB1	AT1G29910	2	0
ANTR1	AT2G29650	0	0
transmembrane protein kinase	AT1G72300	1	0

Table 3.7: Co-Immunoprecipitation with N-term RbcS-Cyt c_{6A}-GFP. Chloroplasts of N-term RbcS-Cyt c_{6A}-GFP were isolated and solubilized with digitonin. Co-immunoprecipitation was performed with GFP specific antibodies and results were analyzed by mass spectrometry. Control experiments were performed with wild type chloroplasts. Numbers of identified peptide are presented in the last two columns.

Plants expressing the N-term RbcS-Cyt c_{6A}-GFP displayed a reduced growth and a pale pigmentation (Fig. 3.26). These phenotypical changes can be caused by a gain-of-function of the mislocation or the high concentration of cytochrome c_{6a}. Indeed, targets of cytochrome c_{6a} might be either disulphide bridge containing redox regulated protein in the stroma or, more likely, the acceptor side of photosystem I, whose interaction was shown in the co-immumnoprecipitation experiment. Cytochrome c_{6a} could interfere with the electron transfer processes of photosynthesis by donating electrons or by inhibiting the efficient docking of ferredoxin to its acceptor side to the PSI. A similar, but even more evident, phenotype can be observed in the *psad1-1* mutant, in which the level of the PSI-D subunit is reduced that leads to an impaired docking of ferredoxin to the acceptor side and an overall reduced concentration of PSI. This defect results in decreased photosynthetic and growth performances as well as an altered pigment composition (Ihnatowicz *et al.* 2004).

The impaired phenotype cannot only be caused by the cytochrome c_{6a} protein in the N-term RbcS-Cyt c_{6A}-GFP, but also by the other components of the fusion protein, the transit peptide of rubisco and the green fluorescent protein. To analyse and to exclude this possibility,

plants have to be created that express only the GFP fused to the rubisco transit peptide and their phenotype has to be analyzed.

<div align="center">

Col-0   N-term RbcS-
Cyt c_{6A}-GFP

</div>
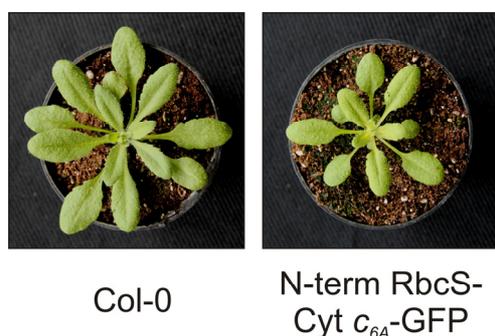
Figure 3.26: Phenotype of Col-0 and N-term RbcS-Cyt c_{6A}-GFP Plants. Five-week-old plants of Col-0 and N-term RbcS-Cyt c_{6A}-GFP propagated in greenhouse are shown.

Photosynthetic parameters showed a reduced PSII performance, measured as maximum and efficient quantum yield (F_V/F_M and Φ_{II}) and a reduced PSI performance by the maximum absorbance under illumination (P_m, P_m') (Tab.3.8).

Parameter	Fv/Fm	ΦII	1-qP	NPQ	Pm, Pm'
Col-0	0.84 ± 0.01	0.76 ± 0.01	0.05 ± 0.01	0.26 ± 0.05	0.064 ± 0.004
N-term RbcS-Cyt c_{6A}-GFP	0.80 ± 0.01	0.70 ± 0.01	0.07 ± 0.01	0.29 ± 0.04	0.051 ± 0.004

Table 3.8: Photosynthetic Performance of Photosystem II and Photosystem I. Parameters of the chlorophyll a fluorescence (F_V/F_M, maximum quantum yield of PSII; Φ_{II}, effective quantum yield of PSII; 1-qP, excitation pressure; NPQ, non-photochemical quenching) and P700 absorption (P_m,P_m') are measured by pulse amplitude modulation (PAM) at 72 µmol photons m^{-2} s^{-1} actinic light. At least five independent five-week-old plants each genotype were measured.

Both phenotype and photosynthetic parameters indicate an impact of the expressed N-term RbcS-Cyt c_{6A}-GFP on the electron transport chain of photosynthesis and supports the idea of interaction with PSI.

4. Discussion

4.1. Challenges of Cytochrome c_{6A}

4.1.1. Absence of the Protein

Since its discovery in 2002 several analyses were published regarding the "new" cytochrome c_6, which was found in higher plants. Most of them were dealing with sequence analysis (Wastl *et al.*, 2002; Weigel *et al.*, 2003b; Wastl *et al.*, 2004) and the dissection of the three dimensional structure of cytochrome c_{6A}, which was obtained by homology modeling (Howe *et al.*, 2006) or X-ray crystallography (Marcaida *et al.*, 2006; Worrall *et al.*, 2007; Worrall *et al.*, 2008). These methods provide a view on structural characteristics, but they are limited in suggesting putative *in vivo* functions of the protein. Anyway, two ideas regarding its function were proposed: the first that sees cytochrome c_{6A} as an electron carrier to PSI, adapted from the function of the original cytochrome c_6 (Gupta *et al.*, 2002), the second that identifies cytochrome c_{6A} as a lumenal redox regulatory protein (Schlarb-Ridley *et al.*, 2006). These hypotheses were tested by the analysis of heterologously expressed proteins in *E. coli* (Molina-Heredia *et al.*, 2003; Wastl *et al.*, 2004) and in *S. cerevisiae.* The latter one is presented in this PhD thesis and published in Pesaresi, Scharfenberg *et al.* (2008). However, in *planta* experiments have never been published so far (Gupta *et al.*, 2002; Weigel *et al.*, 2003a).

The absence of published *in vivo* experiments could be due to the difficulties to detect the protein in plants. During this work several antibodies were generated, which were able to recognize the heterologous expressed protein in *E. coli*, but none of them worked successfully in plants. Different subcellular fractions, such as chloroplasts, stroma and thylakoids and the thylakoid lumen, were isolated to increase the concentration of cytochrome c_{6A}, as well as alternative immuno blot strategies were applied, but they did not provide any positive results. To overcome the problem of a low protein concentration based on a low *ATC6* expression in wild type, transgenic plants with increased transcript level were generated. Although the transcript level was increased up to 70 times, the protein could not

be detected. Cytochrome c_{6A} was even equipped with the polypeptides GFP and HA, to facilitate immuno-detection, but its *in vivo* presence could not be confirmed.

A possible explanation could be that the cytochrome c_{6A} transcript undergoes a post-transcriptional processing, which regulates the translation and the accumulation of protein, independently of the mRNA level. Regulation at transcript level in *Arabidopsis* was already described in floral development processes. An example is given by the RNA 3' End-Processing Factor FY, which mediates the downregulation of the floral repressor *FLC* by controlling the 3' end formation of specific transcripts (Simpson *et al.*, 2003).

The putative regulation of cytochrome c_{6A} seems not to affect the accumulation of protein in plants transformed with the chimeric gene N-term RbcS-Cyt c_{6A}-GFP suggesting the presence of a recognition motive at the 5' mRNA region encoding for the cytochrome c_{6A} transit peptide. Therefore, in this work the lines expressing N-term RbcS-Cyt c_{6A}-GFP were used to express the protein in plants in a sufficient amount, irrespectively whether its localization reflects the natural state.

A method to bypass the difficulties of low protein concentration in presence of high mRNA levels requires the isolation of elements of the post-transcriptional processing. A possibility to analyze proteins binding to the mRNA of cytochrome c_{6A} could be provided by the RNA-IP method (Tenenbaum *et al.*, 2002). Knowing these regulatory mechanisms, new approaches could be designed to facilitate accumulation of the cytochrome c_{6A} protein and to perform *in planta* experiments.

4.1.2. Absence of a Phenotype

Characterization of the *atc6* knock-out mutant by many approaches did not show any phenotypic difference to the corresponding wild type plants. In the course of this work we analyzed the phenotype of mutant plants under normal and various stress conditions, such as high light, heat shock and drought. Moreover, we determined development performances (such as germination capability, hypocotyl length and growth rate) to observe any possible phenotypic difference between mutant and wild type plants. A lack of a phenotype indicates that the role of cytochrome c_{6A} is not crucial for stress response or plant development. Since the protein is present in all higher plants and green algae, a conserved function is likely. To

figure out conditions, which unravel differences that depend on the presence of cytochrome c_{6A}, would give indication about its function and pathways, in which it could be involved in. However, it may be that the role of cytochrome c_{6A} is fulfilled by another not yet identified protein showing functional redundancy. In this case, biochemical approaches to identify the possible function of cytochrome c_{6A}, together with other possible redundant proteins, seem to be more effective.

4.2. Localization of Cytochrome c_{6A}

In Gupta *et al*. 2002, cytochrome c_{6A} was proposed to be located in the thylakoid lumen, as shown by chloroplast fractionation followed by western blot analysis. This result could not be confirmed, even though in this work several approaches to determine the localization *in vivo* were performed. Detection of the protein by Western blot analysis is not feasible, neither in wild type nor in cytochrome c_{6A} overexpressing plants, probably because of its low accumulation. Transient and stable expression of fusion proteins with fluorescence markers (RFP and GFP) and protein tag (HA) followed by plastid fractionation and Western blot analysis failed for the same reason (chapter 3.1.), even though detection of plastocyanin, considered as a lumenal control, was easily possible.

Localization prediction programs, which were shown to be pretty solid and reliable for chloroplast proteins (Armbruster *et al.*, 2009), were applied to analyze the polypeptide sequence of cytochrome c_{6A}. The obtained data did not show a clear result but a *tendency* for a plastidial localization (chapter 3.5.1.). On the other hand, the plastidial localization of cytochrome c_{6A} could be confirmed by *in vitro* import assays (chapter 3.5.3.). A small amount of the protein was imported into the chloroplast. The concentration of imported protein was not sufficient to provide a more detailed characterization by chloroplast fractionation. It remains the question, whether cytochrome c_{6A} is a stromal or lumenal protein. To answer this question a more sensitive cytochrome c_{6A} antibody need to be produced.

4.3. Photosynthesis without Cytochrome c_{6A}

The ancestor algal cytochrome c_6 serves as an electron carrier between the cytochrome b_6f comblex and photosystem I, but this function could not be observed analyzing cytochrome c_{6A} in higher plants. In this work, further characterization of plants lacking cytochrome c_{6A} showed no indications for a new major role in known photosynthetic processes.

In order to detect differences between the *atc6* mutant and wild type plants, the composition of the photosynthetic complexes were tested using 77K fluorescence measurements, BN-PAGE, western blot and pigment analyses (chapter 3.3.1.). Furthermore, photosynthetic performances were measured under different conditions and in mutants characterized by altered photosynthesis (chapter 3.3.2.). Considering all experiments regarding *atc6*, there could not be detected any effect on photosynthesis suggesting that, in adult plants, this process is irrespective of the absence cytochrome c_{6A}.

Indications that a putative new function of cytochrome c_{6A} is related to photosystem I and influences photosynthesis are given by the stromal expression of the chimeric protein in N-term RbcS-Cyt c_{6A}-GFP in plants. The high concentration of this form of the cytochrome c_{6A} in the stroma leads to a decrease in photosynthetic performance (chapter 3.6.2.) and interaction studies proved that subunits of photosystem I could be possible interacting partners with cytochrome c_{6A} (Tab. 3.6 and Tab 3.7). Comments on this new putative function are discribed in chapter 4.6.

4.4. Hypothesis of a Lumenal Redox Regulator

The Schlarb-Ridley hypothesis (Schlarb-Ridley *et al.* 2006) proposes, that plastocyanin and cytochrome c_{6A} might cooperate in the thylakoid lumen, oxidizing target redox lumenal proteins by a *disulphide bridge exchange* reaction. In order to test interactions between cytochrome c_{6A}, plastocyanin and a subset of putative lumenal proteins, which contain at least one disulphide bridge, variants of the yeast two-hybrid approach were applied as described previously. None of the plastocyanin isoforms, PetE1 and PetE2, were interacting with cytochrome c_{6A} in these assays, making the interaction of the proteins *in vivo* unlikely (chapter 3.6.1.). Moreover, also a physical interaction between putative lumenal target

proteins and cytochrome c_{6A} could not be shown giving no support to the hypothesis of a lumenal redox regulatory role of cytochrome c_{6A}.

A putative interaction between cytochrome c_{6A} and plastocyanin was also tested at the genetic level. Based on the hypothesis of Schlarb-Ridley, cytochrome c_{6A} knockout plants with reduced plastocyanin content should be markedly affected in thylakoid functions and the mutations may even be lethal. To test this hypothesis double mutants of the cytochrome c_{6A} knockout line (*atc6*) and *pete1* or *pete2* plants were created (chapter 3.3.2.). The *atc6 pete1* and *atc6 pete2* double mutants and the corresponding single mutants exhibited identical phenotypes, in terms of both photosynthetic performance (chapter 3.3.2.) and growth rate (Pesaresi *et al.*, 2009a).

The hypothesis of Schlarb-Ridley at al. (2006) does not find any support in the approaches of this work and can be considered unlikely, although the existence of a transient weak interaction that escapes detection by the yeast two-hybrid and the ternary trap assays cannot be excluded.

4.5. Cytochrome c_{6A} and Programmed Cell Death (PCD)

4.5.1. Transcriptomic analysis

A genome wide transcriptomic analysis was performed on microarray chip sets to reveal different expression patterns between wild type, *atc6* and Cyt c_{6A} OE lines (chapter 3.4.1.). The transcript levels turned out to be very similar in all genotypes tested. The only gene changed in all conditions was *ATC6* itself indicating no general effect on the overall gene expression by its presence. This is in agreement with the lack of an evident phenotype of the plants (chapter 4.1.2.). In plants showing defects in growth, pigmentation and photosynthetic performance, this unbalance can be confirmed by evident changes of gene expression, like it was shown for the *psad* and the *stn7* mutants (Pesaresi *et al.*, 2009b). The *psad* mutant displays a visible phenotype (Fig.3.16.) that is reflected by the genome transcript level. The transcript level of more than 1,500 genes is significantly changed according to wild type plants. Plants lacking the kinase STN7, which is a key player in light adaptation processes, do not show any visible phenotype. Nevertheless, the expression of

more than 300 genes is changed in the mutant. Compared to these values, the changed expression of only 44 genes in *atc6* leads to the idea of a minor role of this protein in *Arabidopsis*.

This observation is confirmed by testing the microarray data by real-time PCR (Fig.3.18). Most of the tested transcripts, which were significantly up or down regulated, showed a much lower difference to the wild type level if compared to the microarray studies. Clear downregulation could be confirmed for two genes, *CDC48* and *BAG6*.

CDC48 is a homohexameric AAA-ATPase chaperone, highly conserved in eukaryote organisms. It is part of an ubiquitin dependent proteolysis pathway and involved in many cellular processes like protein quality control, transcriptional and metabolic regulation, cell cycle progression and cell death (Stolz *et al.*, 2011). BAG6 (Bcl-2 associated athanogene) is a member of the BAG family that are cochaperones interacting with the heat shock protein HSP70. They are known to regulate PCD cellular pathways (Kang *et al.*, 2005). Since both proteins, CDC48 and BAG6, are involved in cell cycle and PCD processes, cytochrome c_{6A} might have a role in them resulting in the observed strict regulation of its abundance (chapter 4.1.1.). This can be confirmed by an up-regulation of *ATC6* during PCD induction, which is shown by microarray analysis available in the online database Genevestigator[©] (Swidzinski *et al.*, 2002) NASCArrays Experiment Reference number: *NASCARRAYS-30*).

4.5.2. Dimerization of cytochrome c_{6A}

In order to test current hypotheses and new indications for the function of cytochrome c_{6A} we performed interaction studies in yeast and *in vivo*. By yeast two hybrid approaches we could show that cytochrome c_{6A} is capable to build homodimers. This interaction persists even when the two conserved cysteine residues in the LIP (twelve amino acid loop that is missing in the algal form) are replaced by serine residues implying that the formation of homodimers is not dependent on the formation of disulphide bridges. Protein dimerization often serves as regulatory mechanism in signal transduction of biological networks. For example, in the physiological cell death pathway the two proteins Bcl-2 and Bax are regulated by their dimerization state. Bax is able to build homodimers, which promote apoptotic cell death. The two Bax proteins can be separated by Bcl-2 that builds a

heterodimer with one Bax protein preventing programmed cell death (Klemm *et al.*, 1998). It might be possible that dimerization of cytochrome c_{6A} combined with the strict regulation of its concentration are mechanism involved in signaling processes involved in PCD.

4.5.3. Stress treatment

Plants were exposed to different stress treatments to monitor the expression of *ATC6* (chapter 3.4.1.). Under drought condition, the expression was significantly lower than in untreated plants, suggesting a dependency of *ATC6* expression to drought stress response, in which the phytohormone abscisic acid (ABA) plays a central role (Raghavendra *et al.*, 2010). Further characterization of this interdependency by analysis of the transcript level of ABA reporter genes showed that the expression of *ATC6* is regulated in an opposite way than ABA concentration. Indeed, plants with higher level of ABA reporter transcripts show a decreased *ATC6* expression. In contrast, these ABA reporter transcript levels are not influenced by the presence of cytochrome c_{6A}. Additionally, to the mentioned post-transcriptional regulation (4.1.1.), there might be a regulation mechanism on the level of gene transcription that involves the perception of ABA concentrations in the plant cell. This confirms the tight regulation of the protein abundance on several levels of protein biosynthesis.

The expression profile of *ATC6* in young seedlings (chapter 3.4.3.) is consistent with a role in developmental processes and shows its importance in the first period of plant life. During germination and early development, the ABA level is reduced (Finkelstein and Gibson, 2002) and *ATC6* highly expressed, pointing out a probable relation between ABA and cytochrome c_{6A} (chapter 3.4.2.).

A genetic dissection of the relation between the ABA synthesis pathway and the presence of cytochrome c_{6A} by analysis of loss-of-function mutants did not reveal any phenotype changes and gives no indications for a direct connection between the protein and the generation of ABA (chapter 3.4.4.). A direct interaction between ABA1 and NPQ1, the first proteins of the ABA synthesis pathway and cytochrome c_{6A} is also unlikely as shown in yeast two-hybrid assays (chapter 3.6.1.).

Analysis in maize suggested that the balance between ABA and ethylene establishes the onset and progression of endosperm program cell death. An inhibition of ABA synthesis

leads to an acceleration of the execution of the PCD processes in the developing endosperm (Young and Gallie, 1999). A response of cytochrome c_{6A} expression to ABA and its higher concentration in early development stages are further indications for an involvement of the protein in PCD processes.

4.5.4. Hypothesis 1: Cytochrome c_{6A} is involved Program Cell Death Processes

In plants PCD is a mechanism involved in a number of developmental processes, including embryo formation, degeneration of the aleurone layer during monocot seed germination, differentiation of tracheary elements in water conducting xylem tissues, formation of root aerenchyma and epidermal trichomes, anther tapetum degeneration, floral organ abscission, pollen self-incompatibility, remodeling of some types of leaf shape and leaf senescence (Thomas and Franklin-Tong, 2004; Gechev *et al.*, 2006; Gechev *et al.*, 2008). It plays also a role in immunity to biotrophic pathogen and necrosis of tissue upon abiotic and biotic attacks (Swidzinski *et al.*, 2002; Coffeen and Wolpert, 2004; Gechev *et al.*, 2008). Chloroplasts are primary sources of signals initiating plant PCD, via a retrograde signal network from organelle to nucleus (Kleine *et al.*, 2009)**.** Indeed, generation of hydrogen peroxide and superoxide anion radicals by the photosynthetic machinery triggers PCD in the stress response of the plant cell (Gechev *et al.*, 2006). ACD1 and ACD2 (Accelerated Cell Death) are examples of plastidial proteins playing a role in PCD. In plants with suppressed mRNA of ACD1 (a pheophorbide-A oxygenase) the chlorophyll breakdown product pheophorbide-A is accumulating and PCD is induced (Hirashima *et al.*, 2009). ACD2 modulates the extent of PCD triggered by both *Pseudomonas syringae* and protoporphyrin IX (PPIX) treatment (Yao and Greenberg, 2006).

Down-regulation of *BAG6* and *CDC48* when cytochrome c_{6A} is missing, dimerization of cytochrome c_{6A} proteins, response to ABA, up-regulation during PCD induction, strict regulation of its concentration and its higher concentration in young developing plants, are all indications for a putative involvement of cytochrome c_{6A} in PCD processes. Beside the ABA ethylene ratio, which is known to influence PCD induction, ABA inhibits the expression of *ATC6.* By the absence of cytochrome c_{6A}, the two proteins BAG6, a modulator of Bcl-2, and CDC48 are down-regulated. Downregulation of BAG6 could lead to a change in the Bax-

Bcl-2 dimerization behavior and to changes in PCD induction (Fig 4.1). The disulphide formation in the LIP of cytochrome c_{6A} could play an essential role in PCD induction, since involvement of disulphide redox proteins has been shown. The protein *disulphide isomerase 5* (PDI5), which contains two thioredoxin motifs including disulphide bridges, was described to chaperone and inhibit cysteine dependent proteases and it was proposed that it is required for embryogenesis and temporal progression of PCD in seeds (Ondzighi *et al.*, 2008).
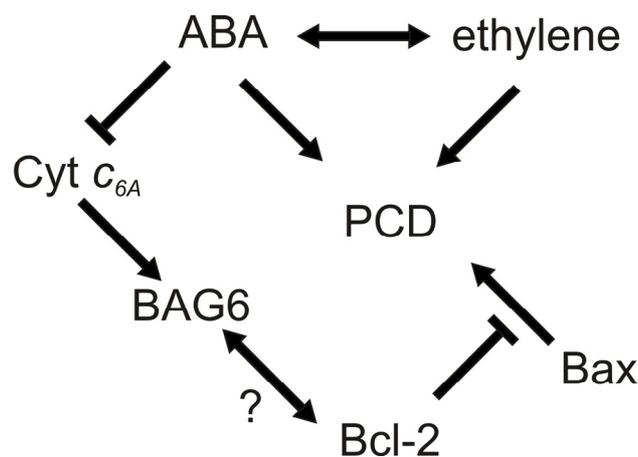
Figure 4.1: Putative Role of Cytochrome c_{6A} in Programmed Cell Death (PCD).

More experiments are required to prove this hypothesis, for instance, a more detailed characterization of the role of cytochrome c_{6A} in PCD-inducing conditions and studies on the expression and interaction studies of the involved proteins.

4.6. Cytochrome c_{6A}, a Stromal Redox Regulating Protein

4.6.1. Yeast interaction studies

The elusive presence of the cytochrome c_{6A} *in planta* prevents gaining any information about the protein characteristics, such as localization or *in vivo* interaction partners. During this work, yeast two hybrid approaches were applied to find possible interactors and pathways involving cytochrome c_{6A}. Beside its homodimerization, interactions with OTP86 and PsaF could be confirmed. A weak interaction between subunit F of the photosystem I and

cytochrome c_{6A} could be detected in split-ubiquitin and ternary yeast assays, which were performed with the total mature protein and with the stromal or lumenal domain of PsaF, respectively. Interestingly, detailed dissection of this interaction revealed that cytochrome c_{6A} only interacts with the stromal domain of PsaF in yeast, but it does not with the lumenal domain. This suggests a stromal localization of cytochrome c_{6A}, in contrast to what was proposed by Gupta et al. (2002) concerning its lumenal targeting. A strong interaction with the stromal RNA editing protein OTP86, total mature protein and different domains like PEX11, could be also confirmed and supports the concept of a cytochrome c_{6A} as stromal protein.

4.6.2. *In vivo* studies

Since studies in yeast are limited because they are artificial systems, expressing a protein in a heterologous organism, the line harboring the chimeric RbcS-Cyt c_{6A}-GFP was used to confirm interactions in *Arabidopsis*. Co-immunoprecipitation experiments with GFP antibodies showed that the stromal portions of photosystem I could be pulled down, confirming the observed interaction with photosystem I subunits in yeast. As a consequence of this interaction, accumulation of RbcS-Cyt c_{6A}-GFP leads to an impaired photosynthetic linear electron flow. These observations indicate that there is not only a peripheral interaction with photosystem I, but that cytochrome c_{6A} is able to influence the electron transfer processes. Similar phenotypes can be observed in *psad1-1* and *psae1-3*, mutants lacking stromal exposed components of photosystem I, which leads to a reduced electron transfer rate (Ihnatowicz *et al.*, 2004; Ihnatowicz *et al.*, 2007).

4.6.3. Hypothesis 2: Cytochrome c_{6A} as a Stromal Redox Regulator

Disulfide/dithiol exchange reactions catalyzed by thioredoxin are an example for a light dependent redox regulation systems in plants. Electrons from photosystem I are transferred via ferredoxin (Fd) and ferredoxin thioredoxin reductase (FTR) to thioredoxin, which is able to reduce target disulphide proteins. Reduced by electrons coming from photosynthesis,

thioredoxin can serve as a switch, in the cell, for light dependent processes, such as the activation of enzymes of the Calvin cycle (Lindahl and Kieselbach, 2009).

The results of interaction studies obtained in this work, can let us suppose a new hypothesis concerning the function of cytochrome c_{6A}, in which cytochrome c_{6A} acts as a redox regulatory protein in the stroma, activating disulphide exchange processes similar to the thioredoxin system (Fig.4.2). Within this frame, cytochrome c_{6A} interacting with OTP86, an mRNA editing protein, could oxidize stromal target reduced proteins by a disulphide exchange reaction involving the cysteines of its LIP. In its reduced form cytochrome c_{6A} might move to photosystem I and leave the target protein in its oxidized state.

Electron transfer in photosystem I is mediated by iron sulphur clusters, which are capable of transferring single electrons along a redox potential cascade, from the donor subunits to the final electron acceptor ferredoxin. Cytochrome c_{6A} might inject the electrons into the photosynthetic machinery by means of its heme group that facilitates a step by step transfer of single electrons, which can be taken over by stromal components of the photosystem I such as PsaF. Electrons are then transferred further to ferredoxin and can be used to build up new reducing power in the stroma by generating NADPH. Another possible pathway of cytochrome c_{6A} mediate electron flow could be the injection back into the ferredoxin/thioredoxin system, which reduces disulphide target proteins in the stroma. This would lead to a kind of cyclic electron flow involving the redox regulation of the stroma. Cytochrome c_{6A} might therefore oxidize stromal redox proteins under reducing conditions to ensure a flexibility of the ferredoxin/thioredoxin system and a possibility to reset the activation switch. Another possible function could be feeding photosystem I and redox systems, which depend on photosystem I, with electrons from other metabolic processes. This might be important in conditions without fully functional light reactions such as darkness or seed development.
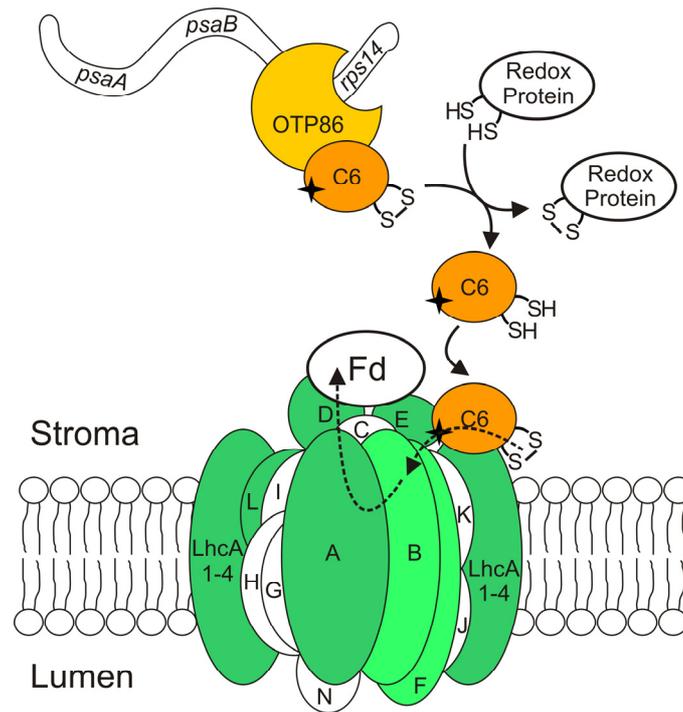
Figure 4.2: Putative Role of Cytochrome c_{6A} in Stromal Redox Regulation. Proteins interacting with cytochrome c_{6A} are colored: yeast assays-tested in orange and CoIP-identified in green. Putative electron transfer is shown with dashed arrows. The black star indicates the heme group of cytochrome c_{6A}.

Combined with a possible involvement of cytochrome c_{6A} in PCD processes (chapter 4.5.), it can be speculated that the oxidized redox proteins in the stroma are part of a signaling network, which includes PCD dependent components. In this scenario cytochrome c_{6A} could act as a crossing-point of photosynthesis and PCD processes. Cytochrome c_{6A} could keep signal proteins in an oxidized and maybe inactive state, during conditions in which the photosynthetic electron transport chain is in a *relaxed* state and the stroma is reduced in a moderate way. Hence, it might contribute to prevent the signal transduction to the nucleus and initiation of the PCD. During excessive light condition, overenergization of photosynthetic complexes and stromal redox regulation occur. Therefore, cytochrome c_{6A} might not be able to stabilize the signal proteins in an oxidized state, because of the strongly reduced stroma together with the impaired electron transfer to the overloaded PSI. In this case, the target signal proteins might be reduced and could communicate the PCD signal from the chloroplast to the nucleus. However, this putative signal transduction pathway might be controlled in redundant and alternative explaining a missing phenotype in plants lacking cytochrome c_{6A}.

4.7. Perspectives

In this work, current hypotheses concerning the function of cytochrome c_{6A} have been tested, but they could not find support in any of the performed experiments. Neither a role of cytochrome c_{6A} in photosynthesis of adult plants (Gupta *et al.*, 2002) nor in lumenal redox regulation (Schlarb-Ridley *et al.*, 2006) are likely. Nevertheless, based on the performed experiments new indications for its function could be found and, considering them, two new hypotheses could be proposed. Future work should deal with testing these hypotheses with new approaches to unravel the function of cytochrome c_{6A}.

First of all the localization of the protein inside the plastidic compartments has to be clarified, because experiments such as interaction studies can only be verified in consideration of the protein location. Published data suggest a lumenal localization of cytochrome c_{6A} (Gupta *et al.*, 2002), whereas in this work only indication for a stromal localization could be found. Indications of its localization could be provided by an *in situ* hybridization assay with an expressed chimeric protein (GFP- or HA-tag), using immuno gold labeling of the protein and detection via electron microscopy. Even though a successful detection might be problematic, due to its very low abundance shown in western blot analyses.

Approaches analyzing the phenotype of adult plants could not provide sufficient indications for the function of cytochrome c_{6A}. However, its higher expression level in seeds and seedlings supports the idea of a function in early development stages. For this reason, future *in vivo* approaches during early-growth period might provide more promising results regarding its role. Comparison of embryo development between the mutant *atc6*, the Cyt c_{6A} OE lines and the wild type should give first hints of presence and function of the protein.

Furthermore, involvement in PCD processes can be investigated in a genetic approach by creating double mutants of plants with altered expression levels of PCD-involved proteins, as BAX, Bax inhibitor 1, PDI5 or Bcl-2.

Concerning the hypothesis about cytochrome c_{6A} as a stromal redox regulator, the interaction of cytochrome c_{6A} with photosystem I should be investigated in more detail. *In vitro* experiments including recombinant expressed cytochrome c_{6A} protein in reduced or

oxidized form and isolated thylakoid membranes might show a possible electron transfer from cytochrome c_{6A} to photosystem I.

Altogether, testing the new ideas emerged concerning the function of cytochrome c_{6A} might unravel its true function, which has changed during the evolutionary process.

Appendix

Primer	Sequence	Experiment
Genotype Screening		
C6seq1s	AGACTTGTTCTCTCTGGTGCCT	Genotyping *atc6*
2Cyt6as	CTTTCGAGGTCTTTTGTGAAAAGC	Genotyping *atc6*
dMWs	CATCCCTTCTTTCACCGGCCT	Genotyping *pete1*
dR4as	CACRATCTTCTCTCCTTTAGC	Genotyping *pete1*
139sl	GAGTTTGCTTTTAGAGCCATCCATTGT	Genotyping *pete2*
75as	TAAAGCCTCAACCATCAAATCATCC	Genotyping *pete2*
psaD1-1s	ATGGCAACTCAAGCCGCCGG	Genotyping *psad1-1*
psaD1-999as	TATGGTTTTGGATCGGAGACT	Genotyping *psad1-1*
dSpm-1-3´7	CTTATTTCAGTAAGAGTGTGGGGTTTT GG	Genotyping *psad1-1*
At4g28750-F	TACAAAATGAACACGATTGCTACA	Genotyping *psae1-3*
At4g28750-R	CATTTCACCATTCTGCAGATTTAC	Genotyping *psae1-3*
Taq3	CTGATACCAGACGTTGCCCGCATAA	Genotyping *psae1-3*
psaf-100s	AAGAATCTAAAGCTCCTCCC	Genotyping *psaf*
psaf732as	GCATAACAATCCGTACTTCC	Genotyping *psaf*
LB3	TAGCATCTGAATTTCATAACCAATCTCGATACAC	Genotyping SAIL lines
aba1.2s	CTAGCATTGGAGCTTGATGA	Genotyping *aba1*
aba1.2as	TCATCTTCAAACCACTCTCG	Genotyping *aba1*
LBb1	GCGTGGACCGCTTGCTGCAACT	Genotyping SALK lines
aba3.2s	GATCCTCATAGGATAGGCTT	Genotyping *aba3*
aba3.2as	TTCTCATCTGCACAGCACGA	Genotyping *aba3*
abi1.2s	ATGGAGGAAGTATCTCCGGC	Genotyping *abi1*
abi1.2as	ACGGATAATGGAAGTGCAGT	Genotyping *abi1*
abi2.1s	AGTAATTCCGGATCCAGAAG	Genotyping *abi2*
abi2.1as	CTAACGAAAACACACACA	Genotyping *abi2*
Gateway Cloning		
GWc6ps	GGGGACAAGTTTGTACAAAAAAGCAGGCTCCAT… …GAGACTTGTTCTCTCTGG	Cloning *ATC6* (full CDS)
GWc6as	GGGGACCACTTTGTACAAGAAAGCTGGGTCTAG… …TCCGTAGATACAGTTG	Cloning *ATC6* (full CDS)
GWc6tagas	GGGGACCACTTTGTACAAGAAAGCTGGGTCGTC… …CGTAGATACAGTTGGCCAGC	Cloning *ATC6* (without stop codon)
PETE2GWs	GGGGACAAGTTTGTACAAAAAACGAGGCTATG… …GCCTCAGTAACCTCAGC	Cloning *PETE2* (full CDS)
PETE2GWframeas	GGGGACCACTTTGTACAAGAAAGCTGGGTCGTT… …AACGGTGACTTTACCGAC	Cloning *PETE2* (without stop codon)
cTPGWs	GGGGACAAGTTTGTACAAAAAAGCAGGCTTCAT… …GGCTTCCTCTATGCTCTCC	Cloning for N-term RbcS-*ATC6*-GFP
C6cTPs	GCGAATTCTCCCAACAGGTCAATGGAAG	Cloning for N-term RbcS-*ATC6*-GFP
cTPas	GCGAATTCCATGCAGCTAACTCTTCCCCC	Cloning for N-term RbcS-*ATC6*-GFP
Topo Cloning		
MC6TOPOs	CACCTCCCAACAGGTCAATGGAAG	Expression in *E. coli*
C6TAGas	CTAGTCCGTAGATACAGTTG	Expression in *E. coli*
Doubles	GAGGATCCTCCCAACAGGTCAATGGAAG	Expression in *E. coli*
Doubleas	CTGGATCCGTCCGTAGATACAGTTGG	Expression in *E. coli*

Real Time PCR

ubis	GGAAAAAGGTCTGACCGACA	RT-PCR reference gene
ubias	CTGTTCACGGAACCCAATTC	RT-PCR reference gene
DesaturaseRTs	GGTTCTATTGGTTTCTACGA	RT-PCR of *AT1G06360*
DesaturaseRTas	GATGTGTCTTTAGTCTTCCA	RT-PCR of *AT1G06360*
MYB75RTs	GACTACTGAAGAAGATAGTCTC	RT-PCR of *AT1G56650*
MYB75RTas	ATTAAAGACCACCTATTCCC	RT-PCR of *AT1G56650*
ATPP2RTs	TATTCTACAGGCTTGATCTC	RT-PCR of *AT1G65390*
ATPP2RTas	ATCTCTATCCGAAATGTCAC	RT-PCR of *AT1G65390*
ARR15RTs	GTTTAGATGGAGACAATGGA	RT-PCR of *AT1G74890*
ARR15RTas	AAGACATTATCACTACTGGG	RT-PCR of *AT1G74890*
nod-like#1RTs	CTTGGATACACAAATGTCTC	RT-PCR of *AT2G16660*
nod-like#1RTas	GATGTAGAGTGAATTAGGCA	RT-PCR of *AT2G16660*
BAG6RTs	AGAAATTGAAGGAGATAGCC	RT-PCR of *AT2G46240*
BAG6RTas	TTATACTAGGATGCAATCCC	RT-PCR of *AT2G46240*
mateRTs	TTGTATCCCTTTAACCTCTG	RT-PCR of *AT3G23550*
mateRTas	GATGATTGTAGATGAATCCC	RT-PCR of *AT3G23550*
QQSNAs	ATGAAGACCAATAGAGAGCA	RT-PCR of *AT3G30720*
QQSNAas	TCAGTAGTTGTAGAACTGAA	RT-PCR of *AT3G30720*
EXPL1RTs	GTAGTCATCTTCCTCTTCTC	RT-PCR of *AT3G45970*
EXPL1RTas	GTAGATAGAAGGGATAGCTG	RT-PCR of *AT3G45970*
CDC48RTs	TAATCAAGGGAAAGAAGAGG	RT-PCR of *AT3G53230*
CDC48RTas	TGAGATTAGACCTAACAACC	RT-PCR of *AT3G53230*
BetaAmyRTs	GATCCCGATATCTACTACAC	RT-PCR of *AT4G15210*
BetaAmyRTas	GAAGCTACTCATGTAATCAC	RT-PCR of *AT4G15210*
HSP26RTs	AGATTCTCACACTTTCTCTG	RT-PCR of *AT4G21870*
HSP26RTas	ATCATATCTATCGATTCCGG	RT-PCR of *AT4G21870*
nod-like#2RTs	AACCTATACCTTATTGGCAG	RT-PCR of *AT4G34950*
nod-like#2RTas	CGTATCCTTTAAGAATCCCT	RT-PCR of *AT4G34950*
CYP79B2RTs	TATGGACAAGTATCATGACC	RT-PCR of *AT4G39950*
CYP79B2RTas	CATTACAAGCTCCTTAATGG	RT-PCR of *AT4G39950*
aba-regRTs	CAAGAACTTCATCAGACAG	RT-PCR of *AT5G05440*
aba-regRTas	CGACACTAAAGCTTATCAC	RT-PCR of *AT5G05440*
EXL3RTs	AGTAGATGGGATGATAAGTG	RT-PCR of *AT5G51550*
EXLRTas	CTATGATCGTTCAACATCTG	RT-PCR of *AT5G51550*
ARR6RTs	ATAGATGTCTTGAAGAAGGG	RT-PCR of *AT5G62920*
ARR6RTas	ACATTCTCTGTTTCTAGCTC	RT-PCR of *AT5G62920*
PSBARTs	GTGCCATTATTCCTACTTCTG	RT-PCR of *ATCG00020*
PSBARTas	AGAGATTCCTAGAGGCATACC	RT-PCR of *ATCG00020*
RPS12ANAs	ATGCCAACCATTAAACAACTTA	RT-PCR of *ATCG00065*
RPS12ANAas	ATACACCCGAGTACATGTTCC	RT-PCR of *ATCG00065*
PSABRTs	GGCTGAGTGGCATGTATTTC	RT-PCR of *ATCG00340/ATCG00350*
PSABRTas	TTGTATTCCTCGGAAGCCTC	RT-PCR of *ATCG00340/ATCG00350*
RBCLNAs	GGCAGCATTCCGAGTAACTC	RT-PCR of *ATCG00490*
RBCLNAas	GATTCGCAGATCCTCTAGAC	RT-PCR of *ATCG00490*
PETGNAs	ATGATTGAAGTTTTTTTATTTGG	RT-PCR of *ATCG00600*
PETGNAas	TTAAAAGTCCAACTGATCAC	RT-PCR of *ATCG00600*
PSBBRTs	TGATCCAATGTGGAGACAAG	RT-PCR of *ATCG00680*
PSBBRTas	TACCCAATGCCAAATAGCTG	RT-PCR of *ATCG00680*
RPS12NAs	ACTATCACCCCCAAAAAACC	RT-PCR of *ATCG00905*
RPS12NAas	TTATTTTGGCTTTTTGACCC	RT-PCR of *ATCG00905*
PSAFRTs	CTCTCAATGCTCAGATCGAG	RT-PCR of *AT1G31330*
PSAFRTas	TTCATCGCGGGTTTCTTCTC	RT-PCR of *AT1G31330*

COR15aRTs	AAGAAGTCGTTGATCTACG	RT-PCR of *AT2G42540*
COR15aRTas	TTTCTCAGCTTCTTTACCC	RT-PCR of *AT2G42540*
KIN2RTs	TCAGAGACCAACAAGAATG	RT-PCR of *AT5G15970*
KIN2RTas	TTGTCCTTCACGAAGTTAA	RT-PCR of *AT5G15970*

Yeast Two Hybrid and Split Ubiquitin Assays

C6wtps	CGGAATTCCAACAGGTCAATGGAAGAGGA	Cloning *ATC6* (CDS without cTP)
c6TAGas	GCGGTCGACTAGTCCGTAGATACAGTTGG	Cloning *ATC6* (CDS without cTP)
C6SERs	TCCACACCGAGAGGACAATCTACCTTTGGACCG	Cloning *ATC6* (cys/ser mutation)
C6SERas	CGGTCCAAAGGTAGATTGTCCTCTCGGTGTGGA	Cloning *ATC6* (cys/ser mutation)
PETE1s	GCGTCGACGGGCTGGAAATGCGGATGGCCATG	Cloning *AT1G76100* (CDS without cTP)
PETE1as	GCGTCGACTTACTTGACGGTGAGTTTCCC	Cloning *AT1G76100* (CDS without cTP)
PETE2s	GCGAATCCGCCGTAGCGGCTGCAGCTTC	Cloning *AT1G20340* (CDS without cTP)
PETE2as	GCGGATCCTTAGTTAACGGTGACTTTACCG	Cloning *AT1G20340* (CDS without cTP)
FKBP13s	CGGTCGACCTATGAGCTCCTTGGGGTTTTC	Cloning *AT5G45680* (CDS without cTP)
FKBP13as	CGGTCGACTCAAGCTTTACCTATGTACTC	Cloning *AT5G45680* (CDS without cTP)
PsbO1s	CGGAATTCATGGCAGCCTCTCTCCAATC	Cloning *AT5G66570* (CDS without cTP)
PsbO1as	CGGTCGACTCACTCAAGTTGACCATACC	Cloning *AT5G66570* (CDS without cTP)
PsbO2s	CGGAATTCATGGCAACTTCTCTCCAAGC	Cloning *AT3G50820* (CDS without cTP)
PsbO2as	CGGTCGACTCACTCAATCTGACCGTACC	Cloning *AT3G50820* (CDS without cTP)
HCF164SUs	CGCTCTAGAAAAATGGGATTCCCTGAATCTC	Cloning *AT4G37200* (CDS without cTP)
HCF164SUas	ATGGAGGCCTCGTCCATGGCTTAAGGGATCAG	Cloning *AT4G37200* (CDS without cTP)
17.4s	CGGAATTCATGGCTTCGCTTCCTGTTCA	Cloning *AT5G53490* (CDS without cTP)
17.4as	CGGTCGACCTATCGGCATCCCAACACAAG	Cloning *AT5G53490* (CDS without cTP)
NPQ1ADBDs	GACCCG GGACTTGGCATTACAAGAAAGAG	Cloning *AT1G08550* (CDS without cTP)
NPQ1ADas	GTATCGATGCTACCTGACCTTCCTGATTG	Cloning *AT1G08550* (CDS without cTP)
NPQ1BDas	CAGTCGACCCCTACCTGACCTTCCTGATTG	Cloning *AT1G08550* (CDS without cTP)
ABA1ADBDs	GACCCGGGGAGCTTTGGAAGCTATTGATAT	Cloning *AT5G67030* (CDS without cTP)
ABA1ADas	CTGGATCCCTCAAGCTGTCTGAAGTAAT	Cloning *AT5G67030* (CDS without cTP)
ABA1BDas	CAGTCGACCCTCAAGCTGTCTGAAGTAAT	Cloning *AT5G67030* (CDS without cTP)
PrxQ57s	GCGAATTCTCCTCTTCTCTCAAAGGCTTAA	Cloning *AT3G26060* (CDS without cTP)
PrxQas	CTGGATCCCTCAAGCAGCTTTGAGAAACTTC	Cloning *AT3G26060* (CDS without cTP)
mStn7_NheI_AAAA_s	TAAGCTAGCTAAAAATGGCTCAATTGATCGATACGG	Cloning *AT1G68830* (CDS without cTP)
Stn7_NcoI_r	ATTCCATGGAGCTCCTCTCTGGGGATCCA	Cloning *AT1G68830* (CDS without cTP)
Riewtps	CGCTCTAGAAAAATGGCGTCGAGTATTCCAGCAGA	Cloning *AT4G03280* (CDS without cTP)
Riematas	ATGGAGGCCTCGAGACCACCATGGAGCATCACC	Cloning *AT4G03280* (CDS without cTP)
Up2ADBD2s	GAGAATTCCTCA ACACCGACTGGACTTAC	Cloning *AT1G28520* (CDS without cTP)
Up2AD2as	GTCCCGGGAGTCACTCTAAGAAACTCATGT	Cloning *AT1G28520* (CDS without cTP)
Up1AD2s	GAGAATTCTGCAGATCTGCTTCTCACAAG	Cloning *AT3G15240* (CDS without cTP)
UP1AD2as	GTCCCGGGAGTCAGGGGATATAATAGTCGC	Cloning *AT3G15240* (CDS without cTP)
OTP86PEX11ADBDs	GACCCGGGAAATGCGTTGGTTTCCATGTA	Cloning PEX11 domain of *AT3G63370*
OTP86PEX11ADas	GTATCGATGTTAGTGCAATTCCATTCCTGCCA	Cloning PEX11 domain of *AT3G63370*
OTP86PEX11BDas	CAGTCGACCCTTAGTGCAATTCCATTCCTGCCA	Cloning PEX11 domain of *AT3G63370*
OTP86IntDomADBDs	GACCCGGGAGAGAAATTGTCCGAGGTTACTAGGAAG	Cloning Y3H-domain of *AT3G63370*
IntDomADas	GAGGATCCCCCTAATAAGCAATCGCTATCCTCTCACTATG	Cloning Y3H-domain of *AT3G63370*
IntDomBDas	CAGTCGACCCCTAATAAGCAATCGCTATCCTCTCACTATG	Cloning Y3H-domain of *AT3G63370*
OTP86ADBDs	GACCCGGGAATGGAATACGCGGTAACTAA	Cloning *AT3G63370* (full CDS)
OTP86ADas	ATGAGCTCTCACCAAGAATCTCCGCAAG	Cloning *AT3G63370* (full CDS)
OTP86BDas	ATGTCGACTCACCAAGAATCTCCGCAAG	Cloning *AT3G63370* (full CDS)
hp1ADBDs	GACCCGGGGATGTGTGGTTATGGCTGTTCA	Cloning *AT1G73090* (full CDS)
hp1ADas	GTATCGATGTCATCTGTATTGTTTGACCA	Cloning *AT1G73090* (full CDS)
hp1BDas	CAGTCGACCCTCATCTGTATTGTTTGACCA	Cloning *AT1G73090* (full CDS)
SULhc2s	CATCTAGAAAAATGGCCGTCGCAGCTGATCCAGA	Cloning *AT3G61470* (CDS without cTP)

SULhc2as	CTCCATGGCCCTTGGGTGTGAAAGCAGCGA	Cloning *AT3G61470* (CDS without cTP)
LHCloopADABs	GAGAATTCCTCAACACTCCGTCATGGTA	Cloning *AT3G61470* (lumenal loop)
LHCloopADBDas	CTGGATCCTTAGTCCGTGAAATACTCTTGCT	Cloning *AT3G61470* (lumenal loop)
LHCA2stromas	GAGAATTCCGCGCCGTCGCAGCTGATC	Cloning *AT3G61470* (stromal loop)
LHCA2stromaas	CTGGATCCTCAGCAGTGGACTATCTCGGCTT	Cloning *AT3G61470* (stromal loop)
PSAFSUs	CATCTAGAAAAATGGATATCTCAGGTTTGACTCC	Cloning *AT1G31330* (CDS without cTP)
PSAFSUas	CTCCATGGCCAACATCCTTAGCAATGAGATC	Cloning *AT1G31330* (CDS without cTP)
PSAFADBDs	GAGAATTCGATATCTCAGGTTTGACTCCTTGCAAGGA	Cloning *AT1G31330* (lumenal domain)
PSAFADBDas	CTGGATCCTTATCCCCAATGCCGCTGGTCTC	Cloning *AT1G31330* (lumenal domain)
PSAFADBDmut1bs	GAGAATTCGATATCTCAGGTTTGACTCCTTCCAAGGA	Cloning *AT1G31330* (cys/ser mutation)
PSAFmut2bas	GTCTGACCCGGATAACAAT	Cloning *AT1G31330* (cys/ser mutation)
PSAFmut2bs	ATTGTTATCCGGGTCAGAC	Cloning *AT1G31330* (cys/ser mutation)
PSAFstromas	GAGAATTCGCTATTAGTGGTGAGAAGAA	Cloning *AT1G31330* (stromal domain)
PSAFstromaas	CTGGATCCTCATTAAACATCCTTAGCAATGAG	Cloning *AT1G31330* (stromal domain)
VPS54ADBDs	GACATATGGCTTCAACGAAGCTCCCTG	Cloning *AT4G19490* (CDS without cTP)
VPS54ADBDas	CTGGCCTCCATGGCCTCACTCAGCTTCGCCTGCTT	Cloning *AT4G19490* (CDS without cTP)
DAGs	GAGAATTCACCCGGATGGATAGGTCTGG	Cloning *AT2G35240* (CDS without cTP)
DAGas	CTGGATCCTCAACGCATGTTCTCCCTCC	Cloning *AT2G35240* (CDS without cTP)
PSAEY2Hs	GAGAATTCGCAGCCGAAGATCCTGCTCC	Cloning *AT4G28750* (CDS without cTP)
PSAEY2Has	CTGGATCCTTAAGCTGCAACTTCTTCGA	Cloning *AT4G28750* (CDS without cTP)
PEX11ADBDs	GAGAATTCATGAGTACCCTTGAGACCAC	Cloning *AT1G01820* (full CDS)
PEX11ADBDas	CTGGATCCTCAGACCATCTTGGACTTGG	Cloning *AT1G01820* (full CDS)
PEX11CSUs	GATCTAGAAAAATGAGTACCCTTGAGACCAC	Cloning *AT1G01820* (full CDS)
PEX11CSUas	GACCATGGCCGACCATCTTGGACTTGGGAT	Cloning *AT1G01820* (full CDS)

Abbreviations

(c)DNA	(complementary) Deoxyribonucleic acid		P680	Photosystem II reaction center
(m)RNA	(messenger) Ribonucleic acid		P700	Photosystem I reaction center
35S CaMV	35S promoter of *Cauliflower mosaic virus*		PAGE	polyacrylamide gel electrophoresis
3-AT	3-amino-1,2,4-triazole		PAM	Pulse-amplitude modulation
ABA	Abscisic acid		PCD	Programmed cell death
ADP	Adenosine diphosphate		PCR	Polymerase chain reaction
ATP	Adenosine triphosphate		PDB	Protein Data Bank
Ax	Antheraxanthin		P_i	Phosphate
BN	Blue native		Pm'	Maximum photosystem I reduction
bp	Basepair		PQ	Plastochinone
Car	Carotenoide		PSI	Photosystem I
CDS	Coding sequence		PSII	Photosystem II
chl	Chlorophyll		Q	Quinone
CoIP	Co-immunoprecipitation		qE	Heat dissipation
Col-0	*Arabidopsis thaliana* background Columbia-0		qI	Photoinhibition
cTP	Chloroplast transit peptide		qP	photochemical quenching
Cub	C-term of Ubiquitin		qT	State transitions
dNTP	Deoxyribonucleotide		RFP	Red fluorescent protein
dsRED	Gene of the red fluorescent protein		RNAi	RNA-interference
DTT	Dithiothreitol		SDS	Sodium dodecyl sulfate
EDTA	Ethylenediaminetetraacetic acid		SSU	Small subunit
FC	Fold change		SU	Split-ubiquitin
FNR	Ferredoxin-NADP oxidoreductase		T-DNA	Transfer-DNA
Fv/Fm	PSII maximum efficiency		TL	Thermolysin
GFP	Green fluorescent protein		UTR	Untranslated region
HA	Hemagglutinin epitope		VAZ	Vx+Ax+Zx
HPLC	High-performance liquid chromatography		VDE	Violaxanthin-de-epoxidase
Ler	*Arabidopsis thaliana* background Landsberg		Vx	Violaxathin
LhcI	Light-harvesting complex I		Y(NA)	Acceptor side limitation of photosystem I
LHCII	Light-harvesting complex II		Y(ND)	Donor side limitation of photosystem I
LIP	Loop insertion peptide		Y2H	Yeast two hybrid assay
Lut	Lutein		Y3H	Ternary trap assay
$NADP^+/H$	Nicotinamide adenine dinucleotide phosphate		ZEP	Zeaxanthin-epoxidase
NPQ	Non-photochemical quenching		Zx	Zeaxanthin
Nub	N-term of Ubiquitin		β-DM	β-dodecyl maltoside
Nx	Neoxanthin		Φ_I	Yield of photosystem I
OE	Overexpressor		Φ_{II}	Yield of photosystem II

References

- **Allen, J.F.** (2002). Photosynthesis of ATP - Electrons, proton pumps, rotors, and poise. Cell **110,** 273-276.

- **Allen, J.F.** (2005). A redox switch hypothesis for the origin of two light reactions in photosynthesis. FEBS Letters **579,** 963-968.

- **Alonso, J.M., Stepanova, A.N., Leisse, T.J., Kim, C.J., Chen, H., Shinn, P., Stevenson, D.K., Zimmerman, J., Barajas, P., Cheuk, R., Gadrinab, C., Heller, C., Jeske, A., Koesema, E., Meyers, C.C., Parker, H., Prednis, L., Ansari, Y., Choy, N., Deen, H., Geralt, M., Hazari, N., Hom, E., Karnes, M., Mulholland, C., Ndubaku, R., Schmidt, I., Guzman, P., Aguilar-Henonin, L., Schmid, M., Weigel, D., Carter, D.E., Marchand, T., Risseeuw, E., Brogden, D., Zeko, A., Crosby, W.L., Berry, C.C., and Ecker, J.R.** (2003). Genome-wide insertional mutagenesis of *Arabidopsis thaliana*. Science **301,** 653-657.

- **Armbruster, U., Hertle, A., Makarenko, E., Zühlke, J., Pribil, M., Dietzmann, A., Schliebner, I., Aseeva, E., Fenino, E., Scharfenberg, M., Voigt, C., and Leister, D.** (2009). Chloroplast proteins without cleavable transit peptides: Rare exceptions or a major constituent of the chloroplast proteome? Molecular Plant **2,** 1325-1335.

- **Arnon, D.I., Allen, M.B., and Whatley, F.R.** (1954). Photosynthesis by isolated chloroplasts. Nature **174,** 394-396.

- **Baena-González, E., and Aro, E.-M.** (2002). Biogenesis, assembly and turnover of photosystem II units. Philos Trans R Soc Lond B Biol Sci. **357,** 1451-1460.

- **Baginsky, S., Siddique, A., and Gruissem, W.** (2004). Proteome analysis of *Tobacco* bright yellow-2 (BY-2) cell culture plastids as a model for undifferentiated heterotrophic plastids. Journal of Proteome Research **3,** 1128-1137.

- **Baniulis, D., Yamashita, E., Zhang, H., Hasan, S.S., and Cramer, W.A.** (2008). Structure - function of the cytochrome b_6f complex. Photochemistry and Photobiology **84,** 1349-1358.

- **Bannai, H., Tamada, Y., Maruyama, O., Nakai, K., and Miyano, S.** (2002). Extensive feature detection of N-terminal protein sorting signals. Bioinformatics **18,** 298-305.

➢ **Bellafiore, S., Barneche, F., Peltier, G., and Rochaix, J.-D.** (2005). State transitions and light adaptation require chloroplast thylakoid protein kinase STN7. Nature **433,** 892-895.

➢ **Ben-Shem, A., Frolow, F., and Nelson, N.** (2003). Crystal structure of plant photosystem I. Nature **426,** 630-635.

➢ **Ben-Shem, A., Frolow, F., and Nelson, N.** (2004). Evolution of photosystem I - from symmetry through pseudosymmetry to asymmetry. FEBS Letters **564,** 274-280.

➢ **Benjamini, Y., and Hochberg, Y.** (1995). Controlling the false discovery rate: A practical and powerful approach to multiple testing. Journal of the Royal Statistical Society. Series B (Methodological) **57,** 289-300.

➢ **Bolle, C.** (2009). Phenotyping of *Arabidopsis* mutants for developmental effects of gene deletions. Methods in Molecular Biology **479,** 1-18.

➢ **Bölter, B., and Soll, J.** (2007). Import of plastid precursor proteins into *pea* chloroplasts. Methods in Molecular Biology **390,** 195-206.

➢ **Bonardi, V., Pesaresi, P., Becker, T., Schleiff, E., Wagner, R., Pfannschmidt, T., Jahns, P., and Leister, D.** (2005). Photosystem II core phosphorylation and photosynthetic acclimation require two different protein kinases. Nature **437,** 1179-1182.

➢ **Buchanan, B., Gruissem, W., and RL, J.** (2002). Biochemistry & Molecular Biology of Plants - 1st edition. John Wiley & Sons.

➢ **Clough, S.J., and Bent, A.F.** (1998). Floral dip: a simplified method for*Agrobacterium*-mediated transformation of *Arabidopsis thaliana*. The Plant Journal **16,** 735-743.

➢ **Coffeen, W.C., and Wolpert, T.J.** (2004). Purification and characterization of serine proteases that exhibit caspase-like activity and are associated with programmed cell death in *Avena sativa*. The Plant Cell Online **16,** 857-873.

➢ **DalCorso, G., Pesaresi, P., Masiero, S., Aseeva, E., Schünemann, D., Finazzi, G., Joliot, P., Barbato, R., and Leister, D.** (2008). A complex containing PGRL1 and PGR5 is involved in the switch between linear and cyclic electron flow in *Arabidopsis*. Cell **132,** 273-285.

➢ **Demmig-Adams, B., and Adams, W.W.** (1993). The xanthophyll cycle, protein turnover, and the high light tolerance of sun-acclimated leaves. Plant Physiology **103,** 1413-1420.

➤ **Eberhard, S., Finazzi, G., and Wollman, F.-A.** (2008). The dynamics of photosynthesis. Annual Review of Genetics **42,** 463-515.

➤ **Egea-Cortines, M., Saedler, H., and Sommer, H.** (1999). Ternary complex formation between the MADS-box proteins SQUAMOSA, DEFICIENS and GLOBOSA is involved in the control of floral architecture in *Antirrhinum majus*. EMBO J. **18,** 5370-5379.

➤ **Emanuelsson, O., Nielsen, H., Brunak, S., and von Heijne, G.** (2000). Predicting subcellular localization of proteins based on their N-terminal amino acid sequence. Journal of Molecular Biology **300,** 1005-1016.

➤ **Emanuelsson, O., Brunak, S., von Heijne, G., and Nielsen, H.** (2007). Locating proteins in the cell using TargetP, SignalP and related tools. Nat. Protocols **2,** 953-971.

➤ **Farber, A., Young, A.J., Ruban, A.V., Horton, P., and Jahns, P.** (1997). Dynamics of xanthophyll-cycle activity in different antenna subcomplexes in the photosynthetic membranes of higher plants (the relationship between zeaxanthin conversion and nonphotochemical fluorescence quenching). Plant Physiology **115,** 1609-1618.

➤ **Finazzi, G., Rappaport, F., and Goldschmidt-Clermont, M.** (2003). From light to life: an interdisciplinary journey into photosynthetic activity. Embo reports **4,** 752-756.

➤ **Finkelstein, R.R., and Gibson, S.I.** (2002). ABA and sugar interactions regulating development: cross-talk or voices in a crowd? Current Opinion in Plant Biology **5,** 26-32.

➤ **Friso, G., Giacomelli, L., Ytterberg, A.J., Peltier, J.-B., Rudella, A., Sun, Q., and Wijk, K.J.v.** (2004). In-depth analysis of the thylakoid membrane proteome of *Arabidopsis thaliana* chloroplasts: New proteins, new functions, and a plastid proteome database. The Plant Cell Online **16,** 478-499.

➤ **Gechev, T.S., Van Breusegem, F., Stone, J.M., Denev, I., and Laloi, C.** (2006). Reactive oxygen species as signals that modulate plant stress responses and programmed cell death. BioEssays **28,** 1091-1101.

➤ **Gechev, T.S., Ferwerda, M.A., Mehterov, N., Laloi, C., Qureshi, M.K., and Hille, J.** (2008). *Arabidopsis* AAL-toxin-resistant mutant *atr1* shows enhanced tolerance to programmed cell death induced by reactive oxygen species. Biochemical and Biophysical Research Communications **375,** 639-644.

➢ **Gietz, R., and Woods, R.** (2006). Yeast transformation by the LiAc/SS carrier DNA/PEG method Methods in Molecular Biology **313,** 107-120.

➢ **Granvogl, B., Reisinger, V., and Eichacker, L.A.** (2006). Mapping the proteome of thylakoid membranes by de novo sequencing of intermembrane peptide domains. PROTEOMICS **6,** 3681-3695.

➢ **Gupta, R., He, Z., and Luan, S.** (2002). Functional relationship of cytochrome c_6 and plastocyanin in *Arabidopsis*. Nature **417,** 567-571.

➢ **Haehnel, W., Jansen, T., Gause, K., Klösgen, R., Stahl, B., Michl, D., Huvermann, B., Karas, M., and Herrmann, R.** (1994). Electron transfer from plastocyanin to photosystem I. EMBO J. **13,** 1028-1038.

➢ **Haldrup, A., Simpson, D.J., and Scheller, H.V.** (2000). Down-regulation of the PSI-F Subunit of Photosystem I (PSI) in *Arabidopsis thaliana*. Journal of Biological Chemistry **275,** 31211-31218.

➢ **Hammani, K., Okuda, K., Tanz, S.K., Chateigner-Boutin, A.-L., Shikanai, T., and Small, I.** (2009). A study of new *Arabidopsis* chloroplast RNA editing mutants reveals general features of editing factors and their target sites. The Plant Cell Online **21,** 3686-3699.

➢ **Hawkins, J., and Bodén, M.** (2006). Detecting and sorting targeting peptides with neural networks and support vector machines. Journal of Bioinformatics and Computational Biology **4,** 1-18.

➢ **Hippler, H., Reichert, J., Sutter, M., Zak, E., Altschmied, L., Schröer, U., Herrmann, R., and W, H.** (1996). The plastocyanin binding domain of photosystem I. EMBO J. **15,** 6374-6384.

➢ **Hippler, M., Drepper, F., Haehnel, W., and Rochaix, J.-D.** (1998). The N-terminal domain of PsaF: Precise recognition site for binding and fast electron transfer from cytochrome c_6 and plastocyanin to photosystem I of *Chlamydomonas reinhardtii*. Proceedings of the National Academy of Sciences **95,** 7339-7344.

➢ **Hippler, M., Drepper, F., Rochaix, J.-D., and Mühlenhoff, U.** (1999). Insertion of the N-terminal part of PsaF from *Chlamydomonas reinhardtii* into photosystem I from *Synechococcus elongatus* enables efficient binding of algal plastocyanin and cytochrome c_6. Journal of Biological Chemistry **274,** 4180-4188.

➢ **Hirashima, M., Tanaka, R., and Tanaka, A.** (2009). Light-independent cell death induced by accumulation of pheophorbide a in *Arabidopsis thaliana*. Plant and Cell Physiology **50,** 719-729.

➢ **Horton, P., Park, K.-J., Obayashi, T., Fujita, N., Harada, H., Adams-Collier, C.J., and Nakai, K.** (2007). WoLF PSORT: protein localization predictor. Nucleic Acids Research **35,** W585-W587.

➢ **Hoth, S., Morgante, M., Sanchez, J.-P., Hanafey, M.K., Tingey, S.V., and Chua, N.-H.** (2002). Genome-wide gene expression profiling in *Arabidopsis thaliana* reveals new targets of abscisic acid and largely impaired gene regulation in the *abi1-1* mutant. J Cell Sci **115,** 4891-4900.

➢ **Howe, C.J., Schlarb-Ridley, B.G., Wastl, J., Purton, S., and Bendall, D.S.** (2006). The novel cytochrome c_6 of chloroplasts: a case of evolutionary bricolage? Journal of Experimental Botany **57,** 13-22.

➢ **Hyun Lee, B., Hibino, T., Takabe, T., Weisbeek, P.J., and Takabe, T.** (1995). Site-directed mutagenetic study on the role of negative patches on silene plastocyanin in the interactions with cytochrome *f* and photosystem I. Journal of Biochemistry **117,** 1209-1217.

➢ **Ihnatowicz, A., Pesaresi, P., and Leister, D.** (2007). The E subunit of photosystem I is not essential for linear electron flow and photoautotrophic growth in *Arabidopsis thaliana*. Planta **226,** 889-895.

➢ **Ihnatowicz, A., Pesaresi, P., Varotto, C., Richly, E., Schneider, A., Jahns, P., Salamini, F., and Leister, D.** (2004). Mutants for photosystem I subunit D of *Arabidopsis thaliana*: effects on photosynthesis, photosystem I stability and expression of nuclear genes for chloroplast functions. The Plant Journal **37,** 839-852.

➢ **Irizarry, R.A., Hobbs, B., Collin, F., Beazer-Barclay, Y.D., Antonellis, K.J., Scherf, U., and Speed, T.P.** (2003). Exploration, normalization, and summaries of high density oligonucleotide array probe level data. Biostatistics **4,** 249-264.

➢ **Jain, N., Thatte, J., Braciale, T., Ley, K., O'Connell, M., and Lee, J.K.** (2003). Local-pooled-error test for identifying differentially expressed genes with a small number of replicated microarrays. Bioinformatics **19,** 1945-1951.

➢ **James, P., Halladay, J., and Craig, E.A.** (1996). Genomic Libraries and a Host Strain Designed for Highly Efficient Two-Hybrid Selection in Yeast. Genetics **144,** 1425-1436.

➢ **Kang, C.H., Jung, W.Y., Kang, Y.H., Kim, J.Y., Kim, D.G., Jeong, J.C., Baek, D.W., Jin, J.B., Lee, J.Y., Kim, M.O., Chung, W.S., Mengiste, T., Koiwa, H., Kwak, S.S., Bahk, J.D., Lee, S.Y., Nam, J.S., Yun, D.J., and Cho, M.J.** (2005). AtBAG6, a novel calmodulin-binding protein, induces programmed cell death in yeast and plants. Cell Death Differ **13,** 84-95.

➢ **Katoh, S.** (1960). Crystallization of an algal cytochrome, *Porphyra tenera*-cytochrome 553. Nature **186,** 138-139.

➢ **Kleffmann, T., Russenberger, D., von Zychlinski, A., Christopher, W., Sjölander, K., Gruissem, W., and Baginsky, S.** (2004). The *Arabidopsis thaliana* chloroplast proteome reveals pathway abundance and novel protein functions. Current Biology **14,** 354-362.

➢ **Kleine, T., Voigt, C., and Leister, D.** (2009). Plastid signalling to the nucleus: messengers still lost in the mists? Trends in Genetics **25,** 185-192.

➢ **Klemm, J.D., Schreiber, S.L., and Crabtree, G.R.** (1998). Dimerization as a regulatory mechanism in signal transduction. Annu. Rev. Immunol. **16,** 569-592.

➢ **Li, X.-P., Bjorkman, O., Shih, C., Grossman, A.R., Rosenquist, M., Jansson, S., and Niyogi, K.K.** (2000). A pigment-binding protein essential for regulation of photosynthetic light harvesting. Nature **403,** 391-395.

➢ **Lindahl, M., and Kieselbach, T.** (2009). Disulphide proteomes and interactions with thioredoxin on the track towards understanding redox regulation in chloroplasts and cyanobacteria. Journal of Proteomics **72,** 416-438.

➢ **Liu, Y.-G., Mitsukawa, N., Oosumi, T., and Whittier, R.F.** (1995). Efficient isolation and mapping of *Arabidopsis thaliana* T-DNA insert junctions by thermal asymmetric interlaced PCR. The Plant Journal **8,** 457-463.

➢ **Marcaida, M.J., Schlarb-Ridley, B.G., Worrall, J.A.R., Wastl, J., Evans, T.J., Bendall, D.S., Luisi, B.F., and Howe, C.J.** (2006). Structure of cytochrome c_{6A}, a novel dithio-cytochrome of *Arabidopsis thaliana*, and its reactivity with plastocyanin: Implications for function. Journal of Molecular Biology **360,** 968-977.

➢ **Maxwell, K., and Johnson, G.N.** (2000). Chlorophyll fluorescence-a practical guide. Journal of Experimental Botany **51,** 659-668.

➢ **Merchant, S., and Dreyfuss, B.W.** (1998). Posttranslational assembly of photosynthetic metalloproteins. Annual Review of Plant Physiology and Plant Molecular Biology **49,** 25-51.

➢ **Molina-Heredia, F.P., Wastl, J., Navarro, J.A., Bendall, D.S., Hervas, M., Howe, C.J., and De la Rosa, M.A.** (2003). Photosynthesis (communication arising): A new function for an old cytochrome? Nature **424,** 33-34.

➢ **Munekage, Y., Hojo, M., Meurer, J., Endo, T., Tasaka, M., and Shikanai, T.** (2002). PGR5 is involved in cyclic electron flow around photosystem I and is essential for photoprotection in *Arabidopsis*. Cell **110,** 361-371.

➢ **Nakai, K., and Horton, P.** (2007). Computational prediction of subcellular localization. In Methods in Molecular Biology, pp. 429-466.

➢ **Nelson, N., and Yocum, C.F.** (2006). Structure and function of photosystems I and II. Annual Review of Plant Biology **57,** 521-565.

➢ **Nicholls, P.** (1992). What form of cytochrome c oxidase reacts with oxygen in vivo? Biochem J. **288,** 1070-1072.

➢ **Nield, J., Kruse, O., Ruprecht, J., da Fonseca, P., Büchel, C., and Barber, J.** (2000). Three-dimensional structure of *Chlamydomonas reinhardtii* and *Synechococcus elongatus* photosystem II complexes allows for comparison of their oxygen-evolving complex organization. Journal of Biological Chemistry **275,** 27940-27946.

➢ **Nordling, M., Sigfridsson, K., Young, S., Lundberg, L.G., and Hansson, Ö.** (1991). Flash-photolysis studies of the electron transfer from genetically modified spinach plastocyanin to photosystem I. FEBS Letters **291,** 327-330.

➢ **Ondzighi, C.A., Christopher, D.A., Cho, E.J., Chang, S.-C., and Staehelin, L.A.** (2008). *Arabidopsis* Protein Disulfide Isomerase-5 inhibits cysteine proteases during trafficking to vacuoles before programmed cell death of the endothelium in developing seeds. The Plant Cell Online **20,** 2205-2220.

➢ **Peltier, J.-B., Emanuelsson, O., Kalume, D.E., Ytterberg, J., Friso, G., Rudella, A., Liberles, D.A., Söderberg, L., Roepstorff, P., von Heijne, G., and van Wijk, K.J.** (2002). Central functions of the lumenal and peripheral thylakoid proteome of

Arabidopsis determined by experimentation and genome-wide prediction. The Plant Cell Online **14,** 211-236.

➢ **Peng, L., Ma, J., Chi, W., Guo, J., Zhu, S., Lu, Q., Lu, C., and Zhang, L.** (2006). LOW PSII ACCUMULATION1 is involved in efficient assembly of photosystem II in *Arabidopsis thaliana*. The Plant Cell Online **18,** 955-969.

➢ **Pesaresi, P., Pribil, M., Wunder, T., and Leister, D.** (2011). Dynamics of reversible protein phosphorylation in thylakoids of flowering plants: The roles of STN7, STN8 and TAP38. Biochimica et Biophysica Acta (BBA) - Bioenergetics **In Press, Corrected Proof**.

➢ **Pesaresi, P., Scharfenberg, M., Weigel, M., Granlund, I., Schröder, W.P., Finazzi, G., Rappaport, F., Masiero, S., Furini, A., Jahns, P., and Leister, D.** (2009a). Mutants, overexpressors, and interactors of *Arabidopsis* plastocyanin isoforms: Revised roles of plastocyanin in photosynthetic electron flow and thylakoid redox state. Molecular Plant **2,** 236-248.

➢ **Pesaresi, P., Hertle, A., Pribil, M., Kleine, T., Wagner, R., Strissel, H., Ihnatowicz, A., Bonardi, V., Scharfenberg, M., Schneider, A., Pfannschmidt, T., and Leister, D.** (2009b). *Arabidopsis* STN7 kinase provides a link between short- and long-term photosynthetic acclimation. The Plant Cell Online **21,** 2402-2423.

➢ **Pfaffl, M.W.** (2001). A new mathematical model for relative quantification in real-time RT-PCR. Nucleic Acids Research **29,** e45.

➢ **Pierleoni, A., Martelli, P.L., Fariselli, P., and Casadio, R.** (2006). BaCelLo: a balanced subcellular localization predictor. Bioinformatics **22,** e408-e416.

➢ **Porra, R.J.** (2002). The chequered history of the development and use of simultaneous equations for the accurate determination of chlorophylls a and b. Photosynthesis Research **73,** 149-156.

➢ **Pribil, M., Pesaresi, P., Hertle, A., Barbato, R., and Leister, D.** (2010). Role of plastid protein phosphatase TAP38 in LHCII dephosphorylation and thylakoid electron flow. PLoS Biol **8,** e1000288.

➢ **Raghavendra, A.S., Gonugunta, V.K., Christmann, A., and Grill, E.** (2010). ABA perception and signalling. Trends in Plant Science **15,** 395-401.

➢ **Schägger, H., and von Jagow, G.** (1987). Tricine-sodium dodecyl sulfate-polyacrylamide gel electrophoresis for the separation of proteins in the range from 1 to 100 kDa. Analytical Biochemistry **166,** 368-379.

➢ **Schein, A.I., Kissinger, J.C., and Ungar, L.H.** (2001). Chloroplast transit peptide prediction: a peek inside the black box. Nucleic Acids Research **29,** e82.

➢ **Schlarb-Ridley, B.G., Nimmo, R.H., Purton, S., Howe, C.J., and Bendall, D.S.** (2006). Cytochrome c_{6A} is a funnel for thiol oxidation in the thylakoid lumen. FEBS Letters **580,** 2166-2169.

➢ **Schubert, M., Petersson, U.A., Haas, B.J., Funk, C., Schröder, W.P., and Kieselbach, T.** (2002). Proteome map of the chloroplast lumen of *Arabidopsis thaliana*. Journal of Biological Chemistry **277,** 8354-8365.

➢ **Schwenkert, S., Umate, P., Bosco, C.D., Volz, S., Mlcochová, L., Zoryan, M., Eichacker, L.A., Ohad, I., Herrmann, R.G., and Meurer, J.r.** (2006). PsbI affects the stability, function, and phosphorylation patterns of photosystem II assemblies in *Tobacco*. Journal of Biological Chemistry **281,** 34227-34238.

➢ **Sessions, A., Burke, E., Presting, G., Aux, G., McElver, J., Patton, D., Dietrich, B., Ho, P., Bacwaden, J., Ko, C., Clarke, J.D., Cotton, D., Bullis, D., Snell, J., Miguel, T., Hutchison, D., Kimmerly, B., Mitzel, T., Katagiri, F., Glazebrook, J., Law, M., and Goff, S.A.** (2002). A high-throughput *Arabidopsis* reverse genetics system. The Plant Cell Online **14,** 2985-2994.

➢ **Sherman, F., Guthrie, C., and Fink, G.** (2002). Getting started with yeast. In Methods in Enzymology (Academic Press), pp. 3-41.

➢ **Shikanai, T.** (2007). Cyclic electron transport around photosystem I: Genetic approaches. Annual Review of Plant Biology **58,** 199-217.

➢ **Simpson, G.G., Dijkwel, P.P., Quesada, V., Henderson, I., and Dean, C.** (2003). FY is an RNA 3' end-processing factor that interacts with FCA to control the *Arabidopsis* floral transition. Cell **113,** 777-787.

➢ **Small, I., Peeters, N., Legeai, F., and Lurin, C.** (2004). Predotar: A tool for rapidly screening proteomes for N-terminal targeting sequences. PROTEOMICS **4,** 1581-1590.

➢ **Sommer, F., Drepper, F., Haehnel, W., and Hippler, M.** (2004). The hydrophobic recognition site formed by residues PsaA-Trp651 and PsaB-Trp627 of photosystem I in *Chlamydomonas reinhardtii* confers distinct selectivity for binding of plastocyanin and cytochrome c_6. Journal of Biological Chemistry **279,** 20009-20017.

➢ **Stolz, A., Hilt, W., Buchberger, A., and Wolf, D.H.** (2011). Cdc48: a power machine in protein degradation. Trends in Biochemical Sciences **In Press, Corrected Proof**.

➢ **Swidzinski, J.A., Sweetlove, L.J., and Leaver, C.J.** (2002). A custom microarray analysis of gene expression during programmed cell death in *Arabidopsis thaliana*. The Plant Journal **30,** 431-446.

➢ **Taiz, L., and Zeiger, E.** (2006). Plant physiology - 4th edition. Spektrum.

➢ **Tenenbaum, S.A., Lager, P.J., Carson, C.C., and Keene, J.D.** (2002). Ribonomics: identifying mRNA subsets in mRNP complexes using antibodies to RNA-binding proteins and genomic arrays. Methods **26,** 191-198.

➢ **Thomas, S.G., and Franklin-Tong, V.E.** (2004). Self-incompatibility triggers programmed cell death in *Papaver* pollen. Nature **429,** 305-309.

➢ **Tikkanen, M., Piippo, M., Suorsa, M., Sirpiö, S., Mulo, P., Vainonen, J., Vener, A., Allahverdiyeva, Y., and Aro, E.-M.** (2006). State transitions revisited-a buffering system for dynamic low light acclimation of *Arabidopsis*. Plant Molecular Biology **62,** 779-793.

➢ **Tissier, A.F., Marillonnet, S., Klimyuk, V., Patel, K., Torres, M.A., Murphy, G., and Jones, J.D.G.** (1999). Multiple independent defective suppressor-mutator transposon insertions in *Arabidopsis*: A tool for functional genomics. The Plant Cell Online **11,** 1841-1852.

➢ **Tsien, R.Y.** (1998). The green fluorescent protein. Annual Review of Biochemistry **67,** 509-544.

➢ **Wagner, R., Dietzel, L., Bräutigam, K., Fischer, W., and Pfannschmidt, T.** (2008). The long-term response to fluctuating light quality is an important and distinct light acclimation mechanism that supports survival of *Arabidopsis thaliana* under low light conditions. Planta **228,** 573-587.

➢ **Wastl, J., Bendall, D.S., and Howe, C.J.** (2002). Higher plants contain a modified cytochrome c_6. Trends in Plant Science **7,** 244-245.

➢ **Wastl, J., Molina-Heredia, F.P., Hervás, M., Navarro, J.A., De la Rosa, M.A., Bendall, D.S., and Howe, C.J.** (2004). Redox properties of *Arabidopsis* cytochrome c_6 are independent of the loop extension specific to higher plants. Biochimica et Biophysica Acta (BBA) - Bioenergetics **1657,** 115-120.

➢ **Weigel, M.** (2006). Molekulargenetische und physiologische Analysen von Plastocyanin und Cytochrom c_x – Mutanten bei *Arabidopsis thaliana*. Dissertation.

➢ **Weigel, M., Pesaresi, P., and Leister, D.** (2003b). Tracking the function of the cytochrome c_6-like protein in higher plants. Trends in Plant Science **8,** 513-517.

➢ **Weigel, M., Varotto, C., Pesaresi, P., Finazzi, G., Rappaport, F., Salamini, F., and Leister, D.** (2003a). Plastocyanin is indispensable for photosynthetic electron flow in *Arabidopsis thaliana*. Journal of Biological Chemistry **278,** 31286-31289.

➢ **Worrall, J., Luisi BF, Schlarb-Ridley BG, Bendall DS, and CJ., H.** (2008). Cytochrome c_{6A}: Discovery, structure and properties responsible for its low haem redox potential. Biochem Soc Trans. **36,** 1175-1179.

➢ **Worrall, J., Schlarb-Ridley, B.G., Reda, T., Marcaida, M.J., Moorlen, R.J., Wastl, J., Hirst, J., Bendall, D.S., Luisi, B.F., and Howe, C.J.** (2007). Modulation of heme redox potential in the cytochrome c_6 family. Journal of the American Chemical Society **129,** 9468-9475.

➢ **Yao, N., and Greenberg, J.T.** (2006). *Arabidopsis* ACCELERATED CELL DEATH2 modulates programmed cell death. The Plant Cell Online **18,** 397-411.

➢ **Young, T., and Gallie, D.** (1999). Analysis of programmed cell death in wheat endosperm reveals differences in endosperm development between cereals. Plant Molecular Biology **39,** 915-926.

Acknowledgements

I am grateful to Prof. Dr. Dario Leister for supervising and supporting my first steps in the scientific world.

I would like to thank Dr. Paolo Pesaresi. I am especially thankful for his supervision and help during difficult times. With his ideas and enthusiasm for science, he was a resilient support.

To Dr. Simona Masiero from the University of Milan (Italy) for performing the yeast two-hybrid and the ternary trap experiments.

To Dr. Giovanni Dal Corso for correcting my thesis. He is an inexhaustible source of knowledge and positive motivation with the precious ability to make difficult things clear to everybody's mind.

To Dr. Elena Fenino for mastering the challenge of the PhD together with me. A worthy help and friend, who always understands me. "Kohl, with you, it is never boring!"

To my lab colleagues, Henning, Alex, Tobi, Angie, Tatjana, Mathias, Cordelia, Stamy, Sabine, Anne, Thilo, Ashraf, Jafar, Qiuping, Arianna, Ute, the soccer-team and many, many more... for sharing fruitful discussions, ups and downs, sports, chocolate, icecream and buffers.

To my brothers and friends in Cologne for always giving me the homecoming feeling and to Uwe with whom I travelled far more than 100,000 km in 6 years.

To my parents-in-law for supporting me and Nadine in every possible way. A special thank to their fabulous wash-mashine that was suffering many weekends.

To my parents for they always believing in me and for their patience for the longest learning path of their sons. I will miss the question: "Und, wie sieht's aus? Fertig?".

To Nadine, the save haven in my stormy life. Many thanks for supporting this challenging journey. Finally, it is time to come home.

Curriculum vitae

PERSONAL DATA

Name: Michael Scharfenberg

Date of Birth: 24th of March 1981

Place of Birth: Dormagen, Germany

Citizenship: German

RESEARCH EXPERIENCES

April 2007 – April 2011

Ludwig-Maximilians-Universität Munich (Germany), Department Biologie I, Botany

Supervisor: Prof. Dr. D. Leister

- PhD in "Cytochrome c_{6A} – Functional Evolution of a Plastidial Protein"

January 2006 – December 2006

Ludwig-Maximilians-Universität Munich (Germany), Department Biologie I, Botany

Supervisors: Dr. Paolo Pesaresi (Univerity of Milano), Prof. Dr. D. Leister and Prof. Dr. U. I. Flügge (University of Cologne)

- Diploma Research Project: "Evolutionärer Funktionswandel von Cytochrom c_6"

EDUCATION

July 2000 – December 2006

University of Cologne (Germany)

Studies of Biology

External Diploma Thesis at the Ludwig-Maximilians-Universität Munich (Germany)

Department Biologie I, Botany: "Evolutionärer Funktionswandel von Cytochrom c_6"

July 1991 – June 2000

Norbert-Gymnasium Knechtsteden, Germany

A-level Majors: Biology and Mathematics

PUBLICATIONS

Armbruster, U., Pribil, M., Xu, W., Scharfenberg, M., Hertle, A., Rojahn, U., Jensen, P.E., Rappaport, F., Joliot, P., Dörmann, P., Wanner, G., and Leister, D. (2011). "The CURT1 family of membrane proteins controls grana formation." *submitted to Cell*

 # Pesaresi, P., Scharfenberg, M., Weigel, M., Granlund, I., Schröder, W.P., Finazzi, G., Rappaport, F., Masiero, S., Furini, A., Jahns, P., and Leister, D. (2009). "Mutants, overexpressors, and interactors of *Arabidopsis* plastocyanin isoforms: Revised roles of plastocyanin in photosynthetic electron flow and thylakoid redox state." **Molecular Plant** 2, 236-248.

Pesaresi, P., Hertle, A., Pribil, M., Kleine, T., Wagner, R., Strissel, H., Ihnatowicz, A., Bonardi, V., Scharfenberg, M., Schneider, A., Pfannschmidt, T., and Leister, D. (2009). "*Arabidopsis* STN7 kinase provides a link between short- and long-term photosynthetic acclimation." **The Plant Cell** 21, 2402-2423.

Armbruster, U., Hertle, A., Makarenko, E., Zühlke, J., Pribil, M., Dietzmann, A., Schliebner, I., Aseeva, E., Fenino, E., Scharfenberg, M., Voigt, C., and Leister, D. (2009). "Chloroplast proteins without cleavable transit peptides: Rare exceptions or a major constituent of the chloroplast proteome?" **Molecular Plant** 2, 1325-1335.

Publication related to this thesis

Ehrenwörtliche Versicherung

Ich versichere hiermit ehrenwörtlich, dass die vorgelegte Dissertation von mir selbständig und ohne unerlaubte Hilfe angefertigt ist.

München, den ....
                                                          (Unterschrift)